

RESTRICTED

RM L52J03a

NACA RM L52J03a

DEC 30 1952

UNCLASSIFIED

TF



RESEARCH MEMORANDUM

EFFECTS OF TWIST AND CAMBER ON THE LOW-SPEED
 LONGITUDINAL STABILITY CHARACTERISTICS OF A 45° SWEEPBACK
 WING OF ASPECT RATIO 8 AT REYNOLDS NUMBERS FROM 1.5×10^6
 TO 4.8×10^6 AS DETERMINED BY PRESSURE DISTRIBUTIONS,
 FORCE TESTS, AND CALCULATIONS

By George L. Pratt

Langley Aeronautical Laboratory
Langley Field, Va.

FOR REFERENCE

NOT TO BE TAKEN FROM THIS ROOM

CLASSIFIED DOCUMENT

This material contains information affecting the National Defense of the United States within the meaning of the espionage laws, Title 18, U.S.C., Secs. 793 and 794, the transmission or revelation of which in any manner to an unauthorized person is prohibited by law.

NATIONAL ADVISORY COMMITTEE FOR AERONAUTICS

WASHINGTON

December 19, 1952

UNCLASSIFIED

CLASSIFICATION CANCELLED

Authority: J.W. Crowley Date: 12/27/53
48-11521
 By: 20727A 12/18/53 See NACA
P-7 1664

RESTRICTED

NACA LIBRARY
LANGLEY AERONAUTICAL LABORATORY
Langley Field, Va.

~~RESTRICTED~~

UNCLASSIFIED

NATIONAL ADVISORY COMMITTEE FOR AERONAUTICS

RESEARCH MEMORANDUM

EFFECTS OF TWIST AND CAMBER ON THE LOW-SPEED
LONGITUDINAL STABILITY CHARACTERISTICS OF A 45° SWEEPBACK
WING OF ASPECT RATIO 8 AT REYNOLDS NUMBERS FROM 1.5×10^6
TO 4.8×10^6 AS DETERMINED BY PRESSURE DISTRIBUTIONS,
FORCE TESTS, AND CALCULATIONS

By George L. Pratt

SUMMARY

The low-speed longitudinal stability characteristics of a 45° swept-back wing of aspect ratio 8 having twist and cambered airfoil sections were investigated by means of force and pressure-distribution measurements at Reynolds numbers from 1.5×10^6 to 4.8×10^6 in the Langley 19-foot pressure tunnel. The effects of Reynolds number, leading-edge roughness, upper-surface fences, and leading-edge and trailing-edge flaps have been determined. The results obtained on the twisted and cambered wing have been compared with the results obtained on a similar untwisted wing having symmetrical airfoil sections of the same thickness distribution. The experimental pressure-distribution loadings have been compared to calculated loadings.

A comparison of the twisted and cambered wing with the untwisted and uncambered wing indicates that the camber and twist improved the stability characteristics in the lift-coefficient range from 0.25 to 0.7. Twist and camber increased the maximum lift coefficient from 1.01 to 1.30 at angles of attack of 20° and 27° , respectively. Upper-surface fences substantially improved the stability characteristics of both wings by improving the stalling characteristics of the outboard sections of the wing. The twisted and cambered wing in conjunction with the upper-surface fences, however, had considerably better stability characteristics at maximum lift. This improvement in stability has been shown (NACA RM L52J03) to be particularly effective when a properly located horizontal tail is used in conjunction with fences on the twisted and cambered wing.

The load distributions calculated by the Multhopp solutions having either 15 or 23 spanwise control points were in good agreement with the experimental load distributions.

~~RESTRICTED~~

UNCLASSIFIED

INTRODUCTION

In order to provide information with which to evaluate sweptback wings for use on long-range high-speed airplanes, the low-speed longitudinal stability characteristics of two 45° sweptback wings of aspect ratio 8 have been investigated in the Langley 19-foot pressure tunnel. The first wing incorporated NACA 631A012 airfoil sections and no geometric twist; whereas the second wing incorporated twist and camber to provide a uniform chordwise loading and an elliptical span loading at a lift coefficient of 0.7 for a Mach number of 0.9. The results of the investigation of the untwisted and uncambered wing are presented in references 1 to 3 while the longitudinal characteristics of the twisted and cambered wing as determined from force tests are presented in references 4 and 5. The present paper includes the results of pressure-distribution measurements on the twisted and cambered wing to determine in more detail than is available from force tests the effects of Reynolds number, leading-edge roughness, upper-surface fences, and leading-edge and trailing-edge flaps. A comparison is made between the results obtained on the twisted and cambered wing and the results obtained on the untwisted and uncambered wing.

The spanwise load distributions calculated by methods (refs. 6 and 7) of determining the loading of sweptback wings have been compared with the loadings obtained from the pressure distributions.

The majority of the tests were made at a Reynolds number of 4.0×10^6 and a Mach number of 0.19. The effects of Reynolds number were obtained from force tests at Reynolds numbers from 1.5×10^6 to 4.8×10^6 on the plain twisted and cambered wing. Pressure distributions were obtained at Reynolds numbers of 1.5×10^6 and 4.0×10^6 on the twisted and cambered wing.

SYMBOLS

The data are referred to the wind axes with the origin at the projection of the quarter-chord point of the mean aerodynamic chord on the plane of symmetry. The force and pressure-distribution data have been reduced to nondimensional coefficient form as follows:

- C_L lift coefficient, $\frac{L}{qS_w}$
- c_l section lift coefficient

$$c_l = \cos(\alpha + \epsilon) \int_0^1 (S_u - S_l) d\left(\frac{x}{c}\right) - \sin(\alpha + \epsilon) \int_{-(z/c)_{\max}}^{(z/c)_{\max}} (S_r - S_f) d\left(\frac{z}{c}\right)$$

c_{l_b} section lift coefficient due to stream misalignment

c_{l_i} section design lift coefficient (camber)

c_{l_α} section lift-curve slope

C_D drag coefficient, $\frac{D}{qS_w}$

c_d section pressure drag coefficient

$$c_d = \sin(\alpha + \epsilon) \int_0^1 (S_u - S_l) d\left(\frac{x}{c}\right) + \cos(\alpha + \epsilon) \int_{-(z/c)_{\max}}^{(z/c)_{\max}} (S_r - S_f) d\left(\frac{z}{c}\right)$$

C_m pitching-moment coefficient, $\frac{M}{qS_w c^2}$

C_{m_0} pitching-moment coefficient at zero lift

c_m section pitching-moment coefficient about local quarter-chord point

$$\int_0^1 (S_u - S_l) \left(0.25 - \frac{x}{c}\right) d\left(\frac{x}{c}\right) + \int_{-(z/c)_{\max}}^{(z/c)_{\max}} (S_r - S_f) \frac{z}{c} d\left(\frac{z}{c}\right)$$

L lift, lb

D drag, lb

M pitching moment about $0.25c'$, ft-lb

H free-stream total pressure, lb/sq ft

S_w wing area (based on untwisted plan form), sq ft

S pressure coefficient, $\frac{H - p}{q}$

R	Reynolds number, $\frac{\rho V c'}{\mu}$
V	free-stream velocity, ft/sec
α	angle of attack of root-chord line, deg
α_0	angle of attack at zero lift, deg
α_p	section angle of attack due to stream misalignment, deg
ϵ	angle of twist measured with respect to root-chord line, washout is minus, deg
ρ	density of air, slugs/cu ft
μ	coefficient of viscosity, slugs/ft-sec
a	mean line
b	wing span, ft
c	local wing chord parallel to plane of symmetry, ft
c'	mean aerodynamic chord, $\frac{2}{S_w} \int_0^{b/2} c^2 dy$, ft
\bar{c}	mean chord, $\frac{S_w}{b}$, ft
p	local static pressure, lb/sq ft
q	dynamic pressure, $\frac{1}{2} \rho V^2$, lb/sq ft
t_{max}	local section maximum thickness, ft
x	distance along section chord line measured from local leading edge parallel to plane of symmetry (rearward positive), ft
\bar{x}	location of section chordwise center of pressure measured from section quarter-chord point (rearward positive), ft
y	lateral distance from plane of symmetry measured perpendicular to plane of symmetry, ft

z	vertical ordinate of airfoil section measured from and perpendicular to chord line (positive up), ft
z_c	vertical ordinate of mean camber line measured from and perpendicular to chord line (positive up), ft
\bar{z}	location of section vertical center of pressure measured perpendicular to chord line (positive up), ft
\bar{y}	lateral distance measured from and perpendicular to plane of symmetry to wing center of pressure, ft
$dC_L/d\alpha$	wing lift-curve slope
$dC_m/d\alpha$	rate of change of pitching moment with angle of attack
dC_m/dC_L	rate of change of pitching moment with lift coefficient

Subscripts:

u	upper surface
l	lower surface
f	forward of maximum thickness
r	rearward of maximum thickness

Terminology

In the discussion that follows, the wing without twist and camber will be referred to as the plane wing; whereas the usage of the word "plain" refers to either wing without high-lift and stall-control devices deflected.

MODEL AND APPARATUS

The model had an aspect ratio of 8.02, a taper ratio of 0.45, and 45° sweepback of the quarter-chord line before incorporating twist about the 0.80c line (fig. 1). The airfoil sections parallel to the plane of symmetry were of the NACA 63₁A012 thickness distribution about a slightly modified NACA $a = 1.0$ mean line having the desired design section lift coefficient (camber). Figure 2 presents the spanwise distribution of twist and design lift coefficient incorporated into the wing. The section mean camber line was obtained by multiplying the design lift

coefficient by the ordinates of the camber line for a design lift coefficient of 1.0 (table I). Additional details of the design of the wing may be found in reference 4.

The model was constructed of a steel core covered with approximately a 1/8-inch layer of an alloy of bismuth and tin. The left semispan of the model was equipped with 215 orifices flush with the surface of the wing distributed chordwise on the upper and lower surface at eight spanwise stations as indicated in figure 1. Table II presents the airfoil ordinates at the various orifice locations. The tubing from the orifices was conducted through the bismuth and tin layer and brought out on the lower surface of the right-hand wing panel approximately 20 percent of the semispan out from the wing root. The tubes were then conducted rearward through a pipe fixed to the wing parallel to the plane of symmetry and then down through a fairing to the outside of the tunnel to multitube manometers. The pressures on the lower surface at station $2y/b = 0.03$ and x/c equal 0.35 and 0.65 were measured by means of a static-pressure survey tube located about 0.004c from the wing surface. The pressures indicated in the manometers were simultaneously recorded photographically. The tube-conducting pipe was replaced by a flush cover plate for the force tests.

Figures 3 and 4 present photographs of the model as installed in the wind tunnel for force and pressure-distribution tests, respectively.

The upper-surface fences were installed as indicated in figure 5. The fences were constructed of 1/16-inch-thick sheet steel and were attached to the model parallel to the plane of symmetry. The attachment brackets were made as small as was feasible to minimize their interference with the air stream.

The trailing-edge flaps were split flaps having a chord equal to 20 percent of the local wing chord in the undeflected position and were deflected 52° from the local chord line parallel to the plane of symmetry. The trailing-edge flaps extended over the inboard semispan of the wing with the 80-percent-chord line as the hinge axis.

The leading-edge flaps had a span equal to $0.45b/2$ extending from $0.525b/2$ to $0.975b/2$. The flaps were deflected 47.5° from the plane formed by the root-chord line and the twist axis of the wing (80-percent-chord line). Further details of the flaps may be found in figure 5. Although it is not shown in figure 5, pressure orifices were distributed on both leading- and trailing-edge flaps along lines parallel to the air stream and at spanwise stations corresponding to the orifice stations on the plain wing.

Leading-edge roughness consisted of No. 60 (0.011-inch-diameter) carborundum grains applied to a thin coating of shellac on 0.08 chord

of the leading edge of the wing measured along the periphery of the upper and lower surfaces.

TESTS

The model was tested in the Langley 19-foot pressure tunnel with the air compressed to approximately 33 pounds per square inch absolute pressure. Lift, drag, and pitching-moment data were obtained from force tests and pressure distributions through an angle-of-attack range from -3.5° to 31° based on the angle of attack of the root-chord line. The force tests on the plain wing were conducted through a Reynolds number range with a corresponding Mach number range as follows:

Reynolds number	Mach number
1.5×10^6	0.07
2.2	.11
3.0	.14
4.0	.19
4.8	.25

Pressure-distribution data were obtained at Reynolds numbers of 1.5×10^6 and 4.0×10^6 on the plain wing and at a Reynolds number of 4.0×10^6 for the configurations having fences, flaps, and leading-edge roughness.

CORRECTIONS TO DATA

The lift, drag, and pitching-moment data obtained by force tests have been corrected for the model support tare and interference effects. The angle of attack and the drag and pitching-moment coefficients obtained from the force and pressure-distribution measurements have been corrected for jet-boundary effects as applied to the untwisted and uncambered wing in reference 1 and are as follow:

$$\Delta\alpha = 0.39C_L$$

$$\Delta C_D = 0.0063C_L^2$$

$$\Delta C_m = 0.0035C_L$$

As pointed out in reference 1, there was a spanwise variation of the air-stream flow angle in the region occupied by the model which produced the equivalent of a basic loading along the span of the model. Since the model of reference 1 had symmetrical sections, it was possible to obtain the magnitude of this air-stream misalignment by assuming the inaccuracies of model construction to be small. For the model of these tests, the basic loading contributed by the camber and twist prohibited the isolation of the basic loading due to air-stream angle. To account in part for this spanwise variation of air stream, the section lift and pitching-moment data have been corrected by using the spanwise variation in air-stream angle obtained by tunnel survey with the model removed (fig. 6). (The method of obtaining the values of air-stream angle is discussed in ref. 1.) The basic lift distribution was obtained by multiplying these angles by the slopes of the section lift curves obtained from the pressure measurements and is presented in figure 6. These values of basic loading were subtracted at all angles of attack from the lift coefficient obtained by the integration of the chordwise pressure-distribution data. No attempt was made to correct the individual pressure coefficients for air-stream variations.

No corrections were applied to take into account spanwise variations of the jet-boundary-induced angle or the model twist due to aerodynamic loading.

PRESENTATION OF DATA

Pressure-coefficient data obtained on the plain twisted and cambered wing through the angle-of-attack range at a Reynolds number of 4.0×10^6 are tabulated in table III. Figures 7 and 8 present the force data obtained on the plain wing through the Reynolds number range and on the wing with fences and wing with roughness at a Reynolds number of 4.0×10^6 . Chordwise pressure distributions are presented in figure 9 for a representative number of angles of attack for the plain wing, wing with fences, and wing with leading-edge roughness. An omitted symbol indicates that data are not available for the configuration at that particular angle of attack. Figures 10 to 13 present the section lift, pitching-moment, and drag coefficients and centers of pressure obtained from the integrated chordwise pressure data for the plain wing, wing with fences, and wing with roughness. The stalling characteristics of the wing may be evaluated from the tuft studies presented in figure 14. Figure 15 presents the spanwise distribution of lift, pitching-moment, and drag loading parameters for the plain wing through the angle-of-attack range at a Reynolds number of 4.0×10^6 . The spanwise distribution of lift at a Reynolds number of 4.0×10^6 and 1.5×10^6 for the wing with fences and wing with roughness for several representative angles of attack are

compared in figure 16 whereas figure 17 presents the variation of the spanwise center of pressure with angle of attack. A comparison of the force and pressure-distribution results obtained on the twisted and cambered wing with the results obtained on a wing having a similar plan form with untwisted, symmetrical sections (ref. 1) is presented in figures 18 and 19. The effect of flaps and upper-surface fences on the two wings is presented in figures 20 to 23. A comparison of the experimental span loadings with the loadings calculated by the methods of Weissinger and Multhopp (refs. 6 and 7) is presented in figures 24 to 26.

TWISTED AND CAMBERED WING

Lift and Pitching-Moment Characteristics

Plain wing ($R = 4.0 \times 10^6$).— The results of the force tests on the twisted and cambered wing (fig. 7) show that the wing longitudinal stability and lift-curve slope were nearly constant up to a lift coefficient of approximately 0.7 and a corresponding angle of attack of 10° . With a further increase in angle of attack, the pitching moment became unstable and the lift increased at a much lower rate. The section lift data (fig. 10) obtained from the integration of the pressure distributions indicate that this loss of stability and lower lift-curve slope is a result of a loss in lift effectiveness over the midsemispan of the wing which chordwise pressure distributions (figs. 9(i) to 9(n)) indicate to be a result of trailing-edge separation occurring on the midsemispan sections of the wing and which spread outboard and forward with further increases in angle of attack. The stations near the wing root have only a slight decrease in lift-curve slope through the angle-of-attack range.

The contribution of the various sections to the total wing pitching moment is indicated in figure 11(c) which presents the section pitching-moment loading parameter $\left(\frac{c_{m_c}}{l}, \frac{c^2}{cc'} \right)$ plotted against wing lift coefficient.

The contribution of the outboard sections to the stabilizing (negative) pitching moment decreases sharply above a lift coefficient of 0.8 while the destabilizing (positive) pitching-moment contribution of the inboard sections increases at a greater rate with increase of lift coefficient. Actually these trends may be attributed to the fact that the wing lift-curve slope is reduced above $C_L = 0.8$ and this reduction is reflected in any plots against wing lift coefficient. When the pitching-moment loading parameter is plotted against angle of attack (fig. 12(b)), however, the contribution of the inboard stations to the wing pitching moment increases at an approximately constant rate throughout the angle-of-attack range. Thus, it can be seen that the adverse pitching-moment

characteristics of the wing are wholly due to changes over the tip sections of the wing and the resulting redistribution of load. That these adverse effects are due primarily to a loss in lift effectiveness is further borne out by figure 11(b) which indicates that the section pitching-moment coefficients about the local section quarter-chord point were almost always negative (stabilizing). The large movement of the section chordwise centers of pressure indicated in figure 11(b) and in figure 13(a) can be shown to have only a small effect on the contribution of the section to the wing pitching moment. Similarly, the movement of the section vertical centers of pressure (fig. 13(b)) has little effect on stability. (The discontinuities in the center-of-pressure curves occur in the region of zero force where the centers of pressure tend toward infinite values.)

At maximum lift ($C_L = 1.30$) the pitching moment broke in a stable direction which resulted from a sudden increase in lift over the tip sections of the wing and a loss inboard at $2y/b = 0.30$ as shown by the section lift curves (fig. 10). The chordwise pressure-distribution plots of figure 9 (see figs. 9(k) to 9(n)) indicate these lift changes to result from a broadening of the pressure distribution over the rear part of the tip sections at the high angles of attack.

Effect of Reynolds number.- The effects of Reynolds number on the over-all wing-lift and pitching-moment characteristics are indicated in the force and pressure-distribution results presented in figures 7, 9, 10, and 12. At negative values of wing lift coefficient, the force and pressure-distribution data indicate that separation occurs on the outboard lower surface of the wing and is particularly predominant at the lower Reynolds number (1.5×10^6). The separation from the lower surface can be attributed to the large amount of camber and twist incorporated into the wing. Two-dimensional tests of an NACA 64-series section having 0.8 camber (ref. 8) indicate similar effects of flow separation occurring on the lower surface at low angles of attack.

In the low positive lift range, ($C_L = 0$ to 0.3) the force-test results indicate that the lower Reynolds number (1.5×10^6) resulted in increased longitudinal stability over that obtained at a Reynolds number of 4.0×10^6 . The chordwise pressure distributions (fig. 9) indicate these effects to be a result of slightly higher upper-surface pressure coefficients over the outboard stations at the low Reynolds number at low and moderate angles of attack which results in a greater lift effectiveness on the outboard stations of the wing (fig. 10). As was the case at the negative lift coefficients, these effects appear to be a continued effect of the large amount of camber in conjunction with the twist inasmuch as no such effects were noted in the tests of an uncambered and untwisted wing of similar plan form (ref. 1).

An increase in Reynolds number resulted in more nearly linear pitching-moment curves through the low and moderate lift range to approximately $C_L = 0.7$ (fig. 7). Above $C_L = 0.7$, the stalling characteristics of the wing were so adverse that little significant improvement in the stability with an increase in Reynolds number can be noted.

At the highest force-test Reynolds number (4.8×10^6), there is an indication that a further slight gain in maximum lift might possibly be obtained by extending the angle of attack or increasing the Reynolds number. At the higher angles of attack, the chordwise pressure distributions (figs. 9(l) to 9(n)) show peak pressures remaining on the outboard leading edge of the wing at a Reynolds number of 4.0×10^6 and, at a Reynolds number of 1.5×10^6 , completely separated flow occurring over the outboard sections. In the angle-of-attack range in which the adverse lift and pitching-moment characteristics occur, the chordwise pressure diagrams (figs. 9(g) to 9(k)) indicate little significant difference in the pressure gradients at the two test Reynolds numbers (1.5×10^6 and 4.0×10^6). It appears open to considerable conjecture from the available data, therefore, whether a further increase in Reynolds number would or would not result in a substantial improvement in the lift and pitching-moment characteristics.

Effect of leading-edge roughness.- The force tests of the wing at a Reynolds number of 4.0×10^6 with roughness added to the leading edge indicate an appreciable effect of roughness on the lift and pitching-moment characteristics (fig. 8). With roughness the wing has a reduced lift-curve slope above a lift coefficient of 0.3, considerable variation in stability in the low lift range, an unstable break in the pitching-moment curve occurring at $C_L = 0.5$ as compared to $C_L = 0.7$ for the smooth wing, and a decrease in maximum lift coefficient from 1.30 to 1.18. The section lift curves presented in figure 10 indicate that the effects of roughness result primarily from lift changes over the outboard stations. The inboard stations showed little effect of roughness on the section characteristics up to an angle of attack of approximately 22° . At higher angles of attack, roughness caused an increase in lift on the inboard stations ($2y/b = 0$ and $2y/b = 0.3$) which the chordwise distributions show to be a result of the broadening of the pressure distribution over the rear part of the section (figs. 9(m) and 9(n)). At the high angles of attack and at negative angles of attack, the chordwise pressure distribution obtained on the wing with roughness at a Reynolds number of 4.0×10^6 is similar to the pressure distributions obtained at the same angles of attack on the smooth wing at the low Reynolds number (1.5×10^6).

Effect of fences.- Force tests of the wing with various stall-control devices which were presented in reference 4 show that, as in

the case of the untwisted and uncambered wing (ref. 2), very appreciable improvements in the lift and pitching-moment characteristics could be obtained by installing chordwise fences on the upper surface of the wing (see fig. 5). Force-test results of the twisted and cambered wing with fences located at 0.45, 0.70, and 0.89b/2 are presented in figure 8. Pressure distributions obtained with this fence arrangement show considerable improvement in the chordwise loading over the outboard stations of the twisted and cambered wing at angles of attack above the angle at which the first indication of trailing-edge separation on the upper surface appears on the plain wing (figs. 9(h) to 9(n)). The improved chordwise loading reduced the movement of the centers of pressure of the outboard sections throughout the moderate and upper angle-of-attack range (fig. 13(a)) and extended the section lift curves up to maximum lift of the wing (fig. 10). The smaller improvement at 0.90b/2 relative to that obtained at the other outboard stations can probably be attributed to a localized effect of the fence at 0.89b/2 on the pressure coefficient on both the upper and lower surfaces of the wing at 0.90b/2 (see figs. 9(j) to 9(n)).

Drag Characteristics

The section drag characteristics of the twisted and cambered wing (fig. 11(d)) were obtained from the integration of the pressure distributions and do not include the drag forces due to frictional forces. The data of figure 11(d) indicate the rapid increase in pressure drag over the root sections with an increase in lift which appears to be characteristic of sweptback wings (e.g., ref. 1). This drag is offset somewhat by forward thrust produced over the tip sections throughout a considerable portion of the lift range. At the outermost tip station (0.96b/2) for instance, a thrust force is maintained from a wing lift coefficient of approximately 0.15 to approximately 1.08. This range extends from the angle of attack at which separation from the lower surface is eliminated (approx. $\alpha = 1.7^\circ$) to an angle of attack of 22° which is well beyond the angle of 10° at which the wing lift and pitching moment are first affected by trailing-edge separation. The reduction of suction pressures over the rear part of the section due to the trailing-edge separation would be expected to be beneficial from a pressure-drag standpoint. A comparison of the chordwise pressure distributions (figs. 9(g) to 9(n)) with the pressure-drag curves (fig. 11(d)) indicates that it is not until the trailing-edge separation has moved forward of the point of maximum thickness (0.40x/c) that the pressure drag becomes positive over the tip sections. On the root sections, the lack of peak suction pressures over the forward part of the section and large suction pressures over the rear part of the section contribute to the large values of pressure drag. The forward inclination of the section normal-force vectors due to the wing twist is also a large contributing factor to the low pressure-drag forces over the tip stations as compared to those at the root.

Stalling Characteristics

Plain wing.- The spread of trailing-edge separation outward over the tip stations, as previously indicated, apparently effects the spanwise pressure gradient and produces the beneficial effect on the chordwise pressure-distribution gradient at the $0.10b/2$ and $0.30b/2$ stations. This resulted in an appreciable improvement in lift over station $2y/b = 0.30$ (fig. 10) after the initial tendency of the lift curve at that station to level off in a manner similar to the outboard stations. At an angle of attack of 22° , there was a small localized bubble defined by the pressure diagram near the trailing edge of the $0.30b/2$ station which remained until the angle of attack of maximum wing lift had been reached (figs. 9(k) and 9(l)). At the highest angles of attack attained (31.1°), the region of trailing-edge separation had moved forward to near the leading edge on the outboard stations. Peak pressures remain near the leading edge of the highest angle of attack, however, over the outboard stations but there was a complete breakdown of the pressure diagram over the section at $2y/b = 0.30$. In order to evaluate the direction of tufts in terms of the stalling characteristics of the wing, a line indicating the extent of trailing-edge separation as indicated by approximately zero pressure gradient in the chordwise pressure distribution is superposed on the stall diagrams of figure 14.

At the high angles of attack, the pressure data do not indicate separated flow inboard of the $0.30b/2$ station although the tufts appear to indicate separation on the basis of the preceding concept. The resistance of the inboard stations to stalling can be attributed to the outward drainage of the boundary-layer air from the inboard sections which turns the tufts parallel to the long axis of the wing but prevents separation from occurring. The boundary layer flows outward along the span of the wing which results in a premature thickened boundary layer and probably hastens the onset of trailing-edge separation on the outboard sections. On the basis of the results presented in figure 14, it would appear that although tuft studies are a useful aid in interpreting the stalling characteristics of a sweptback wing, a knowledge of the flow characteristics of the sweptback wing is necessary to prevent misinterpretation of tuft motion.

The initial occurrence of stalling on the midsemispan stations and the spread outboard and forward with an increase in angle of attack is evident in figure 14.

Effect of fences.- The effect of fences on the stalling of the wing as indicated by the pressure distributions can be seen in figure 9. The outward and forward spread of the area of separated flow was delayed to a considerably higher angle of attack on the stations outboard of the fences. There was little significant change in the pressure distribution over the stations located inboard of the fences (0 to $0.30b/2$)

throughout the angle-of-attack range and over the outboard stations at angles of attack less than 11.9° .

The fences interfere with the outward drainage of the boundary-layer air delaying the build-up of a thickened boundary layer and thereby preventing early separation from the rear part of the outboard sections. In addition, the sections outboard of a fence probably benefit from the spanwise drainage of the boundary-layer air in a manner similar to that obtained in the root sections. The build-up of the boundary layer on the inboard side of a fence eventually results in stalling inboard of the fence as indicated by tuft studies (ref. 4) and pressure-distribution measurements (as indicated for the wing of ref. 1). The net effect of the fences on the stability of the wing, therefore, appears to result from a balance of the forces resulting from the improved lift characteristics outboard of the fences and stalling inboard of the fences. These effects would appear to relate the number and location of fences on the wing by which benefits would be obtained (see ref. 4).

The values of section lift coefficient obtained on the inboard stations of the plain wing and all the stations on the wing with fences are considerably higher than might be expected from adjusting two-dimensional maximum-lift characteristics by simple sweep concepts. The three-dimensional effects of sweepback which include a large spanwise variation in the chordwise locations of the section centers of pressure at a particular angle of attack (see figs. 13(a) and 26) make it improbable that any of the sections of the wing are concurrently acting as two-dimensional sections except in coincidental instances. A comparison of the experimental-lift characteristics on a sweptback wing with those estimated from two-dimensional data is presented in reference 9 and indicates experimental maximum section lift coefficients considerably higher than the estimated values over a large part of the span. The analysis presented in reference 9, however, makes it difficult to account for the benefits derived from the installation of fences on the wing discussed in the present report.

Loading Characteristics

The loss in lift loading over the tip sections of the plain wing and the effect on the pitching moment above angles of attack of 9.9° can be seen in figures 15(a) and 15(b). The attendant inboard movement of the spanwise center of pressure with the loss in tip loading is indicated in figure 17. The low values of pressure drag over the tip stations up to angles of attack well beyond the angle at which adverse lift and pitching-moment characteristics occur and the rapid increase of drag over the inboard stations is indicated in figure 15(c). The large improvement in the loading distribution at angles of attack above 9.9° with the fences installed can be seen in figure 16. Figure 17 shows that

there was very little movement of the spanwise centers of pressure through the upper lift range with the fences installed. The large effect of Reynolds number on the tip sections has a considerable effect on the loading distribution at the lower angles (fig. 16).

EFFECT OF CAMBER AND TWIST

Plain wing.- In figures 18, 19, and 21 the lift, drag, and pitching-moment characteristics of the plain twisted and cambered wing as determined from force and pressure-distribution measurements are compared with the corresponding results obtained on the plane wing (ref. 1). The force-test results (fig. 18) show that in the low lift range, the lift-curve slope and the location of the aerodynamic center (slope of pitching-moment curve) were approximately the same for both wings. This would be expected for wings of similar plan form in unseparated flow in this lift range. Camber and twist would be expected to result merely in a change in α_0 and C_{m_0} . At a moderate lift coefficient (approx. 0.30), the lift and pitching-moment curves began to diverge due to the different stalling characteristics of the two wings and showed little similarity at higher lift coefficients. As pointed out in the section on stalling characteristics of the twisted and cambered wing, stalling began over the midsemispan of the wing and spread outward and forward; whereas stalling began on the plane wing over the rear part of the tip sections and spread inboard and forward. The section lift curves of figure 19 indicate that the loss in lift effectiveness over the outboard stations of the plane wing began at an approximately 4° lower angle of attack than for the twisted and cambered wing. The section lift curves also indicate that the initial stalling affected a larger part of the twisted and cambered wing and, when it occurred, the changes in wing lift and pitching-moment curves were accordingly abrupt in comparison with the changes that occurred on the plane wing.

The force tests show that camber and twist resulted in an increase in maximum lift from 1.01 for the plane wing to 1.30 for the twisted and cambered wing at angles of attack of 20° and 27° , respectively. The section lift curves indicate, however, that although considerable camber was incorporated into the twisted and cambered wing, the stalling characteristics were such that there was little increase in section maximum lift coefficient on the outboard stations over that obtained on the plane wing. There appears to be no correlation indicated between the section maximum lift coefficients and the maximum lift coefficient of the wing. From the erratic variation of section lift coefficient over the outboard stations at angles of attack above that at which the section initially reached a maximum, it appears that it would be extremely difficult to predict any maximum-lift characteristics of these wings.

The force-test drag curves (fig. 18(b)) indicate that incorporating camber and twist into the sweptback wing increased the minimum drag coefficient appreciably but that, at the low Mach number of these tests, the drag was significantly reduced through the upper lift range. Inasmuch as a wing of this plan form is designed primarily for high-speed flight, any conclusions as to the effectiveness of twist and camber in improving aircraft performance must necessarily await tests at high speed.

Effect of fences.- The effect of twist and camber with fences installed on the wing can be seen from a comparison of the force-test results presented in figure 20. Upper-surface fences substantially improved the stability characteristics of both the twisted and cambered and the plane wings. Pressure distributions indicate the improved stability to be a result of improved stalling characteristics on the outboard stations of the wing (see section on stalling characteristics and ref. 1). In reference 4 it was shown that although the fences did not completely eliminate the instability of the twisted and cambered wing throughout the lift range, satisfactory stability could be obtained at maximum lift with several of the fence arrangements investigated. None of the fence arrangements tested on the plane wing (ref. 2) resulted in satisfactory stability at maximum lift. It appears, therefore, that fences in combination with twist and camber may result in substantial improvements in the low-speed stability characteristics of high-aspect-ratio sweptback wings having trailing-edge-type separation. The effectiveness of the twisted and cambered wing with fences installed is further indicated in reference 5 where the effects of a horizontal tail on the stability characteristics of the two wings are presented.

Effect of flaps.- The lift, pitching-moment, and lift-distribution characteristics of the plane wing and the twisted and cambered wing with flaps and fences installed are compared in figures 21 to 23. Equal spans of leading-edge flaps and split-type trailing-edge flaps were installed on both wings and the fences were placed at the same spanwise locations. The twist and camber distribution prevented identical flap deflections being obtained on both wings; however, the differences in flap deflection are small and additional geometric details of the flaps and fences installed on the plane wing are presented in reference 2 and on the twisted and cambered wing in figure 5. It should be pointed out that the flap spans and fence locations are not necessarily the optimum for either wing. More detailed investigations of the effects of flaps and fences on the two wings are presented in references 2 and 4.

The force-test data with flaps and fences installed (fig. 21) when compared with the data for the wings without flaps or fences (fig. 18) indicate that the increment in lift due to the flaps is slightly greater for the flaps on the plane wing than for the flaps on the twisted and cambered wing. The flaps and fences on the plane wing resulted in an

increment of maximum lift coefficient of 0.28 as compared to an increment of 0.18 on the twisted and cambered wing. At zero angle of attack, the increments of lift due to the flaps and fences were 0.41 and 0.37 for the plane wing and the twisted and cambered wing, respectively.

The section lift data for the two wings with flaps and fences are presented in figure 22. The section lift-curve slopes are little affected by the twist and camber or the flaps and fences in the lower angle-of-attack range. The increment of section lift coefficient over the inboard stations, which is principally affected by the trailing-edge flaps, is slightly greater for the flaps on the twisted and cambered wing. On the outboard stations, which are primarily affected by the leading-edge flaps, there is very little increment of lift due to the flaps and fences on the twisted and cambered wing which may be due to the large amount of camber incorporated in this wing. The leading-edge flaps on the plane wing produce a slight increment of section lift coefficient on the outboard stations. The increased effectiveness of the trailing-edge flaps and the decreased effectiveness of the leading-edge flaps on the section lift data on the twisted and cambered wing as compared to the effectiveness of the flaps on the plane wing can also be attributed partially to the differences in flap deflection on the two wings.

The variations in stability were greater throughout the lift range with the flaps deflected on the twisted and cambered wing (fig. 21). In the low lift range, the variation of stability on the twisted and cambered wing may be attributed to stalling from the lower surface of the leading-edge flap on the outboard stations; whereas the instability that occurred at high lift coefficients, as indicated from figure 22 and unpublished chordwise pressure distributions, resulted from flow separation over the outboard sections of the wing.

A comparison of the span-load distributions at several angles of attack for the two wings with flaps and fences is made in figure 23. The data have been faired to give integrated values of lift coefficient approximately equal to the force-test lift coefficients obtained at the same angle of attack with the assistance of tuft studies to indicate the stalled areas. The data have then been reduced to a unit loading coefficient for comparison. At the low angle of attack there is a considerable difference in loading due to the flaps and the twist and camber. The differences in loading decrease with angle of attack and at maximum lift the spanwise distribution of the loading is almost identical.

COMPARISON OF EXPERIMENTAL AND CALCULATED LOADINGS

Methods of Solution

In reference 10 the experimental loading on the plane wing is compared with loadings calculated by several methods of solution of loadings on sweptback wings. In figures 24 and 26 the loadings calculated by the methods of Weissinger (as presented in ref. 6) and Multhopp (ref. 7) including the effects of twist and camber are compared with the experimental loadings obtained on the twisted and cambered wing. The method of identifying the solutions set up in reference 10 will be used when referring to specific solutions. For example, the Multhopp 15 x 2 solution refers to a Multhopp solution having two chordwise control points at each of 15 stations distributed along the span of the wing.

Theoretically, the loading on a twisted and cambered wing may be considered to be made up of a basic loading and an additional loading. The additional loading varies only with angle of attack and is the loading obtained on a wing having no twist. The basic loading is independent of angle of attack and corresponds to the zero-lift loading ($C_L = 0$) on a twisted wing and on a wing in which the camber varies from root to tip. The algebraic sum of the basic loading and the additional loading is the total loading. A wing having a constant amount of camber and no twist along the span can be considered as having an additional type of loading with a shift in angle of zero lift which may be considered to be the slope of the section camber line at some specified chordwise location. For the solutions having one chordwise control point this chordwise location is taken to be at the 3/4-chord point inasmuch as both the Weissinger solution and the Multhopp solution having one chordwise control point measure the downwash at the 3/4-chord point. For wings having a spanwise variation in camber such as the wing of this investigation, the variation of slope of the camber line along the 3/4-chord line can be combined with the geometric twist to give an effective twist distribution.

In the Multhopp 15 x 2 solution, the chordwise control points are taken at 0.9045c and 0.3455c. The slope of the camber line at these chordwise points is used in obtaining the effective twist on the twisted and cambered wing.

The loadings calculated by the Weissinger 7 x 1 solution and the Multhopp 15 x 1, 15 x 2, and 23 x 1 solutions are compared with the experimental results obtained on the twisted and cambered wing and on the plane wing in figure 24. The experimental data are presented for an angle of attack of 4.7° for both wings and at an angle of attack of -0.7° for the twisted and cambered wing. At an angle of attack of 4.7°

there is no indication of flow separation on either wing. At an angle of attack of -0.7° , which corresponds to the angle of attack at zero lift of the wing, there is an indication of flow separation from the lower surface of the outermost wing stations of the twisted and cambered wing (fig. 9(c)). This lower surface separation causes a change in section lift-curve slope at the two outermost stations in the angle-of-attack range being considered in the calculations (see fig. 10).

Reference 10 has shown that the Multhopp solutions most accurately predict the shape of the span-loading curve on the plane wing. The excellent agreement between experiment and calculation by the Multhopp solutions may be seen by the comparison with the plane wing data presented in figure 24. The three Multhopp solutions (15×1 , 15×2 , and 23×1) gave practically identical loadings on the plane wing at the lift coefficient presented. The inaccuracy of the Weissinger 7×1 solution in predicting the span loading on the plane wing has been shown in reference 10 to result from the low number of spanwise control points. When the number of spanwise control points was increased to 15, the Weissinger method gave results comparable to those of the Multhopp solutions.

Basic Loading

The basic loading due to the spanwise distribution of twist and camber calculated by the methods having one chordwise control point at $0.75c$ (Weissinger 7×1 and Multhopp 15×1 and 23×1) are in good agreement (fig. 24). The small difference between the Weissinger and Multhopp solutions appears to result from the use of the interpolation function presented in reference 6 for obtaining additional values between the known values of the Weissinger solution.

The use of two chordwise control points alters the basic loading significantly from that obtained by the use of one chordwise control point in the Multhopp solutions. This apparently is a result of the addition of a higher-order sine term in the chordwise loading in the 15×2 solution which accounts for the camber of the section more accurately than the lower-order assumed loading of the solutions having one chordwise control point (ref. 7). The net effect of the Multhopp 15×2 solution on the basic loading of the twisted and cambered wing appears, from figure 24, to be equivalent to a reduction in effective twist as compared to the solutions having one chordwise control point.

The agreement between the calculated basic loadings and the experimental zero-lift loading is very good over a major portion of the span of the twisted and cambered wing, although near the root stations, the calculated values for all methods of solution overestimate the loading while at the $0.96b/2$ station the calculated loading underestimates the experimental value.

██████████

Total Loading

At a lift coefficient of 0.34, the combined additional and basic loadings result in good agreement with the experimental data obtained on the twisted and cambered wing. Although the Multhopp solutions show somewhat better agreement with experiment than the Weissinger solution, all the methods slightly underestimate the loading over the inboard stations and overestimate the loading over the outboard stations.

The effectiveness of the Multhopp methods in predicting the additional loading on both wings can be seen in figure 25. The experimental section lift-curve slopes are taken through the linear portion of the angle-of-attack range where no separation exists on the wing. The good agreement between the experimental lift-curve slopes for the plane wing and the twisted and cambered wing further substantiates the premise on which the calculated methods are based that additional loading is a function of plan form and varies only with angle of attack.

COMPARISON OF CALCULATED AND EXPERIMENTAL WING COEFFICIENTS

The values of the wing lift-curve slope, aerodynamic-center location, angle of attack at zero lift, and pitching-moment coefficient at zero lift calculated by the various methods are tabulated in the following table:

Parameter	Experiment		Calculated twisted and cambered wing			
	Plane wing	Twisted and cambered wing	Multhopp			Weissinger
			15 × 1	15 × 2	23 × 1	7 × 1
$dC_L/d\alpha$. . .	0.069	0.067	0.065	0.066	0.064	0.0620
α_0 , deg . .	0	-0.7	-0.30	-0.79	0.50	0.20
dC_m/dC_L . .	-0.085	-0.087	-0.070	-0.063	-0.082	-0.113
C_{m_0}	0	0.019	0.119	0.018	0.116	0.116

The Multhopp 15 × 2 solution predicts the wing characteristics much better than the solutions having one chordwise control point. The values of lift-curve slope, angle of attack at zero lift, and pitching-moment coefficient at zero lift calculated by the Multhopp 15 × 2 method are all in very good agreement with the experimental results. The angle of attack at zero lift and the pitching-moment coefficient at zero lift

██████████

in particular are predicted considerably closer by the Multhopp 15×2 solution. The agreement of the Multhopp 15×2 solution with experiment can be attributed to the use of two chordwise control points which accounts for the camber of the sections much more accurately than the solutions having one chordwise control point. The angle of attack at zero lift and the pitching-moment coefficient at zero lift of an airfoil section are both determined by camber.

The pitching-moment coefficients at zero lift computed by the methods having one chordwise control point vary appreciably from the experimental results. The experimental data in figure 13 show the section centers of pressure to be considerably behind the local quarter-chord point. Good agreement was obtained between the experimental wing coefficients and the values calculated by the Multhopp 15×2 solution (fig. 26).

CONCLUDING REMARKS

The following remarks may be made in conclusion of an investigation to determine the low-speed longitudinal stability characteristics of a 45° sweptback wing of aspect ratio 8 having twist and cambered airfoil sections:

1. A comparison of the twisted and cambered wing with the plane wing indicates that camber and twist improved the stability characteristics in the lift-coefficient range from 0.25 to 0.7.
2. Twist and camber increased the maximum lift coefficient from 1.01 to 1.30 at angles of attack of approximately 20° and 27° , respectively.
3. Upper-surface fences substantially improved the stability characteristics of both wings by improving the stalling characteristics of the outboard sections of the wing. The twisted and cambered wing in conjunction with the fences, however, had considerably better stability characteristics at maximum lift.
4. Twist and camber resulted in initial stalling occurring in the form of trailing-edge separation on the midspan sections of the wing at a lift coefficient of approximately 0.7. The area of stalled flow spread outward and forward with further increase in lift coefficient.
5. Similar spans of leading-edge and trailing-edge flaps and fence locations resulted in less desirable stability characteristics on the twisted and cambered wing than on the plane wing. The optimum span of

leading- and trailing-edge flaps, however, were not established during the course of the investigation.

6. The loadings calculated by the Multhopp solutions having 15 or 23 spanwise control points are in good agreement with the experimental results where no separation exists on the wing.

7. Leading-edge roughness had an adverse effect on the lifting characteristics of the outboard sections of the twisted and cambered wing which resulted in a lower wing lift-curve slope above a lift coefficient of approximately 0.3 and large variations in stability throughout the lift range.

Langley Aeronautical Laboratory,
National Advisory Committee for Aeronautics,
Langley Field, Va.

REFERENCES

1. Graham, Robert R.: Low-Speed Characteristics of a 45° Sweptback Wing of Aspect Ratio 8 From Pressure Distributions and Force Tests at Reynolds Numbers from 1,500,000 to 4,800,000. NACA RM L51H13, 1951.
2. Pratt, George L., and Shields, E. Rousseau: Low-Speed Longitudinal Characteristics of a 45° Sweptback Wing of Aspect Ratio 8 With High-Lift and Stall-Control Devices at Reynolds Numbers From 1,500,000 to 4,800,000. NACA RM L51J04, 1952.
3. Salmi, Reino J., and Jacques, William A.: Effect of Vertical Location of a Horizontal Tail on the Static Longitudinal Stability Characteristics of a 45° Sweptback-Wing-Fuselage Combination of Aspect Ratio 8 at a Reynolds Number of 4.0×10^6 . NACA RM L51J08, 1952.
4. Salmi, Reino J.: Low-Speed Longitudinal Aerodynamic Characteristics of a Twisted and Cambered Wing of 45° Sweepback and Aspect Ratio 8 With and Without High-Lift and Stall-Control Devices and a Fuselage at Reynolds Numbers From 1.5×10^6 to 4.8×10^6 . NACA RM L52C11, 1952.
5. Foster, Gerald V.: Effects of Twist and Camber, Fences, and Horizontal-Tail Height on the Low-Speed Longitudinal Stability Characteristics of a Wing-Fuselage Combination With a 45° Sweptback Wing of Aspect Ratio 8 at a Reynolds Number of 4.0×10^6 . NACA RM L52J03, 1952.
6. DeYoung, John, and Harper, Charles W.: Theoretical Symmetric Span Loading at Subsonic Speeds for Wings Having Arbitrary Plan Form. NACA Rep. 921, 1948.
7. Multhopp, H.: Methods for Calculating the Lift Distribution of Wings (Subsonic Lifting Surface Theory). Rep. No. Aero 2353, British R.A.E., Jan. 1950.
8. McCullough, George B., and Haire, William M.: Low-Speed Characteristics of Four Cambered, 10-Percent-Thick NACA Airfoil Sections. NACA TN 2177, 1950.
9. Hunton, Lynn W.: Effects of Finite Span on the Section Characteristics of Two 45° Swept-Back Wings of Aspect Ratio 6. NACA RM A52A10, 1952.

10. Schneider, William C.: A Comparison of the Spanwise Loading Calculated by Various Methods With Experimental Loadings Obtained on a 45° Sweptback Wing of Aspect Ratio 8 at a Reynolds Number of 4.0×10^6 . NACA RM L51G30, 1952.

TABLE I.- WING CAMBER-LINE ORDINATES FOR A DESIGN SECTION
LIFT COEFFICIENT OF 1.0.

All values are given in percent of chord

x/c	z/c*	x/c	z/c*
0	0	40	5.310
.5	.262	45	5.407
.75	.369	50	5.428
1.25	.566	55	5.372
2.5	.991	60	5.240
5.0	1.689	65	5.028
7.5	2.256	70	4.733
10	2.731	75	4.350
15	3.496	80	3.861
20	4.070	85	3.257
25	4.525	90	2.490
30	4.874	95	1.522
35	5.132	100	0

$$\left(\frac{z}{c}\right)_{c_{l1}=1} = \frac{1}{1.05} \left[\left(\frac{z}{c}\right)_{a=1} + \frac{1}{6} \left(\frac{z}{c}\right)_{230} \right]$$

$\left(\frac{z}{c}\right)_{a=1}$ ordinates for a mean line of the type $a = 1$; $c_{l1} = 1$.

$\left(\frac{z}{c}\right)_{230}$ ordinates for an NACA 230 series mean line; $c_{l1} = 0.3$.



TABLE II.- AIRFOIL ORDINATES AT ORIFICE LOCATIONS

Orifice location	Airfoil ordinate, $\frac{z}{a}$								
	$\frac{x}{c}$	$\frac{2y}{b} = 0$	$\frac{2y}{b} = 0.03$	$\frac{2y}{b} = 0.10$	$\frac{2y}{b} = 0.30$	$\frac{2y}{b} = 0.55$	$\frac{2y}{b} = 0.75$	$\frac{2y}{b} = 0.90$	$\frac{2y}{b} = 0.96$
Upper surface	0	0	0	0	0	0	0	0	0
	.0010	-----	-----	.0091	.0096	.0103	.0113	.0122	.0127
	.0025	.0117	-----	.0119	.0123	.0131	.0141	.0150	.0154
	.0050	.0149	-----	.0151	.0157	.0165	.0175	.0186	.0191
	.0125	.0220	.0220	.0222	.0227	.0235	.0244	.0254	.0259
	.0250	.0305	.0305	.0307	.0312	.0321	.0331	.0341	.0347
	.0500	.0432	.0433	.0434	.0439	.0448	.0458	.0468	.0473
	.0850	.0565	.0566	.0568	.0573	.0583	.0594	.0606	.0611
	.15	.0738	.0739	.0741	.0748	.0761	.0775	.0790	.0798
	.25	.0896	.0897	.0900	.0909	.0924	.0942	.0960	.0970
	.35	.0969	-----	.0974	.0984	.1000	.1019	.1039	.1049
	.45	-----	.0971	.0974	.0984	.1001	.1020	.1040	.1049
	.50	.0953	-----	-----	-----	-----	-----	-----	-----
	.55	-----	-----	.0915	.0924	.0938	.0955	.0972	.0980
	.65	-----	.0790	.0793	.0802	.0817	.0834	.0852	.0860
.70	.0702	-----	-----	.0628	.0636	.0649	.0664	.0687	
.75	-----	-----	-----	.0429	.0435	.0444	.0455	.0472	
.85	.0426	-----	-----	.0180	.0182	.0187	.0192	.0200	
.95	.0179	.0179	.0179	-----	-----	-----	.0197	-----	
Lower surface	.0125	-.0095	-.0095	-.0094	-.0093	-.0090	-.0088	-.0084	-.0083
	.0375	-.0142	-.0141	-.0141	-.0140	-.0137	-.0134	-.0131	-.0129
	.0750	-.0180	-.0180	-.0179	-.0175	-.0169	-.0162	-.0155	-.0152
	.15	-.0219	-.0218	-.0217	-.0211	-.0203	-.0193	-.0182	-.0178
	.25	-.0232	-----	-.0230	-.0224	-.0214	-.0203	-.0190	-.0184
	.35	-.0230	-.0229 ^a	-.0226	-.0218	-.0205	-.0189	-.0172	-.0164
	.45	-.0186	-----	-.0183	-.0175	-.0160	-.0144	-.0127	-.0119
	.5	-.0127	-----	-.0123	-.0115	-.0100	-.0083	-.0066	-.0057
	.65	-.0055 ^a	-.0054 ^a	-.0052	-.0044	-.0031	-.0016	0	.0008
	.75	.0013	-----	.0016	.0024	.0036	.0050	.0066	.0073
	.85	.0054	-----	.0053	.0061	.0069	.0079	.0089	.0095
	.95	.0047	.0048	.0048	.0051	.0054	.0058	.0063	.0065



^a Pressures measured at these locations with static pressure survey tube.

TABLE III.- VALUES OF EXPERIMENTAL PRESSURE COEFFICIENT
FOR THE TWISTED AND CAMBERED WING

Uncorrected for basic loading due to spanwise variation of tunnel stream angle; $R = 4.0 \times 10^6$

Orifice location		Pressure coefficient, C_p								
	$\frac{x}{c}$	$\frac{2y}{b} = 0$	$\frac{2y}{b} = 0.03$	$\frac{2y}{b} = 0.10$	$\frac{2y}{b} = 0.30$	$\frac{2y}{b} = 0.55$	$\frac{2y}{b} = 0.75$	$\frac{2y}{b} = 0.90$	$\frac{2y}{b} = 0.96$	
$\alpha = -3.5^\circ$										
Upper surface	0	0.22	1.31	1.19	2.92	----	2.23	2.16	1.58	
	.0010	----	----	.70	1.07	1.78	1.17	1.23	1.12	
	.0025	.10	----	.68	.72	1.45	.87	.94	.81	
	.0050	.18	----	.61	.60	.96	.76	.76	.68	
	.0125	.33	.53	.58	.54	.63	.58	.62	.62	
	.0250	.47	.61	.63	.60	.58	.54	.56	.58	
	.0500	.64	.73	.77	.73	.63	.57	.58	.63	
	.0850	.76	.86	.90	.84	.72	.66	.67	.71	
	.15	.92	1.00	1.05	.99	.89	.82	.81	.87	
	.25	1.08	1.14	1.21	1.16	1.06	.99	----	1.03	
	.35	1.19	----	1.30	1.27	1.17	1.11	1.11	1.14	
	.45	----	1.31	1.34	1.31	1.23	1.18	1.19	1.19	
	.50	1.30	----	----	----	----	----	----	----	
	.55	----	----	1.33	1.30	1.25	1.21	1.21	1.21	
	.65	----	1.26	1.29	1.27	1.21	1.21	1.22	1.21	
	.70	1.30	----	----	----	----	----	----	----	
.75	----	----	1.22	1.22	1.18	1.17	1.20	1.19		
.85	1.27	----	1.15	1.16	1.13	1.16	1.19	1.21		
.95	1.20	1.07	1.02	1.04	1.02	1.06	1.07	1.22		
Lower surface	.0125	1.28	2.03	2.30	----	3.34	2.21	1.82	1.53	
	.0357	1.27	1.43	----	1.98	2.45	----	----	1.54	
	.0750	1.26	1.36	1.50	1.67	1.95	2.14	1.79	1.55	
	.15	1.27	1.29	1.55	1.45	1.60	2.07	1.80	1.55	
	.25	1.26	----	1.29	1.35	1.44	1.83	1.84	1.52	
	.35	1.27	1.25 ^a	1.25	1.28	----	1.48	1.84	1.49	
	.45	1.26	----	1.19	1.23	1.22	1.25	1.68	1.48	
	.55	1.21	----	1.12	1.16	1.13	1.13	1.46	1.45	
	.65	1.15	1.08 ^a	1.05	1.08	1.05	1.05	1.26	1.41	
	.75	1.06	----	.96	1.02	1.00	1.00	1.13	1.35	
	.85	.97	----	.93	.97	.95	.96	1.06	1.28	
	.95	.88	.89	.90	.94	.92	.94	1.02	1.43	
	$\alpha = -1.4^\circ$									
	Upper surface	0	0.15	1.02	0.91	1.99	----	2.94	2.59	2.05
		.0010	----	----	.65	.78	1.30	1.21	1.33	1.29
		.0025	.15	----	.62	.64	1.03	.89	.95	.84
.0050		.24	----	.61	.59	.76	.77	.77	.68	
.0125		.40	.58	.64	.59	.60	.56	.62	.62	
.0250		.55	.69	.71	.66	.60	.55	.56	.58	
.0500		.72	.82	.87	.80	.70	.62	.60	.64	
.0850		.84	.95	1.00	.96	.82	.73	.70	.73	
.15		.99	1.08	1.15	1.11	.99	.91	.86	.90	
.25		1.15	1.22	1.29	1.26	1.15	1.07	----	1.08	
.35		1.26	----	1.38	1.36	1.26	1.18	1.16	1.17	
.45		----	1.37	1.40	1.38	1.30	1.24	1.22	1.22	
.50		1.36	----	----	----	----	----	----	----	
.55		----	----	1.38	1.35	1.30	1.25	1.23	1.23	
.65		----	1.35	1.33	1.31	1.25	1.23	1.22	1.21	
.70		1.36	----	----	----	----	----	----	----	
.75	----	----	1.24	1.24	1.20	1.18	1.19	1.17		
.85	1.34	----	1.15	1.16	1.13	1.14	1.16	1.15		
.95	1.20	1.06	1.01	1.03	1.01	1.01	1.03	1.06		
Lower surface	.0125	1.12	1.68	1.83	2.12	2.86	3.01	2.15	1.97	
	.0357	1.16	1.32	1.47	1.67	2.12	----	----	2.00	
	.0750	1.16	1.25	1.35	1.48	1.74	1.86	1.95	2.01	
	.15	1.19	1.21	1.25	1.34	1.48	1.58	1.79	2.08	
	.25	1.19	----	1.22	1.27	1.36	1.38	1.56	1.85	
	.35	1.21	1.21 ^a	1.19	1.23	----	1.27	1.37	1.46	
	.45	1.20	----	1.15	1.18	1.19	1.16	1.21	1.20	
	.55	1.17	----	1.08	1.12	1.11	1.10	1.12	1.11	
	.65	1.11	1.06 ^a	1.02	1.06	1.03	1.04	1.04	1.06	
	.75	1.03	----	.96	1.00	.98	.98	.98	1.03	
	.85	.95	----	.92	.96	.93	.94	.95	1.01	
	.95	.87	.88	.90	.93	.90	.91	.94	1.03	

^aThese pressures measured with static tube.

TABLE III.- VALUES OF EXPERIMENTAL PRESSURE COEFFICIENT FOR THE TWISTED AND CAMBERED WING - Continued.

Uncorrected for basic loading due to spanwise variation of tunnel stream angle; $R = 4.0 \times 10^6$

Orifice location		Pressure coefficient, S								
	$\frac{x}{c}$	$\frac{2y}{b} = 0$	$\frac{2y}{b} = 0.03$	$\frac{2y}{b} = 0.10$	$\frac{2y}{b} = 0.30$	$\frac{2y}{b} = 0.55$	$\frac{2y}{b} = 0.75$	$\frac{2y}{b} = 0.90$	$\frac{2y}{b} = 0.96$	
$\alpha = -0.8^\circ$										
Upper surface	0	0.14	0.98	0.81	1.76	----	2.67	2.61	2.07	
	.0010	----	----	.61	.76	1.14	1.13	1.23	1.24	
	.0025	.17	----	.59	.65	.96	.84	.94	.82	
	.0050	.25	----	.59	.62	.75	.73	.74	.66	
	.0125	.43	.59	.61	.63	.61	.56	.61	.59	
	.025	.58	.71	.73	.70	.61	.55	.56	.57	
	.050	.74	.85	.91	.86	.74	.65	.61	.65	
	.085	.87	.98	1.04	1.00	.86	.76	.72	.75	
	.15	1.01	1.11	1.18	1.15	1.03	.94	.88	.92	
	.25	1.17	1.25	1.32	1.29	1.19	1.10	----	1.09	
	.35	1.28	----	1.40	1.39	1.30	1.21	1.18	1.19	
	.45	----	1.39	1.42	1.40	1.33	1.27	1.24	1.23	
	.50	1.38	----	----	----	----	----	----	----	
	.55	----	----	1.39	1.37	1.33	1.27	1.25	1.24	
	.65	----	1.36	1.34	1.32	1.27	1.25	1.23	1.22	
	.70	1.35	----	----	----	----	----	----	----	
.75	----	----	1.25	1.25	1.21	1.19	1.20	1.17		
.85	1.31	----	1.15	1.16	1.14	.94	1.15	1.14		
.95	1.20	1.06	1.01	1.03	1.01	.97	1.01	1.03		
Lower surface	.0125	1.07	1.58	1.71	1.94	2.73	2.82	2.22	2.00	
	.0375	1.12	1.28	1.44	1.58	2.02	----	----	2.02	
	.075	1.14	1.21	1.30	1.42	1.68	1.76	1.96	2.03	
	.15	1.16	1.18	1.22	1.30	1.45	1.50	1.73	2.14	
	.25	1.17	----	1.20	1.24	1.35	1.35	1.48	1.84	
	.35	1.19	1.19 ^a	1.17	1.21	----	1.26	1.30	1.36	
	.45	1.19	----	1.13	1.17	1.18	1.17	1.18	1.12	
	.55	1.15	----	1.07	1.11	1.10	1.09	1.09	1.05	
	.65	1.10	1.06 ^a	1.01	1.05	1.02	1.04	1.02	1.01	
	.75	1.02	----	.95	.99	.97	.97	.97	.98	
	.85	.94	----	.91	.95	.92	.93	.94	.96	
	.95	.87	.87	.89	.93	.89	.90	.94	.98	
	$\alpha = -0.7^\circ$									
	Upper surface	0	0.13	0.98	0.75	1.71	----	2.60	2.58	2.05
		.0010	----	----	.62	.72	1.11	1.10	1.22	1.22
		.0025	.17	----	.59	.62	.95	.84	.92	.81
.0050		.26	----	.59	.56	.73	.73	.73	.65	
.0125		.43	.61	.62	.62	.62	.56	.62	.59	
.025		.58	.72	.73	.70	.62	.56	.56	.58	
.050		.75	.85	.91	.86	.74	.65	.62	.66	
.085		.87	.98	1.04	1.01	.86	.77	.73	.76	
.15		1.02	1.11	1.19	1.15	1.04	.95	.89	.92	
.25		1.17	1.25	1.32	1.29	1.19	1.11	----	1.10	
.35		1.28	----	1.40	1.39	1.29	1.21	1.18	1.19	
.45		----	1.39	1.42	1.40	1.33	1.27	1.24	1.24	
.50		1.38	----	----	----	----	----	----	----	
.55		----	----	1.39	1.37	1.33	1.27	1.25	1.24	
.65		----	1.36	1.34	1.32	1.26	1.24	1.23	1.22	
.70		1.35	----	----	----	----	----	----	----	
.75	----	----	1.25	1.25	1.21	1.19	1.20	1.17		
.85	1.28	----	1.15	1.16	1.13	1.14	1.15	1.14		
.95	1.22	1.06	1.01	1.03	1.00	1.00	1.01	1.03		
Lower surface	.0125	1.06	1.56	1.68	1.91	2.69	2.77	2.22	1.99	
	.0375	1.11	1.27	1.39	1.56	2.00	----	----	2.00	
	.075	1.13	1.20	1.29	1.41	1.67	1.74	1.94	2.02	
	.15	1.15	1.18	1.22	1.29	1.44	1.48	1.71	2.12	
	.25	1.17	----	1.20	1.24	1.34	1.34	1.41	1.82	
	.35	1.19	1.18 ^a	1.17	1.20	----	1.25	1.29	1.35	
	.45	1.18	----	1.13	1.17	1.18	1.16	1.17	1.12	
	.55	1.15	----	1.07	1.11	1.10	1.09	1.09	1.05	
	.65	1.09	1.05 ^a	1.01	1.05	1.02	1.03	1.02	1.01	
	.75	1.02	----	.95	.99	.97	.97	.96	.98	
	.85	.94	----	.91	.95	.92	.93	.94	.95	
	.95	.87	.87	.89	.93	.89	.90	.93	.98	

^aThese pressures measured with static tube.

TABLE III.- VALUES OF EXPERIMENTAL PRESSURE COEFFICIENT FOR THE
TWISTED AND CAMBERED WING - Continued.Uncorrected for basic loading due to spanwise variation of tunnel stream angle; $R = 4.0 \times 10^6$

Orifice location		Pressure coefficient, S									
	$\frac{x}{c}$	$\frac{2y}{b} = 0$	$\frac{2y}{b} = 0.03$	$\frac{2y}{b} = 0.10$	$\frac{2y}{b} = 0.30$	$\frac{2y}{b} = 0.55$	$\frac{2y}{b} = 0.75$	$\frac{2y}{b} = 0.90$	$\frac{2y}{b} = 0.96$		
$\alpha = -0.6^\circ$											
Upper surface	0	0.13	0.95	0.79	1.66	----	2.51	2.54	2.05		
	.0010	----	----	.62	.71	1.07	1.07	1.19	1.20		
	.0025	.18	----	.57	.62	.90	.75	.86	.81		
	.0050	.27	----	.59	.56	.73	.69	.70	.64		
	.0125	.44	.61	.62	.62	.61	.55	.59	.59		
	.025	.59	.72	.74	.70	.62	.56	.56	.58		
	.050	.76	.86	.92	.87	.75	.65	.62	.66		
	.085	.88	.90	1.05	1.01	.87	.78	.73	.76		
	.15	1.02	1.11	1.19	1.15	1.04	.95	.89	.93		
	.25	1.18	1.33	1.33	1.30	1.20	1.11	----	1.10		
	.35	1.29	----	1.41	1.39	1.30	1.21	1.19	1.19		
	.45	----	1.40	1.42	1.40	1.33	1.27	1.24	1.23		
	.50	1.38	----	----	----	----	----	----	----		
	.55	----	----	1.39	1.37	1.33	1.27	1.24	1.24		
	.65	----	1.37	1.34	1.32	1.26	1.24	1.23	1.22		
.70	1.36	----	----	----	----	----	----	----			
.75	----	----	1.25	1.24	1.21	1.19	1.20	1.17			
.85	1.31	----	1.15	1.16	1.13	1.14	1.15	1.13			
.95	1.20	1.06	1.01	1.02	1.00	1.00	1.00	1.03			
Lower surface	.0125	1.05	1.54	1.65	1.87	2.68	2.73	2.22	1.98		
	.0375	1.11	1.27	1.38	1.54	1.97	----	----	2.00		
	.075	1.12	1.20	1.28	1.39	1.65	1.73	1.93	2.01		
	.15	1.15	1.17	1.21	1.28	1.43	1.47	1.70	2.10		
	.25	1.16	----	1.19	1.23	1.33	1.33	1.45	1.80		
	.35	1.18	1.18 ^a	1.16	1.20	----	1.25	1.29	1.33		
	.45	1.18	----	1.13	1.16	1.17	1.16	1.17	1.11		
	.55	1.15	----	1.07	1.11	1.09	1.09	1.08	1.04		
	.65	1.09	1.05 ^a	1.01	1.05	1.02	1.03	1.01	1.00		
	.75	1.01	----	.95	.99	.96	.97	.96	.97		
	.85	.94	----	.91	.95	.92	.93	.94	.95		
	.95	.87	.87	.89	.93	.89	.90	.93	.97		
	$\alpha = -0.4^\circ$										
	Upper surface	0	0.13	0.90	0.78	1.61	----	2.42	2.54	2.04	
		.0010	----	----	.61	.70	1.04	.94	1.18	1.19	
.0025		.18	----	.57	.62	.89	.78	.86	.81		
.0050		.27	----	.57	.56	.70	.68	.70	.64		
.0125		.45	.62	.63	.62	.62	.56	.59	.59		
.025		.60	.73	.76	.73	.62	.56	.56	.58		
.050		.76	.86	.94	.89	.76	.66	.63	.66		
.085		.88	1.00	1.07	1.03	.88	.79	.74	.76		
.15		1.03	1.12	1.21	1.17	1.06	.97	.90	.93		
.25		1.19	1.26	1.34	1.32	1.21	1.12	----	1.10		
.35		1.29	----	1.42	1.41	1.31	1.22	1.20	1.20		
.45		----	1.41	1.43	1.42	1.34	1.28	1.25	1.24		
.50		1.39	----	----	----	----	----	----	----		
.55		----	----	1.40	1.39	1.34	1.28	1.25	1.24		
.65		----	1.36	1.35	1.33	1.27	1.25	1.23	1.22		
.70	1.36	----	----	----	----	----	----	----			
.75	----	----	1.25	1.25	1.21	1.19	1.20	1.17			
.85	1.31	----	1.16	1.17	1.14	1.14	1.15	1.13			
.95	1.21	1.06	1.01	1.03	1.00	1.00	1.00	1.02			
Lower surface	.0125	1.04	1.52	1.63	1.83	2.67	2.68	2.25	1.99		
	.0375	1.10	1.26	1.37	1.52	1.94	----	----	2.00		
	.075	1.12	1.19	1.27	1.34	1.63	1.71	1.93	2.01		
	.15	1.14	1.16	1.21	1.28	1.42	1.46	1.69	2.09		
	.25	1.16	----	1.18	1.23	1.33	1.33	1.44	1.78		
	.35	1.18	1.17 ^a	1.16	1.20	----	1.24	1.28	1.32		
	.45	1.18	----	1.12	1.16	1.17	1.16	1.16	1.10		
	.55	1.14	----	1.05	1.11	1.10	1.08	1.08	1.04		
	.65	1.09	1.04 ^a	1.01	1.05	1.02	1.03	1.01	.99		
	.75	1.01	----	.95	.99	.97	.97	.96	.97		
	.85	.94	----	.91	.95	.92	.92	.93	.94		
	.95	.86	.87	.89	.93	.89	.90	.93	.97		

^aThese pressures measured with static tube.

TABLE III.- VALUES OF EXPERIMENTAL PRESSURE COEFFICIENT FOR THE TWISTED AND CAMBERED WING - Continued.

Uncorrected for basic loading due to spanwise variation of tunnel stream angle; $R = 4.0 \times 10^6$

Orifice location		Pressure coefficient, S								
	$\frac{x}{c}$	$\frac{2y}{b} = 0$	$\frac{2y}{b} = 0.03$	$\frac{2y}{b} = 0.10$	$\frac{2y}{b} = 0.30$	$\frac{2y}{b} = 0.55$	$\frac{2y}{b} = 0.75$	$\frac{2y}{b} = 0.90$	$\frac{2y}{b} = 0.96$	
$\alpha = 0.6^\circ$										
Upper surface	0	0.09	0.84	0.70	1.33	----	1.95	2.98	2.09	
	.0010	----	----	.61	.65	.88	.87	1.20	1.10	
	.0025	.21	----	.59	.61	.85	.77	.88	.75	
	.0050	.31	----	.59	.60	.68	.72	.72	.63	
	.0125	.49	.69	.70	.68	.62	.56	.59	.57	
	.025	.64	.78	.82	.79	.67	.58	.57	.59	
	.050	.81	.92	1.00	.94	.83	.71	.65	.69	
	.085	.93	1.05	1.13	1.11	.95	.84	.78	.80	
	.15	1.07	1.17	1.26	1.24	1.12	1.03	.95	.97	
	.25	1.22	1.30	1.38	1.37	1.26	1.18	----	1.14	
	.35	1.33	----	1.46	1.45	1.36	1.27	1.23	1.23	
	.45	1.33	1.43	1.46	1.45	1.36	1.32	1.28	1.26	
	.50	1.41	----	----	----	----	----	----	----	
	.55	----	----	1.42	1.41	1.36	1.31	1.28	1.26	
	.65	----	1.39	1.36	1.34	1.29	1.27	1.25	1.23	
	.70	1.38	----	----	----	----	----	----	----	
	.75	----	----	1.26	1.26	1.23	1.20	1.20	1.17	
	.85	1.32	----	1.16	1.17	1.14	1.14	1.14	1.12	
.95	1.21	1.06	1.01	1.03	1.00	.99	.98	1.00		
Lower surface	.0125	.96	1.36	1.44	1.58	2.37	2.58	2.62	2.01	
	.0375	1.04	1.20	1.27	1.41	1.79	----	----	1.99	
	.075	1.07	1.13	1.21	1.30	1.54	1.61	1.86	1.97	
	.15	1.10	1.12	1.16	1.22	1.37	1.40	1.53	1.91	
	.25	1.12	----	1.15	1.19	1.29	1.29	1.35	1.58	
	.35	1.15	1.14 ^a	1.13	1.17	----	1.22	1.23	1.26	
	.45	1.15	----	1.10	1.14	1.15	1.14	1.14	1.10	
	.55	1.12	----	1.05	1.09	1.08	1.07	1.07	1.03	
	.65	1.07	1.02 ^a	1.00	1.04	1.01	1.01	1.01	.97	
	.75	.99	----	.94	.98	.96	.95	.96	.94	
	.85	.93	----	.90	.94	.91	.91	.93	.90	
	.95	.86	.87	.89	.93	.89	.89	.91	.93	
	$\alpha = 1.7^\circ$									
	Upper surface	0	0.08	0.75	0.65	1.00	----	1.53	2.81	2.41
		.0010	----	----	.61	.62	.76	.73	1.00	1.11
		.0025	.25	----	.56	.61	.68	.65	.75	.75
		.0050	.35	----	.63	.64	.65	.61	.60	.64
		.0125	.54	.72	.77	.77	.62	.56	.56	.59
.025		.69	.84	.89	.87	.73	.63	.59	.61	
.050		.86	.97	1.07	.99	.89	.77	.69	.72	
.085		.97	1.10	1.19	1.18	1.02	.91	.83	.84	
.15		1.11	1.21	1.31	1.30	1.18	1.09	1.00	1.01	
.25		1.26	1.34	1.43	1.42	1.32	1.23	1.00	1.18	
.35		1.36	----	1.50	1.50	1.40	1.32	1.27	1.26	
.45		----	1.46	1.50	1.49	1.41	1.35	1.31	1.28	
.50		1.45	----	----	----	----	----	----	----	
.55		----	----	1.45	1.43	1.39	1.34	1.30	1.27	
.65		----	1.41	1.38	1.36	1.31	1.29	1.26	1.24	
.70		1.40	----	----	----	----	----	----	----	
.75		----	----	1.27	1.27	1.24	1.19	1.21	1.17	
.85		1.33	----	1.16	1.17	1.14	1.14	1.14	1.12	
.95	1.21	1.06	1.01	1.02	1.00	.99	.97	.99		
Lower surface	.0125	.89	1.23	1.27	1.37	2.03	2.40	2.92	2.18	
	.0375	.98	1.13	1.18	1.29	1.64	----	----	2.02	
	.075	1.02	1.08	1.14	1.23	1.44	1.50	1.63	1.86	
	.15	1.06	1.08	1.11	1.17	1.31	1.33	1.41	1.56	
	.25	1.09	----	1.11	1.15	1.25	1.25	1.29	1.30	
	.35	1.12	1.11 ^a	1.11	1.14	----	1.19	1.20	1.18	
	.45	1.12	----	1.08	1.12	1.13	1.12	1.12	1.09	
	.55	1.10	----	1.03	1.08	1.08	1.05	1.05	1.03	
	.65	1.05	1.01 ^a	.98	1.02	1.00	1.00	1.00	.96	
	.75	.93	----	.93	.97	.95	.94	.94	.93	
	.85	.91	----	.89	.94	.91	.90	.91	.90	
	.95	.85	.86	.89	.89	.88	.88	.99	.92	

^aThese pressures measured with static tube.

TABLE III.- VALUES OF EXPERIMENTAL PRESSURE COEFFICIENT FOR THE TWISTED AND CAMBERED WING - Continued.

Uncorrected for basic loading due to spanwise variation of tunnel stream angle; $R = 4.0 \times 10^6$

Orifice location		Pressure coefficient, S								
	$\frac{x}{c}$	$\frac{2y}{b} = 0$	$\frac{2y}{b} = 0.03$	$\frac{2y}{b} = 0.10$	$\frac{2y}{b} = 0.30$	$\frac{2y}{b} = 0.55$	$\frac{2y}{b} = 0.75$	$\frac{2y}{b} = 0.90$	$\frac{2y}{b} = 0.96$	
$\alpha = 2.7^\circ$										
Upper surface	0	0.06	0.65	0.59	0.81	----	1.17	2.26	2.99	
	.0010	----	----	.60	.62	.67	.66	.82	1.06	
	.0025	.29	----	.62	.63	.66	.62	.67	.73	
	.0050	.38	----	.71	.73	.66	.61	.57	.64	
	.0125	.59	.77	.85	.87	.70	.62	.57	.59	
	.025	.74	.90	.97	.97	.81	.69	.64	.64	
	.050	.90	1.03	1.15	1.14	.98	.86	.77	.78	
	.085	1.02	1.16	1.25	1.27	1.09	.99	.91	.90	
	.15	1.15	1.26	1.36	1.38	1.24	1.17	1.08	1.07	
	.25	1.30	1.38	1.47	1.49	1.38	1.29	----	1.23	
	.35	1.40	----	1.54	1.55	1.46	1.37	1.33	1.31	
	.45	----	1.49	1.53	1.52	1.46	1.40	1.35	1.31	
	.50	1.47	----	----	----	----	----	----	----	
	.55	----	----	1.47	1.46	1.42	1.37	1.33	1.25	
	.65	----	1.43	1.30	1.38	1.33	1.31	1.27	1.26	
	.70	1.42	----	----	----	----	----	----	----	
	.75	----	----	1.26	1.28	1.25	1.22	1.21	1.18	
.85	1.35	----	1.15	1.17	1.14	1.14	1.13	1.12		
.95	1.20	1.06	1.01	1.02	1.00	.97	.97	.98		
Lower surface	.0125	.82	1.08	1.11	1.17	1.72	1.98	2.81	2.97	
	.0375	.93	1.04	1.08	1.16	1.46	----	----	1.82	
	.075	.97	1.03	1.08	1.14	1.34	1.38	1.47	1.51	
	.15	1.02	1.04	1.07	1.12	1.25	1.26	1.32	1.32	
	.25	1.05	----	1.08	1.11	1.21	1.20	1.23	1.20	
	.35	1.08	1.08 ^a	1.08	1.10	----	1.15	1.17	1.14	
	.45	1.09	----	1.05	1.09	1.12	1.09	1.09	1.07	
	.55	1.07	----	.99	1.06	1.06	1.03	1.04	1.00	
	.65	1.02	.99 ^a	.96	1.00	.99	.98	.98	.95	
	.75	.96	----	.92	.95	.95	.93	.92	.93	
	.85	.90	----	.88	.93	.95	.89	.87	.89	
	.95	.84	.86	.88	.92	.88	.88	.88	.91	
	$\alpha = 4.7^\circ$									
	Upper surface	0	0.05	0.59	0.61	0.59	----	0.76	1.41	1.96
		.0010	----	----	.73	.71	.60	.62	.63	.77
		.0025	.37	----	.78	.83	.63	.62	.62	.63
		.0050	.48	----	.89	.94	.68	.63	.58	.63
.0125		.69	.93	1.06	1.09	.86	.74	.63	.62	
.025		.84	1.03	1.16	1.19	1.01	.84	.75	.72	
.050		1.00	1.15	1.30	1.26	1.17	1.01	.89	.88	
.085		1.11	1.26	1.41	1.45	1.27	1.15	1.04	1.00	
.15		1.23	1.35	1.50	1.53	1.41	1.31	1.20	1.16	
.25		1.37	1.46	1.57	1.60	1.51	1.42	----	1.31	
.35		1.46	----	1.62	1.63	1.56	1.48	1.42	1.37	
.45		----	1.49	1.59	1.59	1.54	1.48	1.42	1.37	
.50		1.53	----	----	----	----	----	----	----	
.55		----	----	1.52	1.51	1.48	1.43	1.38	1.33	
.65		----	1.46	1.42	1.41	1.37	1.35	1.32	1.28	
.70		1.45	----	----	----	----	----	----	----	
.75		----	----	1.29	1.29	1.27	1.25	1.24	1.19	
.85	1.37	----	1.16	1.17	1.15	1.15	1.15	1.12		
.95	1.23	1.03	1.00	1.02	1.00	.99	.97	.97		
Lower surface	.0125	.70	.88	.87	.86	1.31	1.52	2.00	2.20	
	.0375	.83	.92	.93	.96	1.24	----	----	1.57	
	.075	.89	.94	.97	.99	1.19	1.21	1.31	1.36	
	.15	.94	.97	.98	1.01	1.16	1.15	1.21	1.23	
	.25	.98	----	1.01	1.03	1.14	1.13	1.17	1.16	
	.35	1.02	1.02 ^a	1.02	1.04	----	1.10	1.12	1.11	
	.45	1.04	----	1.00	1.04	1.07	1.06	1.06	1.05	
	.55	1.02	----	.97	1.01	1.02	1.01	1.02	1.00	
	.65	.98	.94 ^a	.93	.98	.96	.97	.96	.95	
	.75	.93	----	.90	.93	.93	.92	.92	.92	
	.85	.88	----	.87	.91	.89	.88	.88	.88	
	.95	.82	.84	.87	.91	.87	.87	.87	.90	

^aThese pressures measured with static tube

NACA

TABLE III.- VALUES OF EXPERIMENTAL PRESSURE COEFFICIENT FOR THE
TWISTED AND CAMBERED WING - Continued.Uncorrected for basic loading due to spanwise variation of tunnel stream angle; $R = 4.0 \times 10^6$

Orifice location		Pressure coefficient, S								
	$\frac{x}{c}$	$\frac{2y}{b} = 0$	$\frac{2y}{b} = 0.03$	$\frac{2y}{b} = 0.10$	$\frac{2y}{b} = 0.30$	$\frac{2y}{b} = 0.55$	$\frac{2y}{b} = 0.75$	$\frac{2y}{b} = 0.90$	$\frac{2y}{b} = 0.96$	
$\alpha = 6.8^\circ$										
Upper surface	0	0.05	0.53	0.72	0.62	----	0.61	0.83	1.19	
	.0010	----	----	1.02	1.10	.78	.74	.59	.63	
	.0025	.47	----	1.04	1.25	.87	.81	.63	.64	
	.0050	.58	----	1.18	1.36	.95	.89	.71	.67	
	.0125	.81	1.09	1.31	1.42	1.17	.98	.81	.76	
	.025	.95	1.17	1.36	1.48	1.25	1.08	.94	.88	
	.050	1.10	1.28	1.49	1.48	1.41	1.24	1.09	1.05	
	.085	1.20	1.38	1.57	1.68	1.47	1.36	1.22	1.16	
	.15	1.31	1.45	1.63	1.72	1.60	1.50	1.38	1.30	
	.25	1.45	1.54	1.68	1.76	1.67	1.57	1.43	1.43	
	.35	1.53	----	1.70	1.75	1.68	1.60	1.54	1.47	
	.45	----	1.61	1.65	1.68	1.63	1.56	1.52	1.45	
	.50	1.59	----	----	----	----	----	----	----	
	.55	----	----	1.56	1.56	1.55	1.51	1.45	1.39	
	.65	----	1.50	1.45	1.45	1.42	1.40	1.37	1.32	
	.70	1.49	----	----	----	----	----	----	----	
	.75	----	----	1.31	1.32	1.30	1.29	1.28	1.22	
.85	1.39	----	1.16	1.18	1.16	1.17	1.17	1.14		
.95	1.23	1.05	1.00	1.01	1.01	1.00	.98	.98		
Lower surface	.0125	.57	.69	.68	.65	.96	1.09	1.40	1.57	
	.0375	.72	.79	.79	.79	1.03	1.03	1.10	1.33	
	.075	.79	.84	.85	.86	1.04	1.04	1.14	1.21	
	.15	.86	.89	.90	.91	1.06	1.04	1.10	1.15	
	.25	.91	----	.94	.95	1.07	1.05	1.09	1.12	
	.35	.96	.95 ^a	.96	.98	----	1.05	1.08	1.09	
	.45	.97	----	.95	.98	1.03	1.02	1.03	1.05	
	.55	.96	----	.92	.97	.99	.97	1.00	1.01	
	.65	.93	.90 ^a	.90	.94	.97	.94	.95	.96	
	.75	.88	----	.86	.91	.91	.89	.91	.93	
	.85	.84	----	.84	.89	.87	.86	.88	.90	
	.95	.79	.82	.86	.89	.86	.85	.87	.92	
	$\alpha = 9.9^\circ$									
	Upper surface	0	0.21	0.56	1.11	1.09	----	0.84	0.59	0.64
		.0010	----	----	1.55	1.97	1.33	1.33	.92	.70
		.0025	.67	----	1.61	2.08	1.44	1.34	1.06	.86
		.0050	.77	----	1.72	2.12	1.53	1.39	1.15	.99
.0125		1.01	1.41	1.77	2.02	1.72	1.47	1.25	1.13	
.025		1.13	1.44	1.77	1.99	1.74	1.53	1.36	1.25	
.050		1.26	1.50	1.81	1.93	1.80	1.63	1.48	1.31	
.085		1.35	1.57	1.83	2.02	1.81	1.70	1.57	1.47	
.15		1.44	1.60	1.84	1.99	1.86	1.79	1.67	1.57	
.25		1.57	1.67	1.85	1.95	1.86	1.80	1.67	1.65	
.35		1.64	----	1.82	1.87	1.82	1.78	1.73	1.65	
.45		----	1.69	1.73	1.76	1.72	1.72	1.68	1.59	
.50		1.66	----	----	----	----	----	----	----	
.55		----	----	1.62	1.62	1.61	1.59	1.56	1.51	
.65		----	1.54	1.49	1.48	1.44	1.46	1.45	1.42	
.70		1.54	----	----	----	----	----	----	----	
.75		----	----	1.32	1.38	1.30	1.32	1.34	1.30	
.85	1.41	----	1.14	1.13	1.14	1.17	1.21	1.22		
.95	1.24	1.05	1.00	1.03	.99	.98	.99	1.05		
Lower surface	.0125	.40	.51	.52	.54	.62	.64	.78	.92	
	.0375	.57	.63	.62	.61	.75	----	----	1.00	
	.075	.66	.70	.71	.70	.82	.81	.91	1.02	
	.15	.74	.77	.73	.78	.90	.87	.95	1.04	
	.25	.80	----	.84	.85	.94	.92	.98	1.06	
	.35	.86	.85 ^a	.87	.89	----	.94	.99	1.06	
	.45	.88	----	.88	.89	.97	.93	.97	1.04	
	.55	.88	----	.87	.92	.95	.90	.95	1.01	
	.65	.97	.85 ^a	.85	.90	.93	.88	.92	.97	
	.75	.83	----	.83	.88	.88	.85	.88	.96	
	.85	.80	----	.82	.88	.87	.82	.86	.93	
	.95	.76	.80	.85	.90	.85	.82	.86	.97	

^aThese pressures measured with static tube.

TABLE III.- VALUES OF EXPERIMENTAL PRESSURE COEFFICIENT FOR THE
TWISTED AND CAMBERED WING - ContinuedUncorrected for basic loading due to spanwise variation of tunnel stream angle; $R = 4.0 \times 10^6$

Orifice location		Pressure coefficient, S								
	$\frac{x}{b}$	$\frac{z}{b} = 0$	$\frac{z}{b} = 0.03$	$\frac{z}{b} = 0.10$	$\frac{z}{b} = 0.30$	$\frac{z}{b} = 0.55$	$\frac{z}{b} = 0.75$	$\frac{z}{b} = 0.90$	$\frac{z}{b} = 0.96$	
$\alpha = 11.9^\circ$										
Upper surface	0	0.16	0.65	1.58	1.68	----	1.34	0.76	0.62	
	.0010	----	----	2.03	2.67	1.86	1.78	1.37	.99	
	.0025	.80	----	2.08	2.69	1.94	1.81	1.46	1.20	
	.0050	.89	----	2.15	2.63	2.06	1.81	1.47	1.30	
	.0125	1.13	1.65	2.17	2.43	2.06	1.91	1.55	1.38	
	.025	1.24	1.63	2.05	2.31	2.04	1.84	1.65	1.48	
	.050	1.37	1.65	2.02	2.16	2.05	1.88	1.71	1.60	
	.085	1.44	1.69	2.00	2.20	2.02	1.91	1.76	1.63	
	.15	1.51	1.69	1.95	2.10	2.03	1.96	1.82	1.69	
	.25	1.63	1.74	1.91	2.02	1.98	1.92	---	1.73	
	.35	1.69	---	1.88	1.94	1.87	1.86	1.82	1.70	
	.45	---	1.74	1.78	1.79	1.76	1.76	1.73	1.63	
	.50	1.70	---	---	---	---	---	---	---	
	.55	---	---	1.64	1.61	1.61	1.62	1.58	1.53	
	.65	---	1.57	1.49	1.42	1.41	1.47	1.47	1.42	
	.70	1.56	---	---	---	---	---	---	---	
.75	---	---	1.31	1.23	1.24	1.30	1.34	1.30		
.85	1.42	---	1.14	1.12	1.10	1.13	1.19	1.21		
.95	1.24	1.03	1.03	1.11	1.06	1.00	.98	1.04		
Lower surface	.0125	.31	.44	.51	.58	.59	.54	.61	.71	
	.0375	.49	.55	.55	.55	.68	---	---	.85	
	.075	.58	.62	.63	.63	.77	.73	.81	.87	
	.15	.67	.70	.71	.72	.87	.82	.88	.97	
	.25	.74	---	.78	.80	.93	.88	.93	1.02	
	.35	.90	.79 ^a	.82	.85	---	.91	.95	1.03	
	.45	.83	---	.83	.86	.95	.91	.94	1.02	
	.55	.83	---	.83	.89	.94	.90	.94	1.01	
	.65	.82	.83 ^a	.82	.89	.92	.88	.91	.97	
	.75	.79	---	.81	.88	.89	.86	.88	.96	
	.85	.76	---	.91	.88	.97	.84	.86	.94	
	.95	.74	.78	.95	.92	.87	.85	.87	.98	
	$\alpha = 13.9^\circ$									
	Upper surface	0	0.25	0.89	2.15	2.53	----	1.85	1.10	0.76
		.0010	----	----	2.61	3.56	2.46	2.32	1.84	1.35
		.0025	.94	----	2.69	3.49	2.52	2.28	1.89	1.49
.0050		1.03	----	2.69	3.29	2.59	2.23	1.85	1.56	
.0125		1.26	1.89	2.58	2.91	2.52	2.11	1.81	1.64	
.025		1.35	1.81	2.36	2.69	2.36	2.11	1.88	1.71	
.050		1.47	1.91	2.23	2.46	2.29	2.09	1.91	1.78	
.085		1.53	1.80	2.18	2.42	2.17	2.08	1.92	1.78	
.15		1.58	1.79	2.08	2.27	2.12	2.07	1.95	1.79	
.25		1.70	1.81	2.01	2.13	2.01	1.98	---	1.80	
.35		1.74	---	1.94	2.00	1.89	1.87	1.86	1.75	
.45		---	1.77	1.82	1.82	1.71	1.74	1.75	1.65	
.50		1.74	---	---	---	---	---	---	---	
.55		---	---	1.67	1.59	1.50	1.57	1.59	1.54	
.65		---	1.58	1.50	1.36	1.26	1.38	1.45	1.42	
.70		1.58	---	---	---	---	---	---	---	
.75	---	---	1.32	1.22	1.17	1.18	1.30	1.29		
.85	1.43	---	1.15	1.19	1.15	1.08	1.13	1.19		
.95	1.24	1.06	1.07	1.21	1.16	1.06	.99	1.03		
Lower surface	.0125	.23	.43	.55	.71	.60	.51	.54	.60	
	.0375	.41	.48	.50	.51	.62	---	---	.75	
	.075	.51	.55	.57	.57	.70	.67	.74	.84	
	.15	.60	.63	.64	.67	.81	.77	.82	.92	
	.25	.68	---	.72	.75	.88	.84	.89	.98	
	.35	.74	.74 ^a	.77	.81	---	.89	.92	1.01	
	.45	.78	---	.79	.85	.94	.90	.92	1.01	
	.55	.79	---	.79	.87	.94	.89	.92	1.00	
	.65	.78	.75 ^a	.79	.87	.91	.88	.91	.98	
	.75	.76	---	.78	.87	.90	.86	.88	.97	
	.85	.74	---	.79	.89	.91	.85	.87	.95	
	.95	.72	.76	.84	.95	.91	.87	.87	.99	

^a These pressures measured with static tube.

NACA

TABLE III.- VALUES OF EXPERIMENTAL PRESSURE COEFFICIENT FOR THE TWISTED AND CAMBERED WING - Continued.

Uncorrected for basic loading due to spanwise variation of tunnel stream angle; $R = 4.0 \times 10^6$

Orifice location		Pressure coefficient, S								
	$\frac{x}{c}$	$\frac{2y}{b} = 0$	$\frac{2y}{b} = 0.03$	$\frac{2y}{b} = 0.10$	$\frac{2y}{b} = 0.30$	$\frac{2y}{b} = 0.55$	$\frac{2y}{b} = 0.75$	$\frac{2y}{b} = 0.90$	$\frac{2y}{b} = 0.96$	
$\alpha = 17.0^\circ$										
Upper surface	0	0.44	1.31	3.21	4.21	---	2.84	1.76	1.13	
	.0010	---	---	3.70	5.23	3.63	3.18	2.51	1.92	
	.0025	1.21	---	3.72	4.88	3.72	3.01	2.47	1.98	
	.0050	1.29	---	3.64	4.49	3.61	2.92	2.30	1.96	
	.0125	1.51	2.35	3.37	3.72	3.23	2.57	2.24	1.99	
	.025	1.56	2.16	2.83	3.37	2.86	2.48	2.18	2.00	
	.050	1.65	2.07	2.64	2.93	2.62	2.35	2.14	1.99	
	.085	1.69	2.01	2.48	2.82	2.43	2.25	2.07	1.95	
	.15	1.72	1.95	2.30	2.54	2.28	2.14	2.02	1.88	
	.25	1.81	1.92	2.15	2.29	2.05	1.94	---	1.82	
	.35	1.84	---	2.04	2.08	1.81	1.74	1.76	1.71	
	.45	---	1.84	1.89	1.81	1.50	1.48	1.57	1.57	
	.50	1.82	---	---	---	---	---	---	---	
	.55	---	---	1.71	1.52	1.30	1.25	1.34	1.43	
	.65	---	1.62	1.52	1.34	1.27	1.21	1.17	1.29	
	.70	1.61	---	---	---	---	---	---	---	
.75	---	---	1.30	1.32	1.27	1.21	1.12	1.14		
.85	1.45	---	1.18	1.34	1.28	1.20	1.11	1.08		
.95	1.26	1.07	1.15	1.38	1.29	1.21	1.09	1.05		
Lower surface	.0125	.13	.49	.74	1.06	.73	.52	.54	.55	
	.0375	.29	.39	.46	.54	.56	---	---	.65	
	.075	.39	.45	.48	.52	.62	.59	.66	.76	
	.15	.50	.53	.55	.59	.73	.69	.76	.87	
	.25	.58	---	.62	.67	.82	.79	.85	.96	
	.35	.65	.65 ^a	.68	.74	---	.85	.90	1.00	
	.45	.69	---	.71	.79	.91	.88	.91	1.01	
	.55	.71	---	.73	.81	.92	.89	.93	1.01	
	.65	.71	.70 ^a	.74	.83	.91	.89	.93	.99	
	.75	.70	---	.74	.85	.91	.88	.91	.98	
	.85	.69	---	.76	.88	.92	.88	.91	.97	
	.95	.68	.73	.82	.96	.95	.93	.93	1.02	
	$\alpha = 22.0^\circ$									
	Upper surface	0	0.78	2.39	5.57	8.24	---	4.01	2.76	1.87
		.0010	---	---	5.94	8.80	5.44	3.98	3.30	2.70
		.0025	1.67	---	5.88	8.07	5.42	3.65	3.08	2.59
.0050		1.72	---	5.57	6.83	5.08	3.54	2.84	2.44	
.0125		1.91	3.25	4.68	5.43	3.90	2.86	2.61	2.38	
.025		1.91	2.75	3.83	4.68	3.51	2.67	2.44	2.28	
.050		1.94	2.53	3.36	3.80	3.01	2.38	2.24	2.12	
.085		1.93	2.35	3.02	3.52	2.59	2.13	2.05	2.00	
.15		1.91	2.19	2.67	2.99	2.14	1.77	1.85	1.79	
.25		1.97	2.10	2.39	2.53	1.57	1.37	---	1.57	
.35		1.97	---	2.20	2.14	1.46	1.32	1.26	1.31	
.45		---	1.95	2.00	1.72	1.46	1.31	1.22	1.18	
.50		1.91	---	---	---	---	---	---	---	
.55		---	---	1.79	1.57	1.47	1.30	1.21	1.16	
.65		---	1.70	1.55	1.50	1.47	1.30	1.21	1.16	
.70		1.67	---	---	---	---	---	---	---	
.75	---	---	1.43	1.62	1.50	1.30	1.20	1.16		
.85	1.48	---	1.31	1.77	1.50	1.29	1.20	1.17		
.95	1.17	1.03	1.20	1.54	1.45	1.29	1.19	1.17		
Lower surface	.0125	.03	.82	1.37	2.09	1.13	.53	.65	.60	
	.0375	.14	.32	.51	.57	.57	---	---	.56	
	.075	.23	.32	.40	.50	.53	.50	.56	.67	
	.15	.34	.39	.43	.48	.62	.60	.67	.79	
	.25	.42	---	.50	.55	.71	.71	.77	.90	
	.35	.49	.52 ^a	.55	.62	---	.79	.84	.96	
	.45	.55	---	.59	.68	.85	.83	.87	.99	
	.55	.58	---	.62	.73	.88	.86	.91	1.00	
	.65	.59	.59 ^a	.64	.76	.89	.87	.91	.99	
	.75	.59	---	.66	.80	.91	.88	.91	.99	
	.85	.59	---	.68	.86	.93	.89	.92	.98	
	.95	.60	.65	.75	.99	1.00	.95	.96	1.06	

^aThese pressures measured with static tube.

TABLE III.- VALUES OF EXPERIMENTAL PRESSURE COEFFICIENT FOR THE
TWISTED AND CAMBERED WING - Continued.

Uncorrected for basic loading due to spanwise variation of tunnel stream angle; $R = 4.0 \times 10^6$

Orifice location		Pressure coefficient, S								
	$\frac{x}{c}$	$\frac{2y}{b} = 0$	$\frac{2y}{b} = 0.03$	$\frac{2y}{b} = 0.10$	$\frac{2y}{b} = 0.30$	$\frac{2y}{b} = 0.55$	$\frac{2y}{b} = 0.75$	$\frac{2y}{b} = 0.90$	$\frac{2y}{b} = 0.96$	
$\alpha = 25.1^\circ$										
Upper surface	0	1.09	3.19	7.39	11.56	----	4.11	3.33	2.37	
	.0010	-----	-----	7.59	11.61	5.14	3.88	3.71	3.18	
	.0025	2.00	-----	7.48	10.40	5.10	3.58	3.42	2.91	
	.0050	2.82	-----	7.00	8.53	4.66	3.32	3.05	2.69	
	.0125	2.18	-----	5.66	6.84	3.39	2.67	2.73	2.54	
	.025	2.11	3.97	4.52	5.60	2.85	2.44	2.45	2.36	
	.050	2.11	3.17	3.82	4.72	2.09	2.07	2.20	2.12	
	.085	2.08	2.55	3.35	3.98	1.69	1.71	1.93	1.94	
	.15	2.02	2.33	2.89	3.28	1.63	1.44	1.58	1.62	
	.25	2.06	2.20	2.53	2.67	1.60	1.42	-----	1.31	
	.35	2.03	-----	2.30	2.17	1.57	1.41	1.29	1.24	
	.45	-----	2.02	2.06	1.84	1.57	1.40	1.28	1.24	
	.50	1.96	-----	-----	-----	-----	-----	-----	-----	
	.55	-----	-----	1.85	1.77	1.57	1.39	1.27	1.24	
	.65	-----	1.74	1.67	1.72	1.58	1.39	1.27	1.24	
	.70	1.70	-----	-----	-----	-----	-----	-----	-----	
	.75	-----	-----	1.52	1.95	1.59	1.38	1.27	1.24	
.85	1.48	-----	1.34	2.42	1.57	1.37	1.27	1.25		
.95	1.21	.99	1.16	1.88	1.53	1.35	1.26	1.26		
Lower surface	.0125	.01	1.16	1.95	2.94	1.20	.67	.75	.68	
	.0375	.08	.33	.62	.94	.56	-----	-----	.53	
	.075	.16	.27	.39	.54	.49	.48	.52	.62	
	.15	.25	.31	.37	.44	.57	.57	.63	.74	
	.25	.34	-----	.43	.49	.67	.68	.73	.86	
	.35	.41	-----	.48	.55	-----	.76	.81	.93	
	.45	.47	-----	.52	.61	.82	.81	.86	.97	
	.55	.50	-----	.55	.66	.86	.84	.90	.98	
	.65	.52	-----	.58	.71	.88	.86	.91	.98	
	.75	.53	-----	.60	.75	.92	.88	.92	.98	
	.85	.54	-----	.63	.84	.94	.89	.94	.99	
	.95	.55	.61	.71	1.05	1.03	.96	.99	1.08	
	$\alpha = 26.1^\circ$									
	Upper surface	0	1.21	3.57	8.08	12.77	----	4.38	3.49	2.54
		.0010	-----	-----	8.18	12.63	4.55	4.04	3.75	3.23
		.0025	2.12	-----	8.08	11.06	4.57	3.71	3.45	2.99
		.0050	2.12	-----	7.60	9.10	4.09	3.24	3.06	2.71
.0125		2.26	4.07	6.00	7.03	2.78	2.70	2.71	2.56	
.025		2.18	3.31	4.76	5.81	2.20	2.42	2.41	2.39	
.050		2.16	2.92	3.99	4.78	1.77	1.97	2.13	2.12	
.085		2.13	2.62	3.45	4.12	1.71	1.63	1.82	1.91	
.15		2.06	2.39	2.96	3.38	1.71	1.49	1.46	1.56	
.25		2.09	2.23	2.58	2.22	1.68	1.47	-----	1.31	
.35		2.06	-----	2.33	1.94	1.67	1.44	1.33	1.29	
.45		-----	2.05	2.09	1.88	1.65	1.42	1.33	1.30	
.50		1.97	-----	-----	-----	-----	-----	-----	-----	
.55		-----	-----	1.87	1.83	1.65	1.42	1.32	1.30	
.65		-----	1.74	1.70	2.21	1.64	1.42	1.32	1.30	
.70		1.71	-----	-----	-----	-----	-----	-----	-----	
.75		-----	-----	1.55	2.86	1.62	1.41	1.32	1.30	
.85	1.48	-----	1.34	1.90	1.59	1.41	1.31	1.31		
.95	1.20	.98	1.14	1.62	1.56	1.38	1.30	1.31		
Lower surface	.0125	.01	1.30	2.17	3.23	1.14	.72	.79	.72	
	.0375	.06	.34	.66	1.01	.56	-----	-----	.53	
	.075	.14	.25	.39	.54	.50	.47	.52	.61	
	.15	.23	.28	.35	.42	.58	.55	.62	.74	
	.25	.31	-----	.40	.46	.67	.72	.73	.86	
	.35	.38	.41 ^a	.45	.52	-----	.78	.81	.93	
	.45	.44	-----	.49	.58	.81	.79	.86	.97	
	.55	.47	-----	.53	.63	.85	.85	.89	.99	
	.65	.49	.50 ^a	.56	.67	.87	.86	.91	.99	
	.75	.50	-----	.58	.71	.91	.88	.92	.99	
	.85	.52	-----	.61	.79	.94	.89	.94	1.00	
	.95	.54	.51	.69	1.00	1.02	.97	1.00	1.10	

These pressures measured with static tube.

TABLE III.- VALUES OF EXPERIMENTAL PRESSURE COEFFICIENT FOR THE TWISTED AND CAMBERED WING - Continued.

Uncorrected for basic loading due to spanwise variation of tunnel stream angle; $R = 4.0 \times 10^6$

Orifice location		Pressure coefficient, S								
	$\frac{x}{c}$	$\frac{2y}{b} = 0$	$\frac{2y}{b} = 0.03$	$\frac{2y}{b} = 0.10$	$\frac{2y}{b} = 0.30$	$\frac{2y}{b} = 0.55$	$\frac{2y}{b} = 0.75$	$\frac{2y}{b} = 0.90$	$\frac{2y}{b} = 0.96$	
$\alpha = 27.1^\circ$										
Upper surface	0	1.33	3.85	8.65	6.11	----	6.75	5.11	3.47	
	.0010	----	----	8.68	4.56	4.07	5.98	5.11	4.17	
	.0025	2.24	----	8.53	3.59	4.12	5.14	4.58	3.65	
	.0050	2.22	----	8.00	3.19	3.79	4.54	3.97	2.96	
	.0125	2.35	4.23	6.28	2.87	2.73	3.83	3.42	2.97	
	.025	2.24	3.44	4.94	2.86	2.37	3.43	2.97	2.70	
	.050	2.21	3.08	4.11	3.31	2.01	2.89	2.53	2.31	
	.085	2.17	3.08	3.56	2.89	1.83	2.48	2.10	1.99	
	.15	2.09	2.42	3.02	2.89	1.82	2.13	1.71	1.58	
	.25	2.11	2.26	2.62	2.81	1.78	1.92	----	1.41	
	.35	2.07	----	2.36	2.66	1.76	1.84	1.51	1.39	
	.45	----	2.07	2.13	2.53	1.76	1.80	1.49	1.38	
	.50	1.98	----	----	----	----	----	----	----	
	.55	----	----	1.90	2.37	1.76	1.79	1.48	1.37	
	.65	----	1.76	1.78	2.22	1.73	1.79	1.47	1.37	
	.70	1.72	----	----	----	----	----	----	----	
.75	----	----	1.64	2.08	1.69	1.78	1.45	1.36		
.85	1.50	----	1.43	1.91	1.65	1.74	1.44	1.37		
.95	1.22	.99	1.21	1.78	1.59	1.62	1.40	1.35		
Lower surface	.0125	.01	1.42	2.35	1.64	1.10	1.08	1.10	.88	
	.0375	.04	.35	.70	.57	.60	----	----	.52	
	.075	.11	.23	.38	.38	.55	.47	.48	.58	
	.15	.20	.26	.25	.39	.62	.52	.57	.70	
	.25	.28	----	.37	.47	.69	.62	.68	.83	
	.35	.35	.39 ^a	.43	.55	----	.70	.77	.91	
	.45	.41	----	.48	.63	.82	.75	.83	.96	
	.55	.45	----	.52	.69	.85	.79	.88	.98	
	.65	.47	.49 ^a	.55	.75	.87	.82	.90	.99	
	.75	.49	----	.59	.81	.89	.85	.92	1.00	
	.85	.51	----	.62	.90	.92	.88	.95	1.01	
	.95	.54	.60	.71	1.09	1.00	.99	1.03	1.12	
	$\alpha = 29.1^\circ$									
	Upper surface	0	1.53	4.60	9.88	4.13	----	7.12	5.13	3.63
		.0010	----	----	9.75	3.01	4.17	6.13	4.92	4.22
		.0025	2.43	----	9.60	2.87	4.17	5.09	4.34	3.66
.0050		2.41	----	8.96	2.80	3.84	4.54	3.69	2.90	
.0125		2.48	4.59	6.87	2.68	2.69	3.73	3.14	2.86	
.025		2.37	3.70	5.35	2.69	2.36	3.28	2.65	2.52	
.050		2.32	3.17	4.40	2.74	2.07	2.75	2.15	2.05	
.085		2.26	2.80	3.75	2.72	1.89	2.41	1.79	1.69	
.15		2.16	2.51	3.17	2.71	1.87	2.18	1.64	1.51	
.25		2.16	2.28	2.73	2.65	1.82	2.05	----	1.48	
.35		2.12	----	2.49	2.57	1.82	2.00	1.58	1.47	
.45		----	2.17	2.30	2.51	1.82	1.97	1.56	1.46	
.50		2.07	----	----	----	----	----	----	----	
.55		----	----	2.07	2.41	1.82	1.95	1.54	1.45	
.65		----	1.89	2.04	2.30	1.79	1.94	1.53	1.44	
.70		1.88	----	----	----	----	----	----	----	
.75	----	----	1.88	2.16	1.75	1.90	1.53	1.43		
.85	1.70	----	1.61	1.99	1.71	1.81	1.50	1.43		
.95	1.37	1.09	1.38	1.94	1.64	1.67	1.45	1.41		
Lower surface	.0125	.04	1.75	2.80	1.47	1.18	1.18	.82	.94	
	.0375	.03	.40	.80	.62	.62	----	----	.53	
	.075	.08	.23	.41	.39	.51	.46	.47	.58	
	.15	.17	.24	.32	.40	.59	.49	.56	.70	
	.25	.25	----	.36	.46	.72	.58	.67	.82	
	.35	.32	.36 ^a	.41	.55	----	.65	.76	.91	
	.45	.38	----	.47	.63	.81	.72	.82	.96	
	.55	.43	----	.51	.70	.84	.76	.87	.99	
	.65	.46	.47 ^a	.56	.76	.86	.80	.90	.99	
	.75	.48	----	.60	.83	.89	.83	.92	1.01	
	.85	.52	----	.65	.93	.92	.87	.95	1.02	
	.95	.56	.63	.77	1.14	1.02	.99	1.04	1.14	

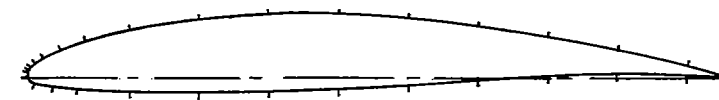
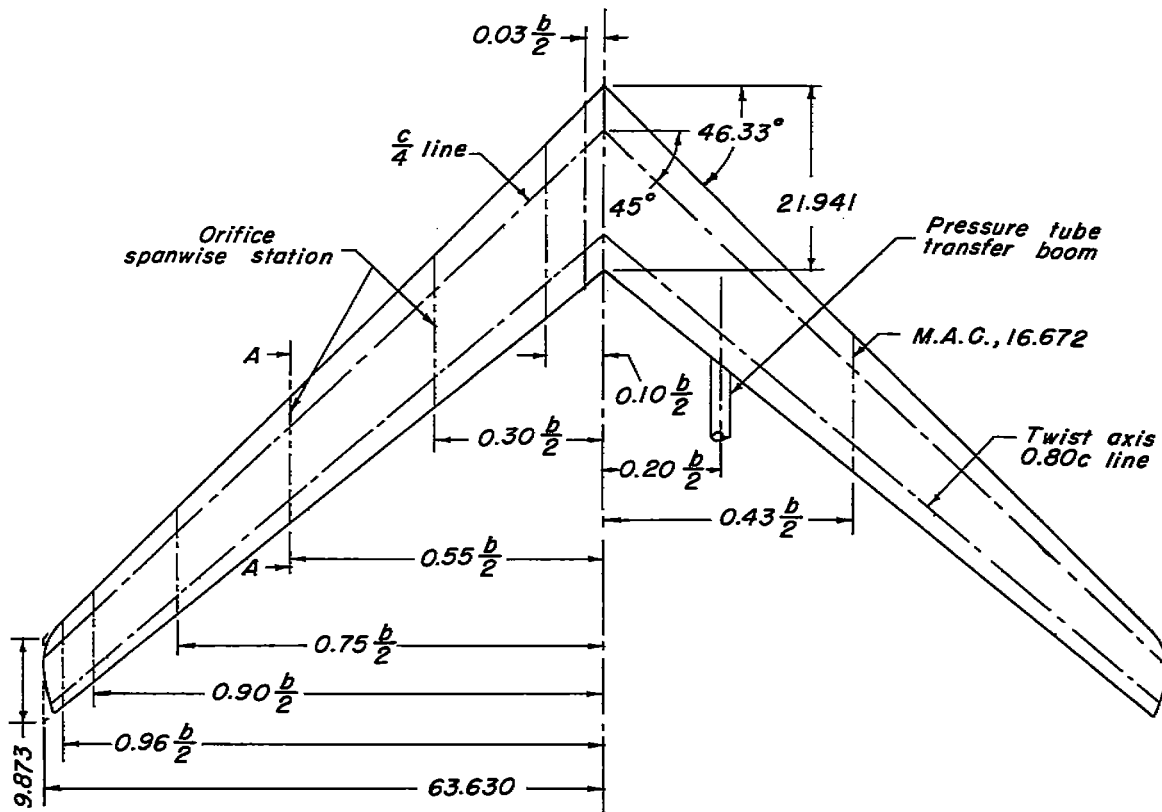
^aThese pressures measured with static tube.

TABLE III.- VALUES OF EXPERIMENTAL PRESSURE COEFFICIENT FOR THE TWISTED AND CAMBERED WING - Concluded.

Uncorrected for basic loading due to spanwise variation of tunnel stream angle; $R = 4.0 \times 10^6$

Orifice location		Pressure coefficient, S							
		$\frac{2y}{b} = 0$	$\frac{2y}{b} = 0.03$	$\frac{2y}{b} = 0.10$	$\frac{2y}{b} = 0.30$	$\frac{2y}{b} = 0.55$	$\frac{2y}{b} = 0.75$	$\frac{2y}{b} = 0.90$	$\frac{2y}{b} = 0.96$
$\alpha = 31.1^\circ$									
Upper surface	0	1.81	5.19	10.54	3.05	----	5.21	3.40	3.85
	.0010	----	----	10.22	2.61	4.08	4.31	3.00	4.32
	.0025	2.66	----	10.10	2.57	4.05	3.56	2.73	3.62
	.0050	2.60	----	9.07	2.57	3.62	3.42	2.51	2.94
	.0125	2.62	4.92	7.04	2.57	2.53	2.88	2.31	2.89
	.025	2.46	3.91	5.41	2.46	2.26	2.65	2.09	2.54
	.050	2.40	3.30	4.32	2.52	2.06	2.44	1.88	2.06
	.085	2.31	2.87	3.60	2.40	1.89	2.29	1.76	1.79
	.15	2.17	2.54	2.95	2.34	1.86	2.19	1.71	1.65
	.25	2.16	2.36	3.02	2.27	1.81	2.10	----	1.63
	.35	2.13	----	3.02	2.25	1.80	2.06	1.62	1.61
	.45	----	2.33	2.86	2.26	1.79	2.02	1.59	1.58
	.50	2.13	----	----	----	----	----	----	----
	.55	----	----	2.61	2.24	1.79	1.99	1.57	1.55
	.65	----	2.27	2.33	2.17	1.76	1.95	1.56	1.54
	.70	2.12	----	----	----	----	----	----	----
	.75	----	----	2.07	2.07	1.72	1.87	1.53	1.52
.85	2.03	----	1.81	1.98	1.68	1.77	1.50	1.51	
.95	1.64	1.36	1.58	1.99	1.62	1.67	1.45	1.47	
Lower surface	.0125	.07	2.02	2.96	1.32	1.22	1.03	.96	1.01
	.0375	.01	.42	.80	.56	.62	----	----	.53
	.075	.05	.20	.37	.40	.52	.43	.49	.56
	.15	.13	.19	.27	.40	.56	.47	.56	.67
	.25	.21	----	.32	.48	.62	.56	.66	.80
	.35	.28	----	.39	.57	----	.64	.75	.89
	.45	.35	----	.46	.65	.79	.71	.81	.94
	.55	.40	----	.52	.72	.83	.76	.86	.97
	.65	.45	----	.58	.78	.85	.80	.89	.98
	.75	.49	----	.64	.85	.89	.83	.92	1.00
	.85	.53	----	.71	.95	.92	.88	.95	1.01
.95	.59	.69	.89	1.15	1.02	1.00	1.03	1.14	

NACA



Station A-A (enlarged)

Typical airfoil section and chordwise orifice location

Figure 1.- Geometric details of model. Aspect ratio, 8.02; taper ratio, 0.45; airfoil section, NACA 63₁A c_l_i 12; wing area, 14.02 square feet. (Dimensions are in inches.) c_l_i defined in figure 2.

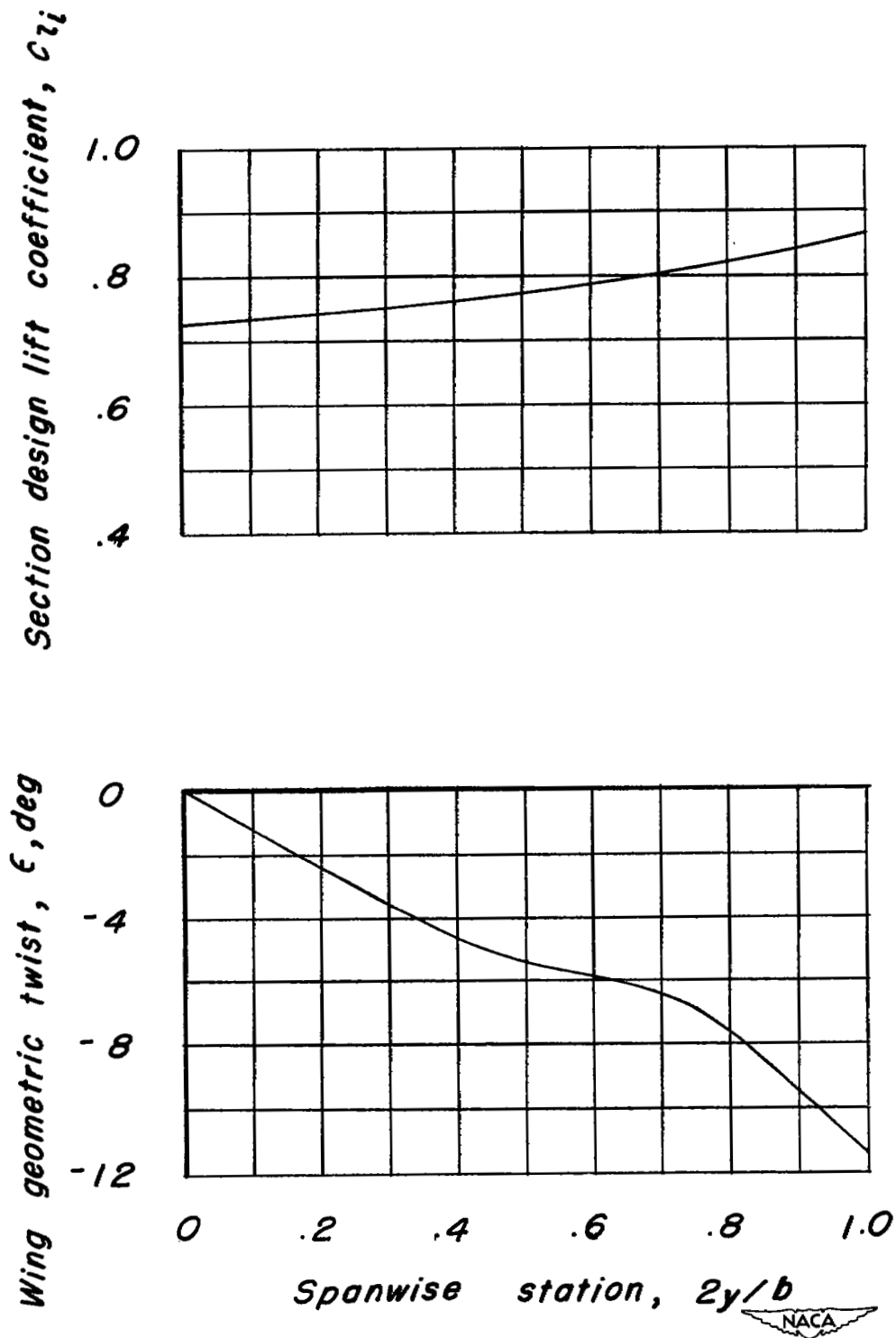


Figure 2.- Spanwise variation of wing geometric twist and design section lift coefficient.

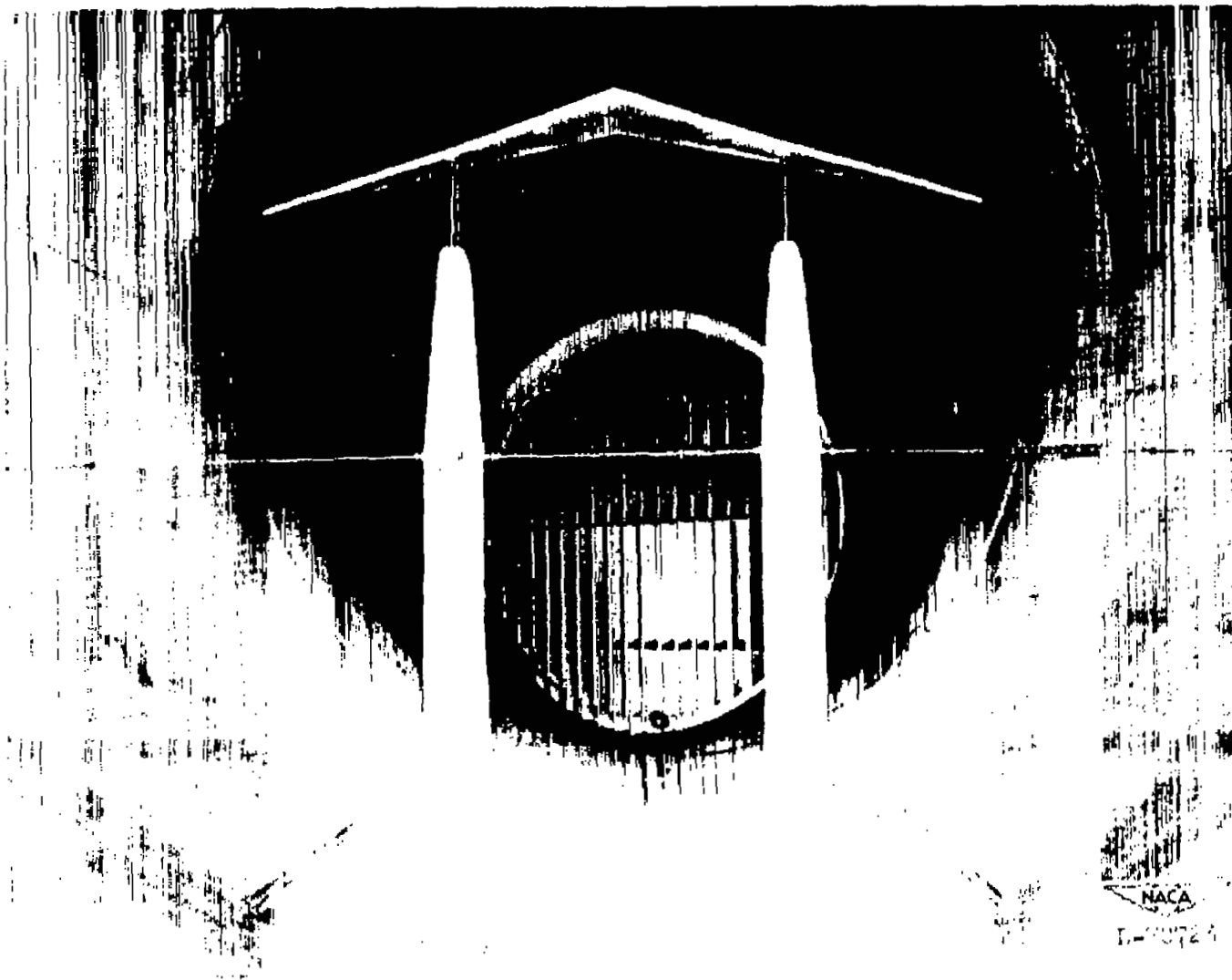


Figure 3.- Model in tunnel for force tests (front view).

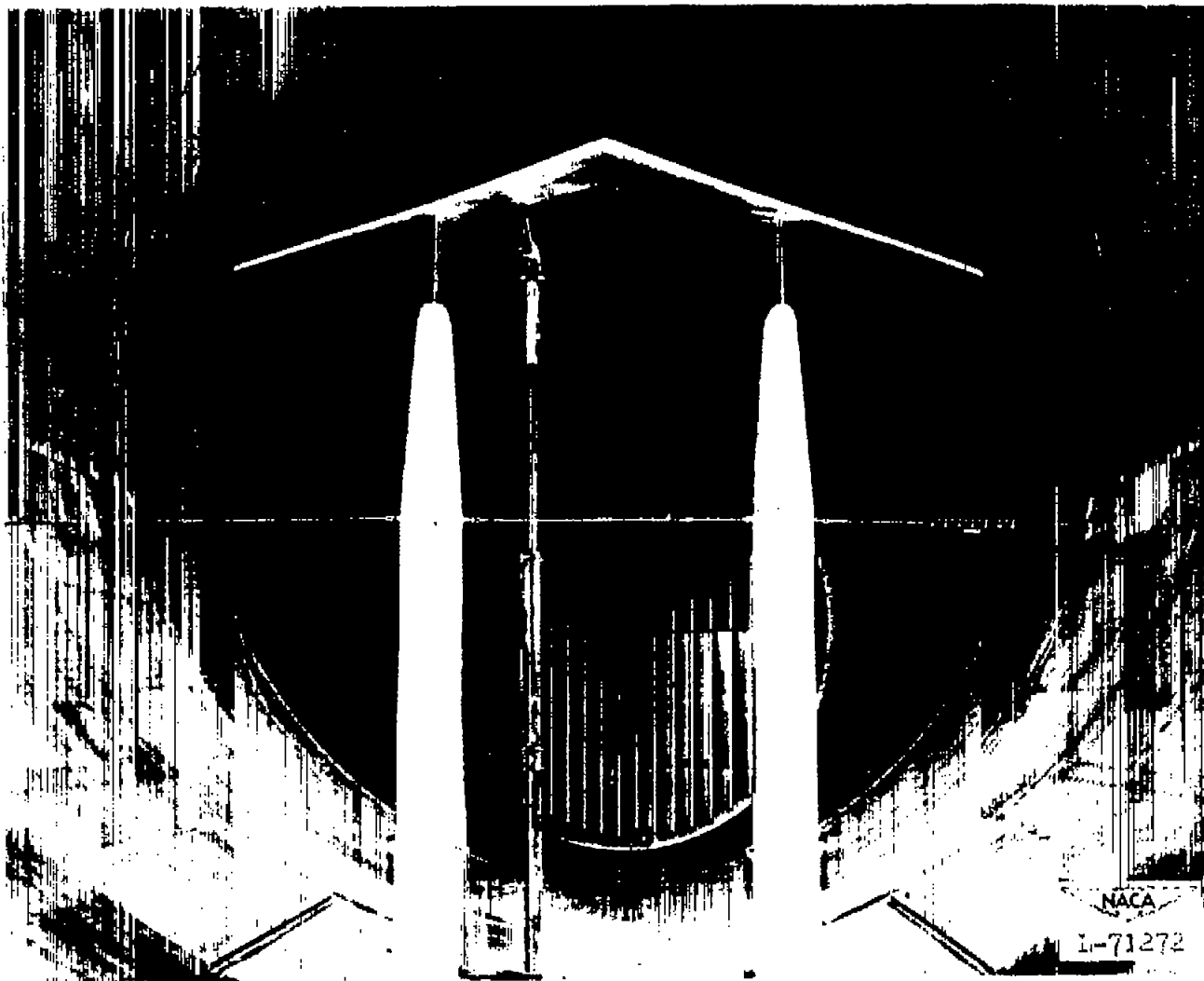


Figure 4.- Model in tunnel for pressure-distribution tests (front view).

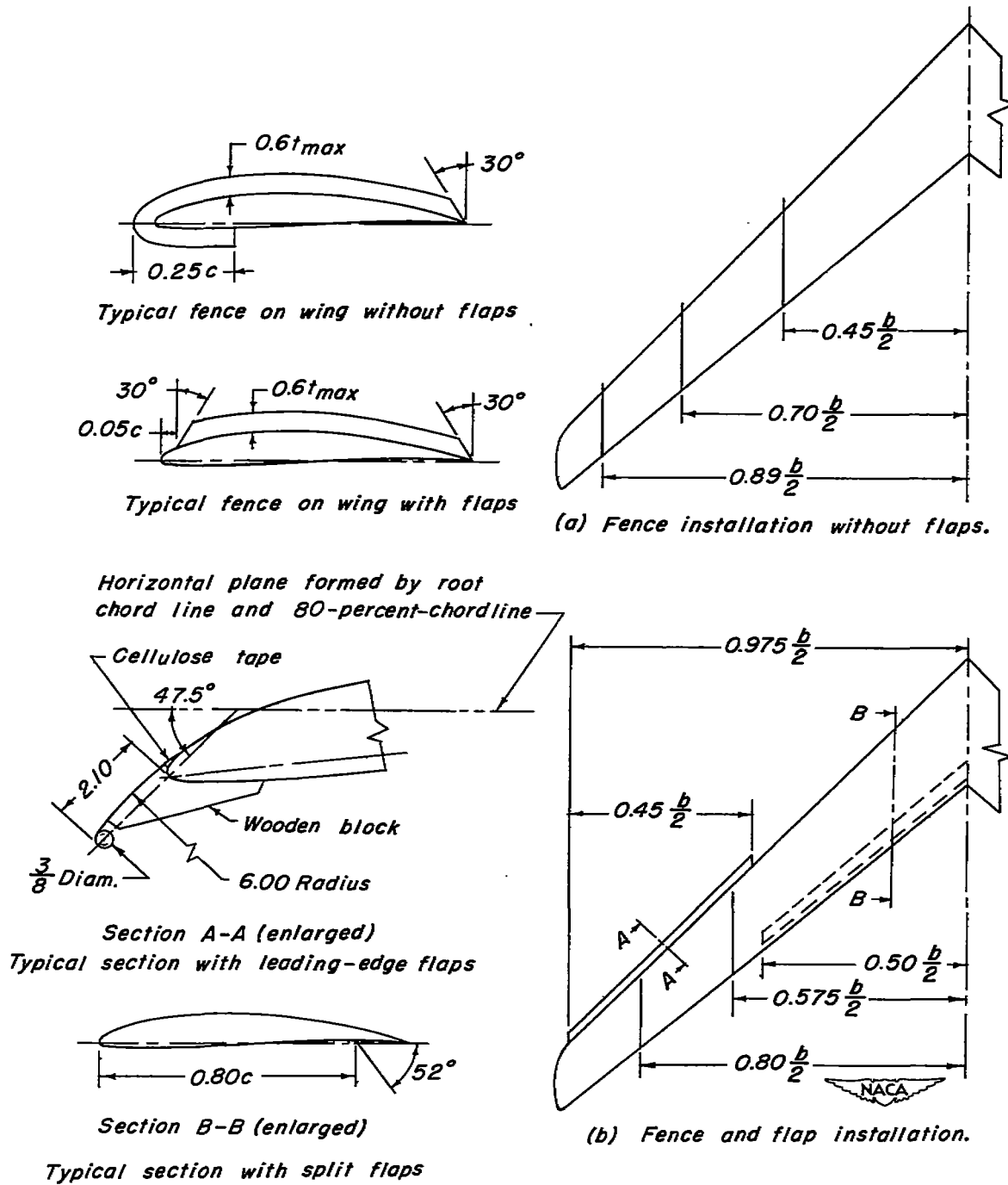


Figure 5.- Details of flaps and fences. (Dimensions are in inches.)

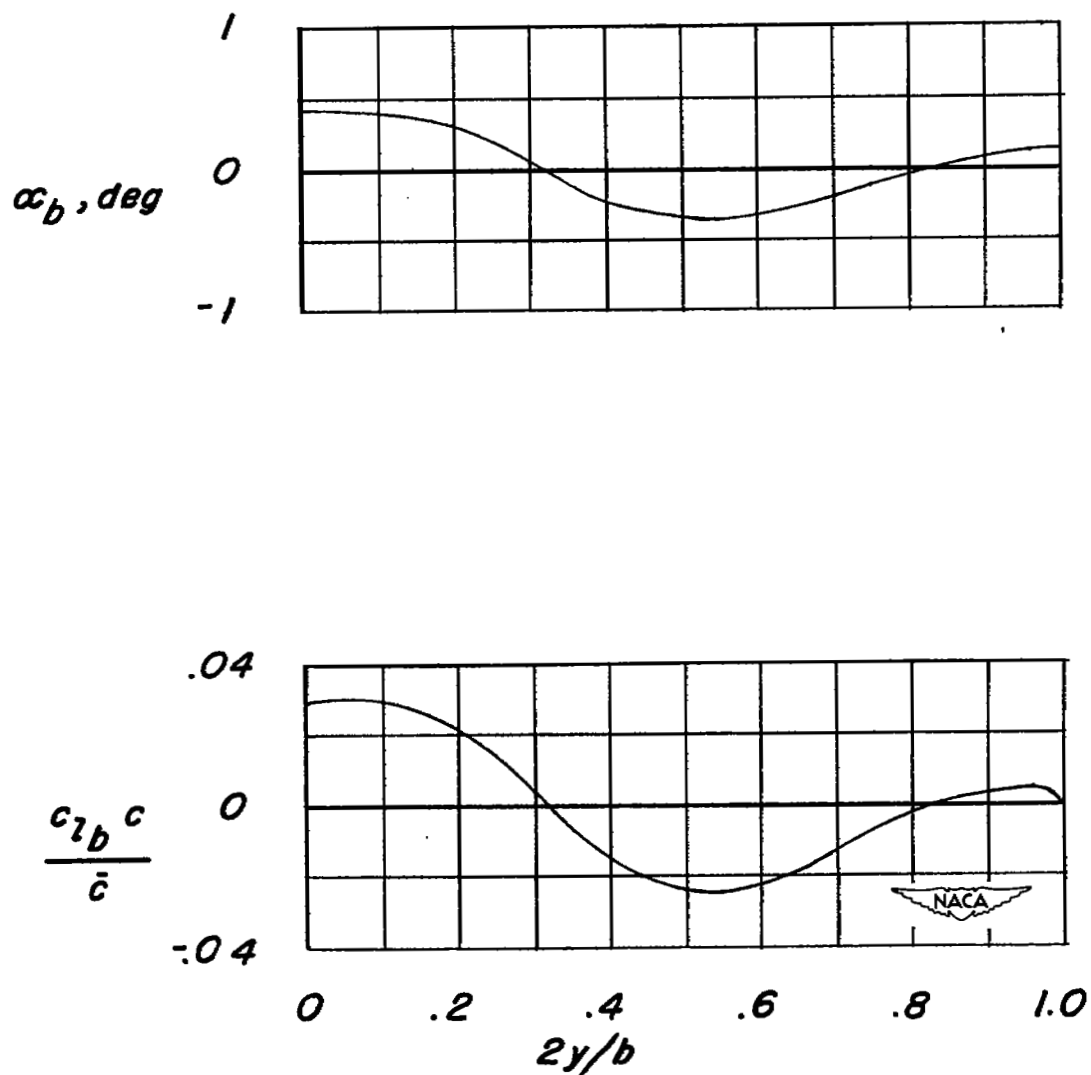
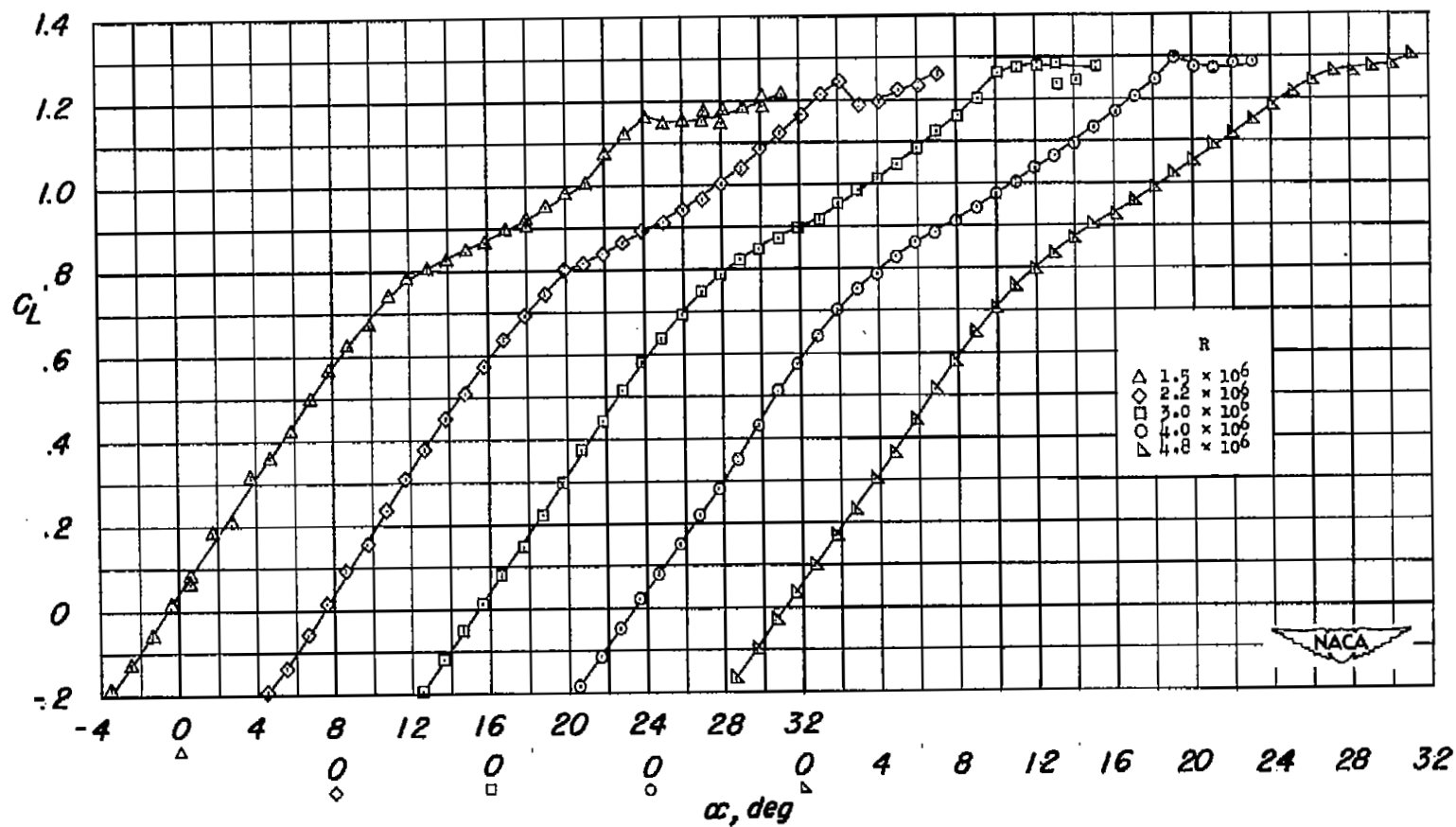
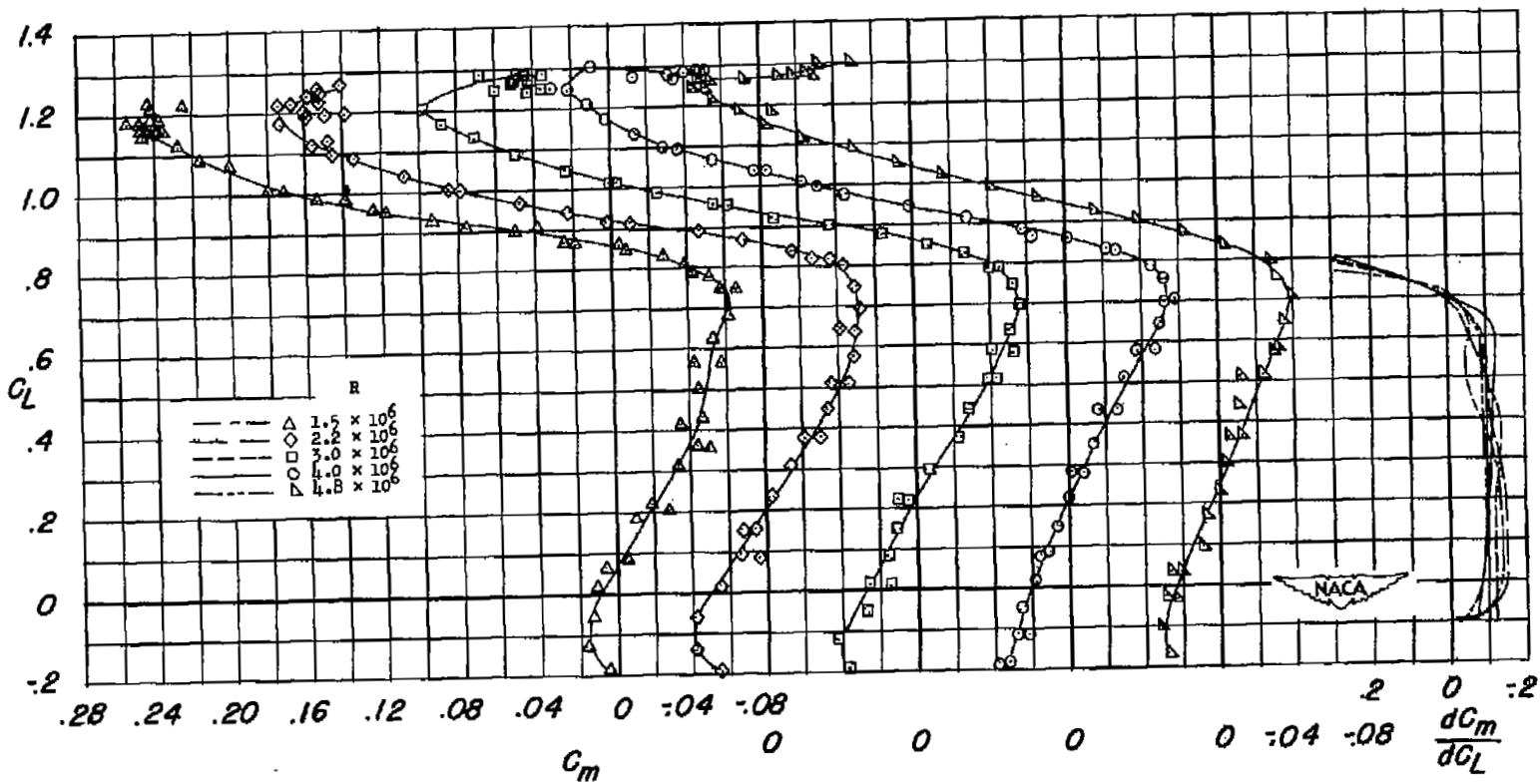


Figure 6.- Spanwise air-stream angle-of-attack variation and basic loading due to air-stream variation.



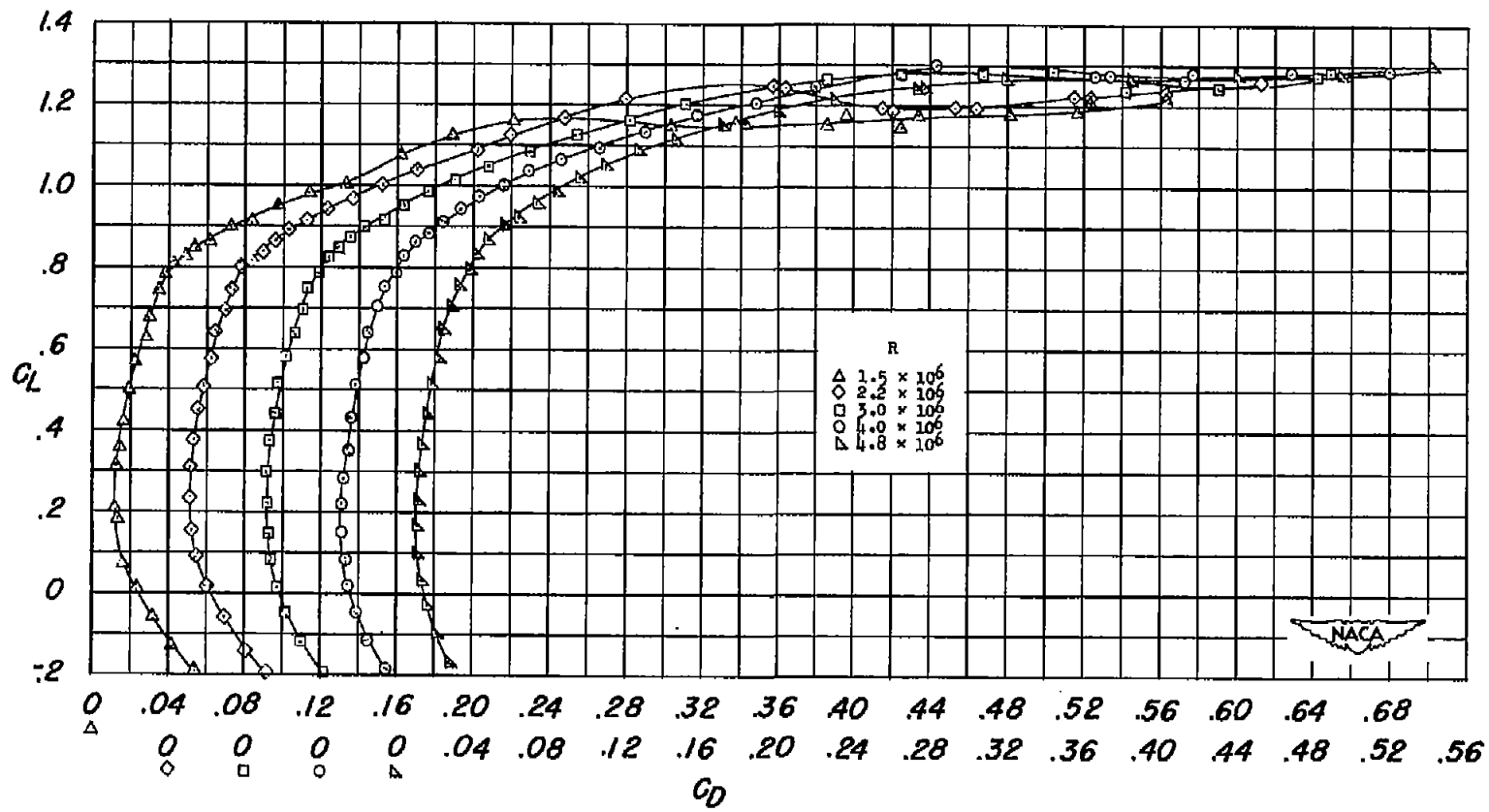
(a) Lift.

Figure 7.- Effect of Reynolds number on the lift, drag, and pitching-moment characteristics of the twisted and cambered wing.



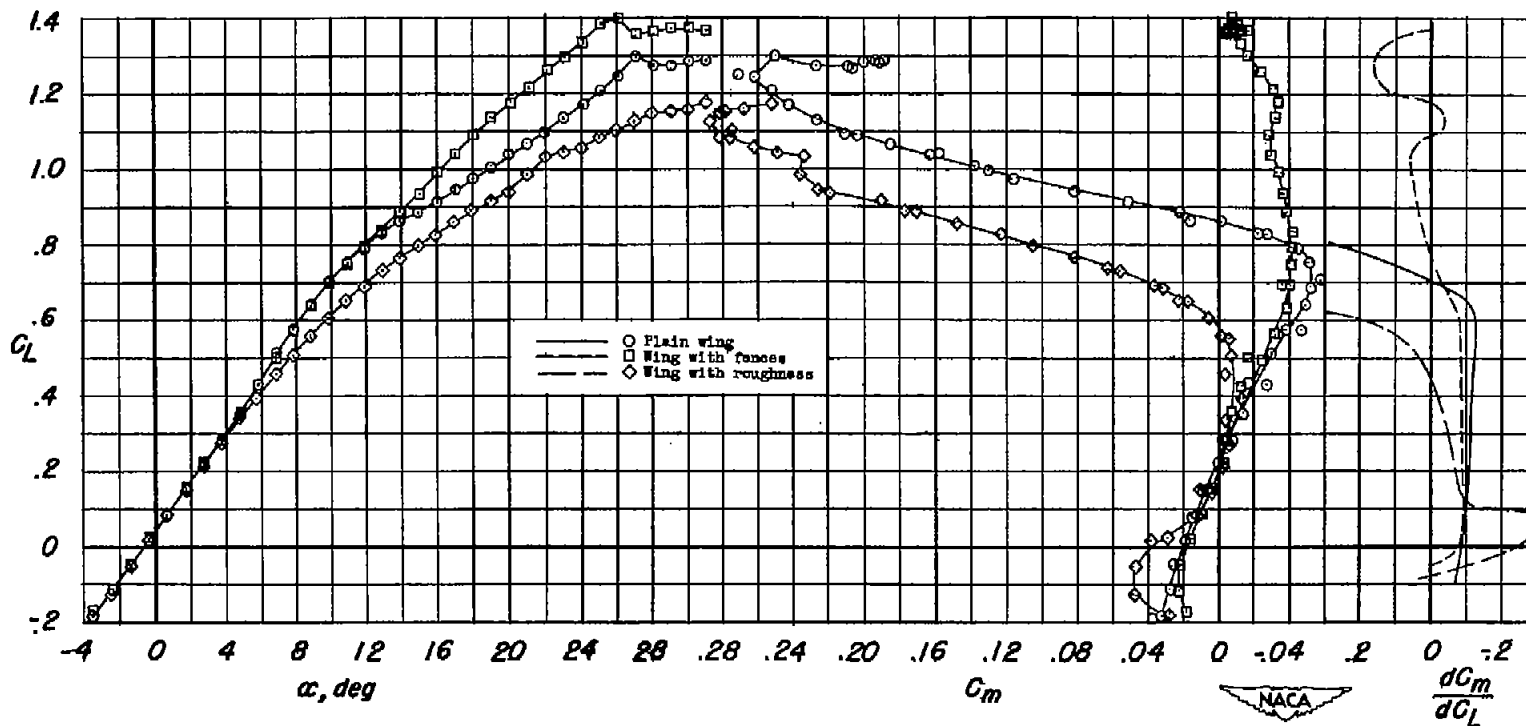
(b) Pitching moment.

Figure 7.- Continued.



(c) Drag.

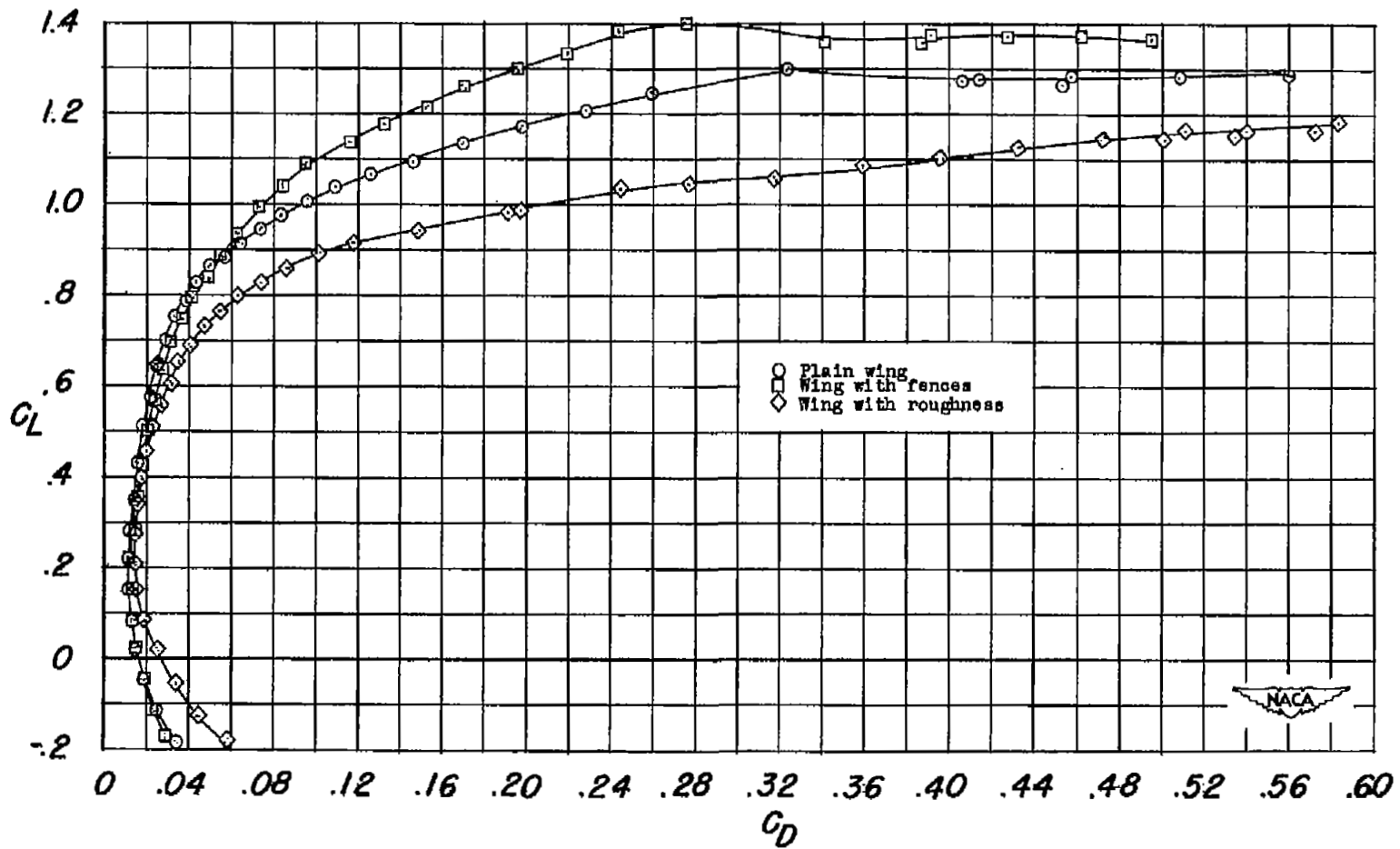
Figure 7.- Concluded.



(a) Lift and pitching moment.

Figure 8.- Effect of fences and leading-edge roughness on the lift, drag, and pitching-moment characteristics of the twisted and cambered wing.

$R = 4.0 \times 10^6$; fence locations, 0.45, 0.70, and 0.89b/2.

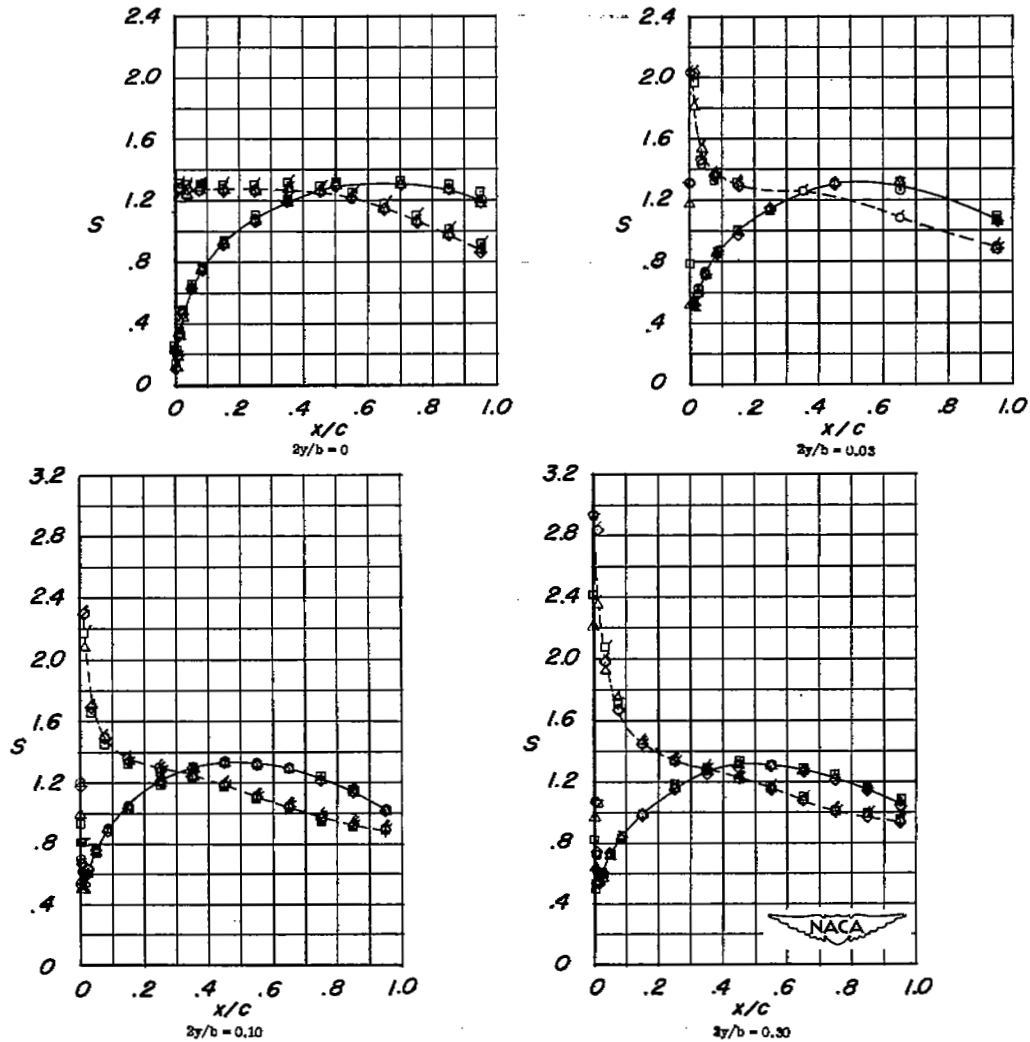


(b) Drag.

Figure 8.- Concluded.

- | | |
|--|-----------------------|
| ○ Plain wing | $R = 4.0 \times 10^6$ |
| □ Plain wing | $R = 1.5 \times 10^6$ |
| ◇ Wing with fences at 0.45, 0.70, and 0.80 $b/2$ | $R = 4.0 \times 10^6$ |
| △ Wing with leading-edge roughness | $R = 4.0 \times 10^6$ |

—○— Upper surface
 - -○- - Lower surface

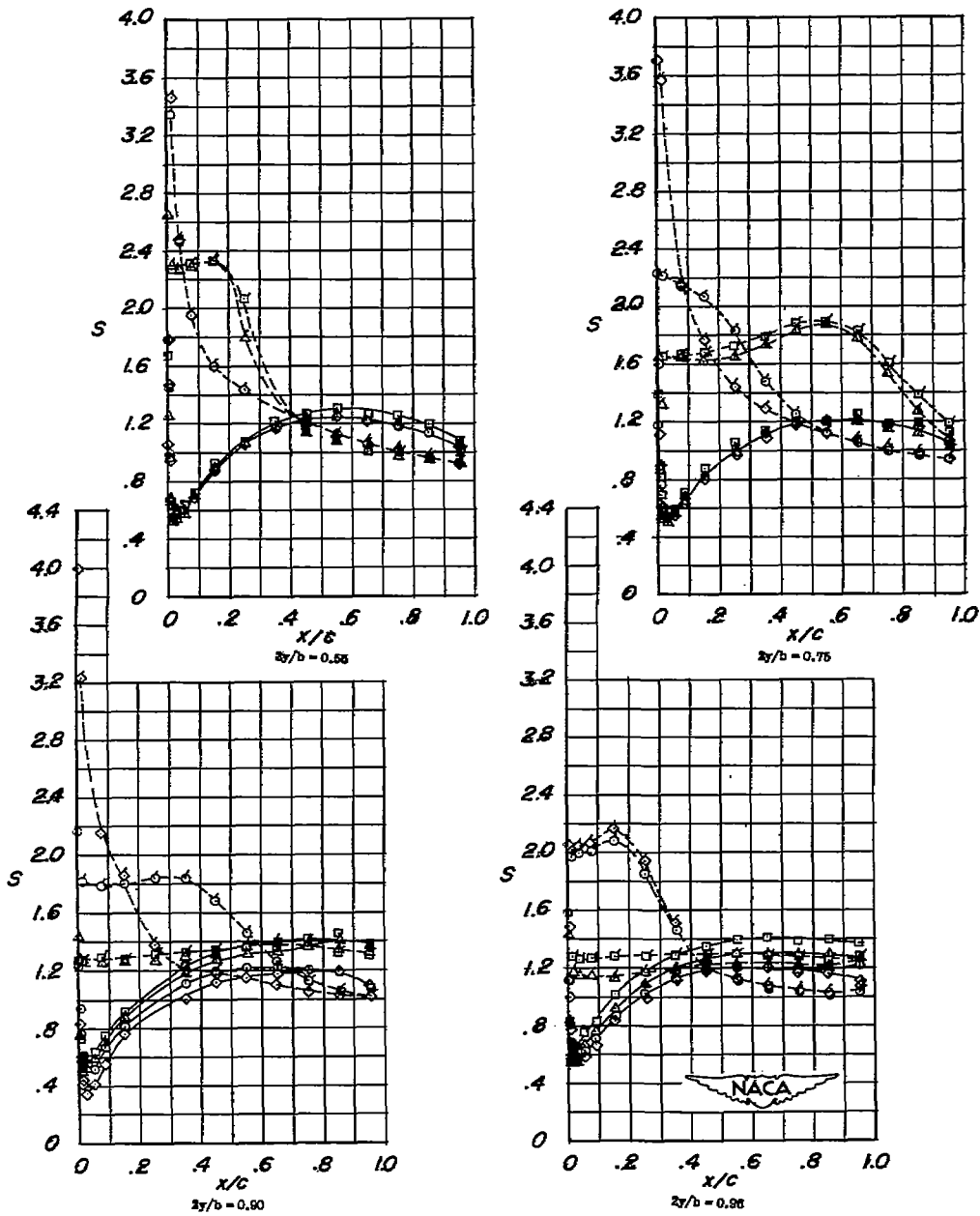


(a) $\alpha = -3.5^\circ$.

Figure 9.- Chordwise pressure diagrams for twisted and cambered wing, wing with fences, and wing with roughness.

- | | |
|--|-----------------------|
| ○ Plain wing | $R = 4.0 \times 10^6$ |
| □ Plain wing | $R = 1.6 \times 10^6$ |
| ◇ Wing with fences at 0.46, 0.70, and 0.89 $b/2$ | $R = 4.0 \times 10^6$ |
| △ Wing with leading-edge roughness | $R = 4.0 \times 10^6$ |

—○— Upper surface
 - - -○- - Lower surface

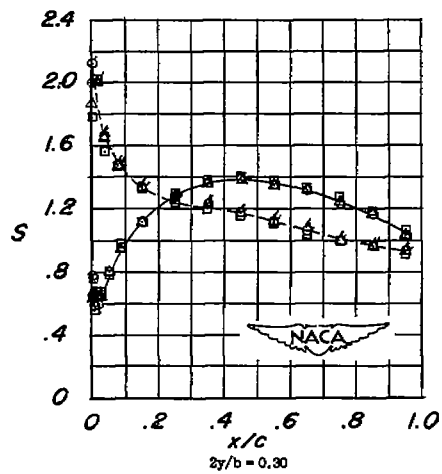
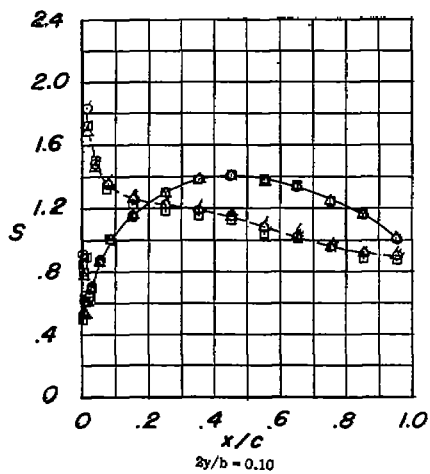
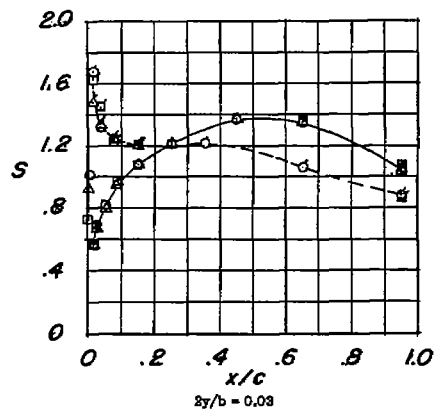
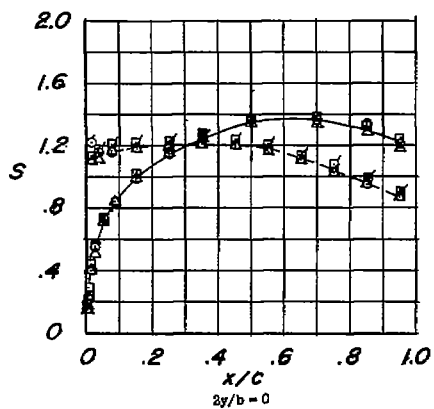


(a) Concluded. $\alpha = -3.5^\circ$.

Figure 9.- Continued.

- | | | |
|---|---------------------------|-----------------------|
| ○ | Plain wing | $R = 4.0 \times 10^6$ |
| □ | Plain wing | $R = 1.6 \times 10^6$ |
| ■ | Wing with fences at 0.46, | $R = 4.0 \times 10^6$ |
| | 0.70, and 0.89 $b/2$ | |
| △ | Wing with leading-edge | $R = 4.0 \times 10^6$ |
| | roughness | |

—○— Upper surface
 - -○- - Lower surface

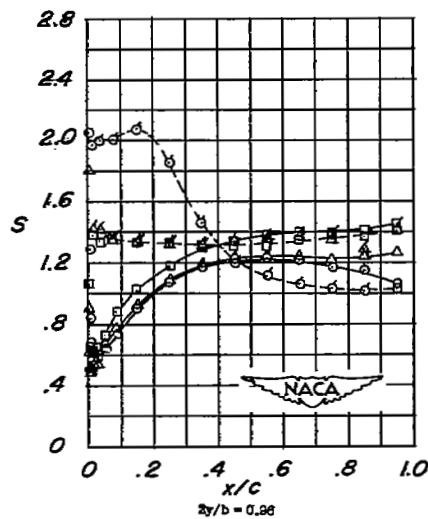
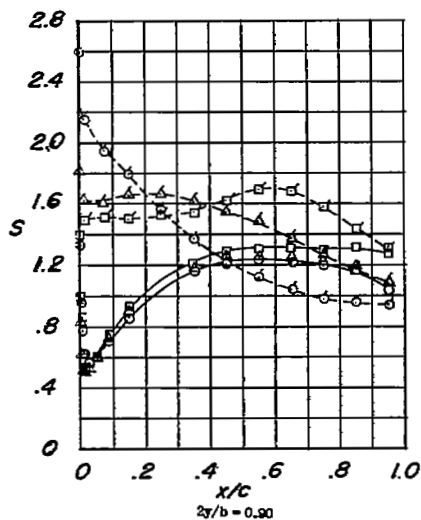
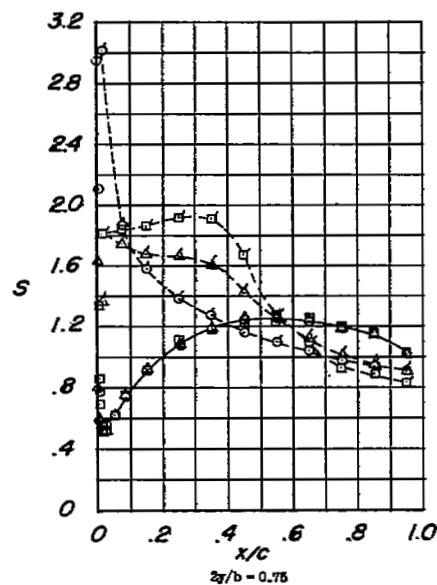
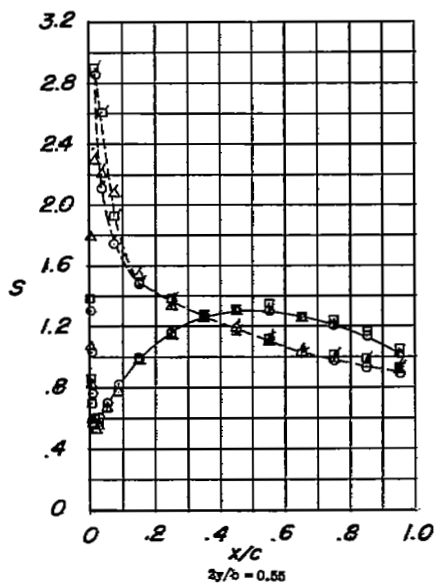


(b) $\alpha = -1.4^\circ$.

Figure 9.- Continued.

- Plain wing $R = 4.0 \times 10^6$
- Plain wing $R = 1.5 \times 10^6$
- Wing with fences at 0.45, $R = 4.0 \times 10^6$
0.70, and 0.89 $b/2$
- △ Wing with leading-edge roughness $R = 4.0 \times 10^6$

—○— Upper surface
- -○- - Lower surface

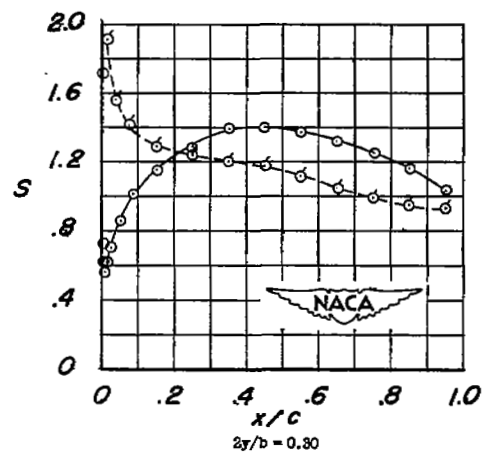
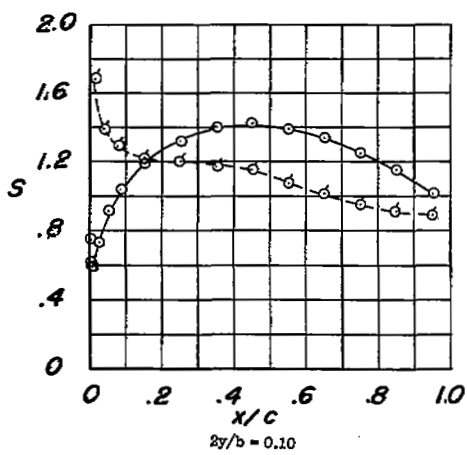
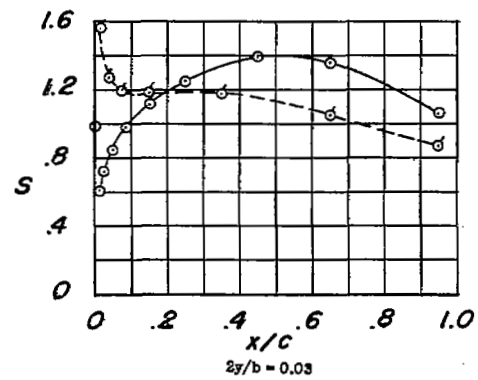
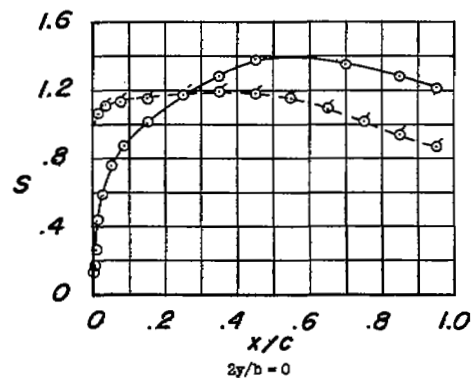


(b) Concluded. $\alpha = -1.4^\circ$.

Figure 9.- Continued.

- Plain wing $R = 4.0 \times 10^6$
 Plain wing $R = 1.6 \times 10^6$
 Wing with fences at 0.45, $R = 4.0 \times 10^6$
 0.70, and 0.89 $b/2$
 Wing with leading-edge roughness $R = 4.0 \times 10^6$

—○— Upper surface
 - - -○- - Lower surface

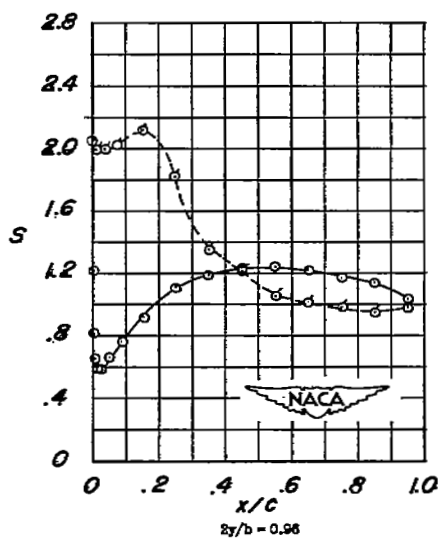
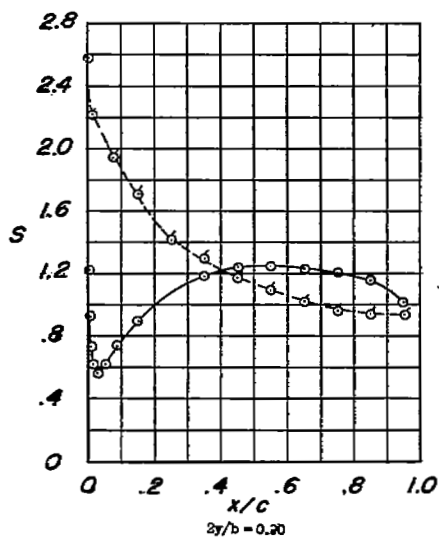
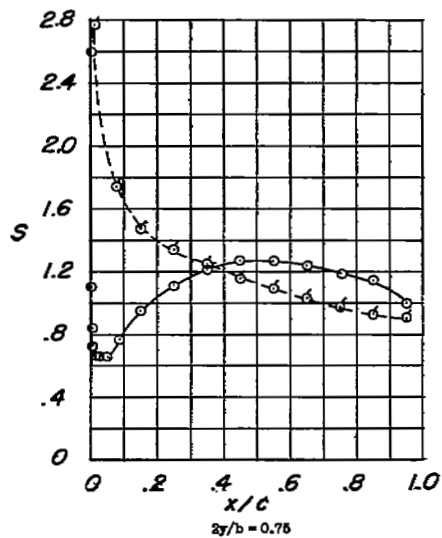
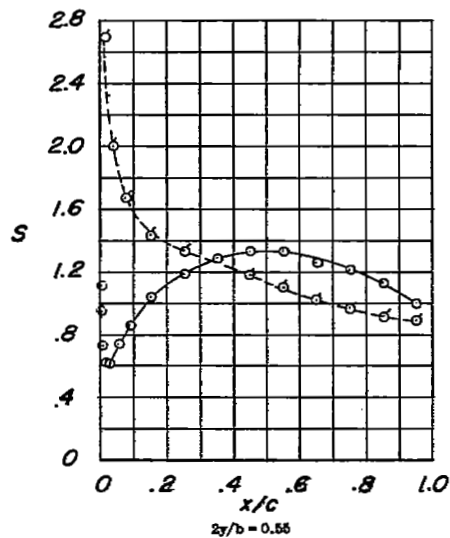


(c) $\alpha = -0.7^\circ$.

Figure 9.- Continued.

○ Plain wing $R = 4.0 \times 10^6$
 Plain wing $R = 1.5 \times 10^6$
 Wing with fences at 0.45, $R = 4.0 \times 10^6$
 0.70, and 0.89 $b/2$
 Wing with leading-edge roughness $R = 4.0 \times 10^6$

—○— Upper surface
 - - -○ - - Lower surface

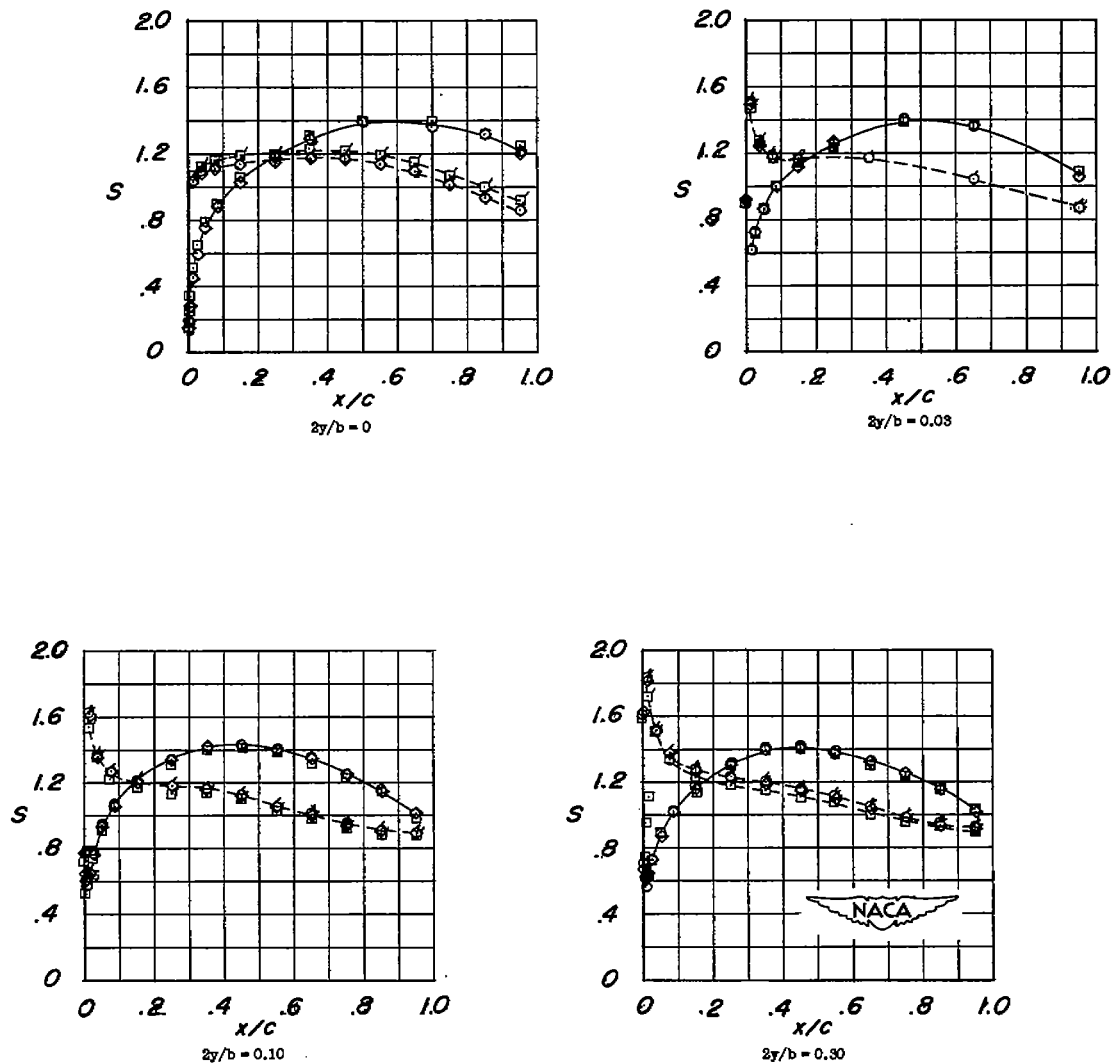


(c) Concluded. $\alpha = -0.7^\circ$.

Figure 9.- Continued.

- | | |
|-----------------------------|-----------------------|
| ○ Plain wing | $R = 4.0 \times 10^6$ |
| □ Plain wing | $R = 1.5 \times 10^6$ |
| ◇ Wing with fences at 0.46, | $R = 4.0 \times 10^6$ |
| 0.70, and 0.89 $b/2$ | |
| Wing with leading-edge | $R = 4.0 \times 10^6$ |
| roughness | |

—○— Upper surface
 - -○- - Lower surface

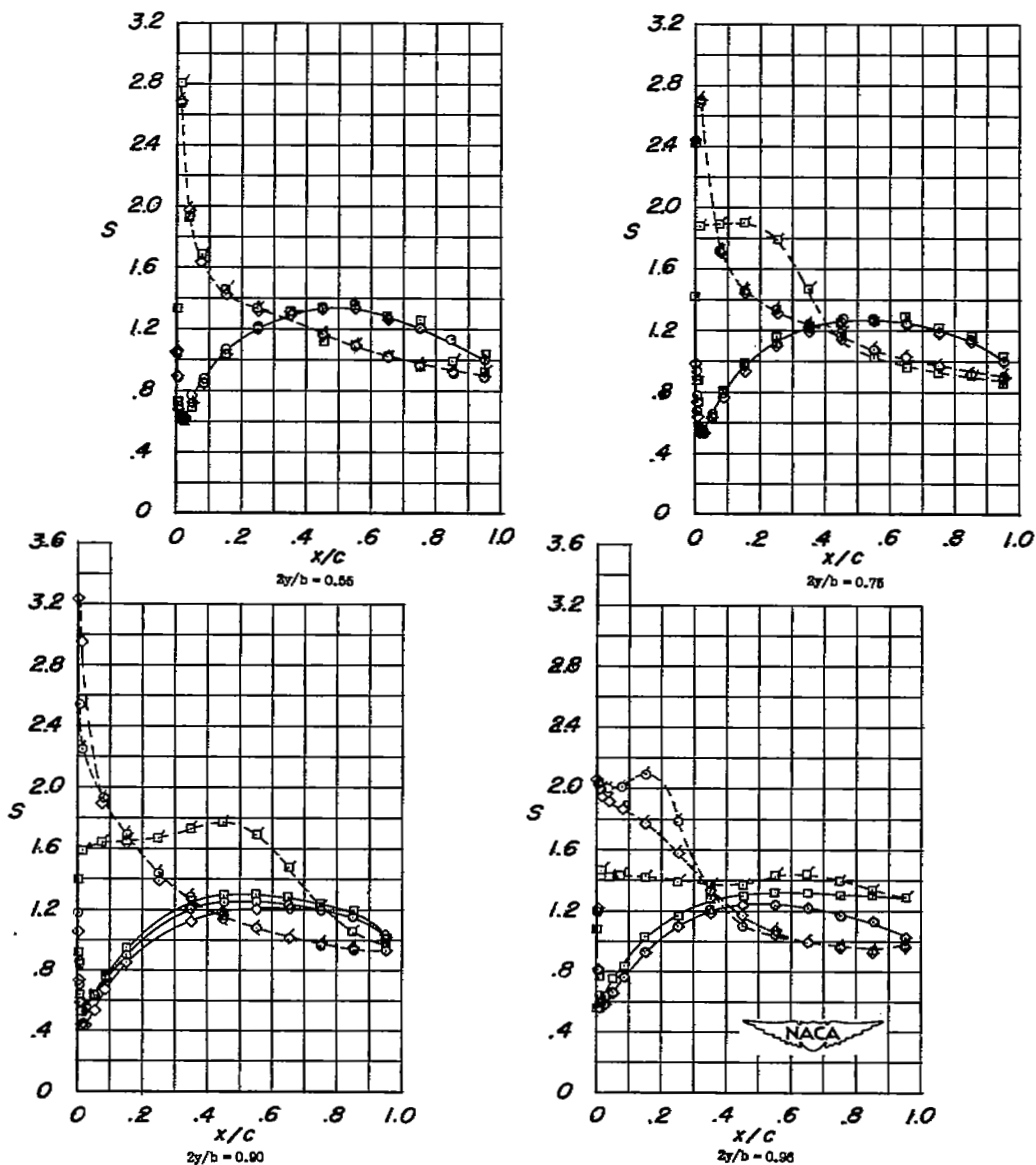


(d) $\alpha = -0.4^\circ$.

Figure 9.- Continued.

○ Plain wing $R = 4.0 \times 10^6$
 □ Plain wing $R = 1.5 \times 10^6$
 ◇ Wing with fences at 0.45, 0.70, and 0.89 by 2 $R = 4.0 \times 10^6$
 Wing with leading-edge roughness $R = 4.0 \times 10^6$

—○— Upper surface
 - - -○- - Lower surface

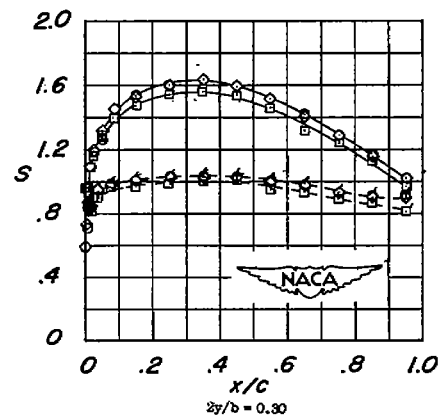
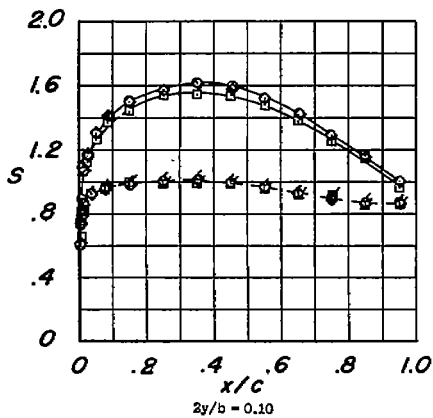
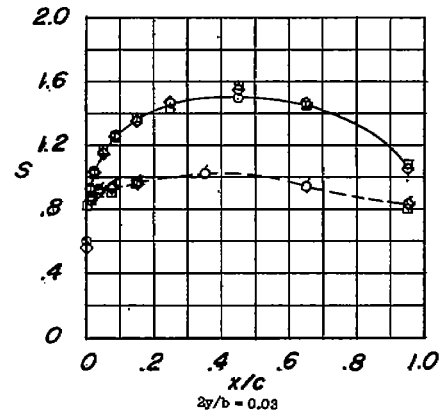
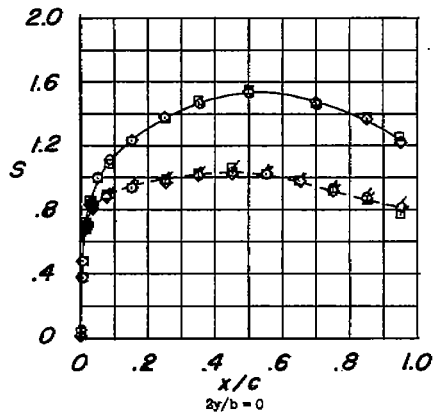


(d) Concluded. $\alpha = -0.4^\circ$.

Figure 9.- Continued.

- | | |
|--|-----------------------|
| ○ Plain wing | $R = 4.0 \times 10^6$ |
| □ Plain wing | $R = 1.5 \times 10^6$ |
| ◇ Wing with fences at 0.45, 0.70, and $0.89 b/2$ | $R = 4.0 \times 10^6$ |
| Wing with leading-edge roughness | $R = 4.0 \times 10^6$ |

—○— Upper surface
 - -○- - Lower surface

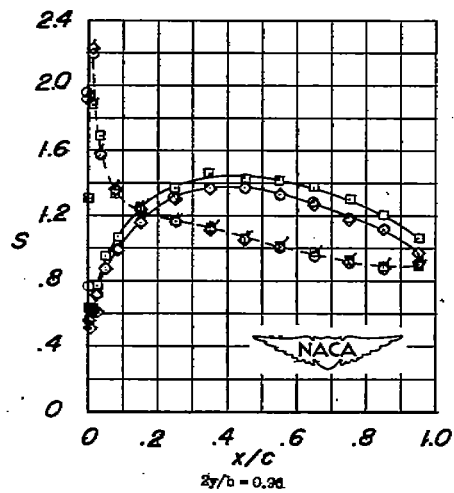
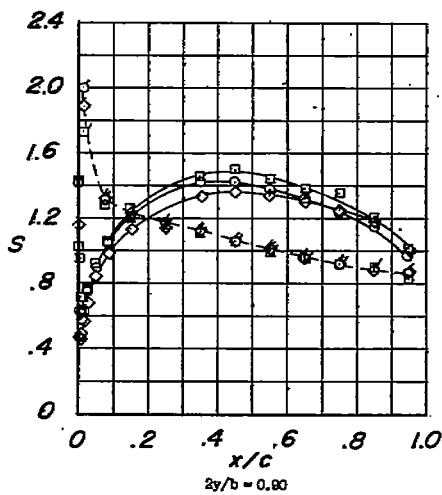
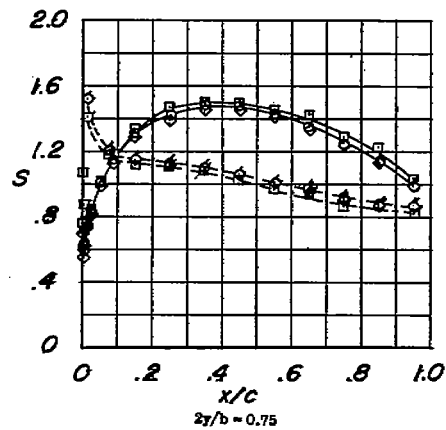
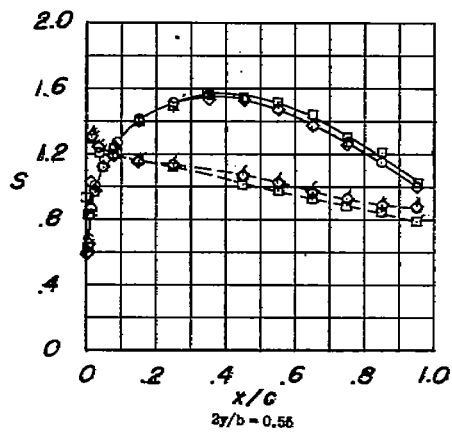


(e) $\alpha = 4.7^\circ$.

Figure 9.- Continued.

- | | |
|--|-----------------------|
| ○ Plain wing | $R = 4.0 \times 10^6$ |
| □ Plain wing | $R = 1.5 \times 10^6$ |
| ◇ Wing with fences at 0.45, 0.70, and 0.89 $b/2$ | $R = 4.0 \times 10^6$ |
| Wing with leading-edge roughness | $R = 4.0 \times 10^6$ |

—○— Upper surface
 - - -○- - Lower surface

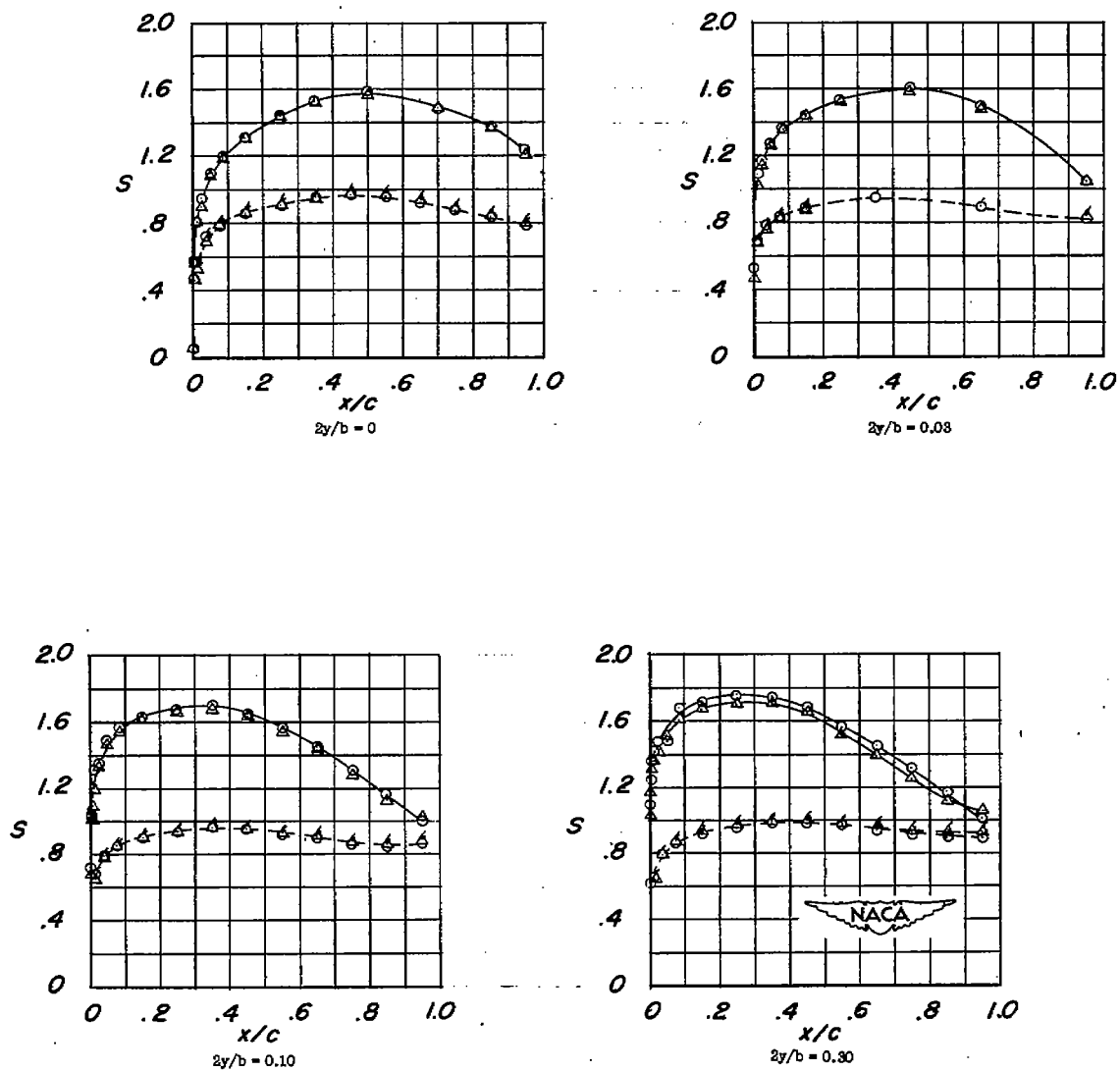


(e) Concluded. $\alpha = 4.7^\circ$.

Figure 9.- Continued.

- | | |
|---|-----------------------|
| ○ Plain wing | $R = 4.0 \times 10^6$ |
| ○ Plain wing | $R = 1.5 \times 10^6$ |
| Wing with fences at 0.45,
0.70, and 0.89 $b/2$ | $R = 4.0 \times 10^6$ |
| △ Wing with leading-edge
roughness | $R = 4.0 \times 10^6$ |

—○— Upper surface
- - -○- - Lower surface

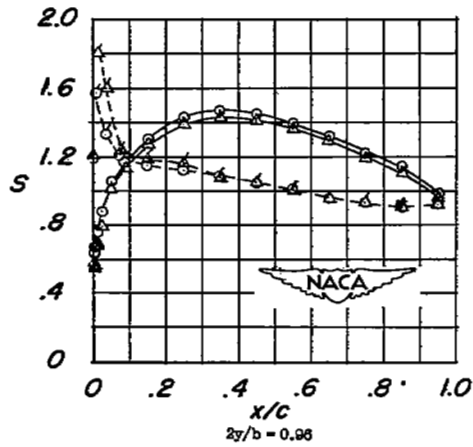
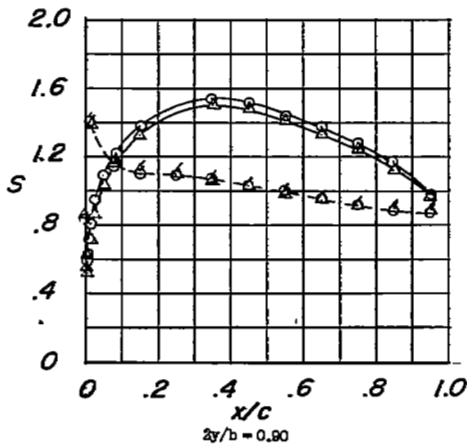
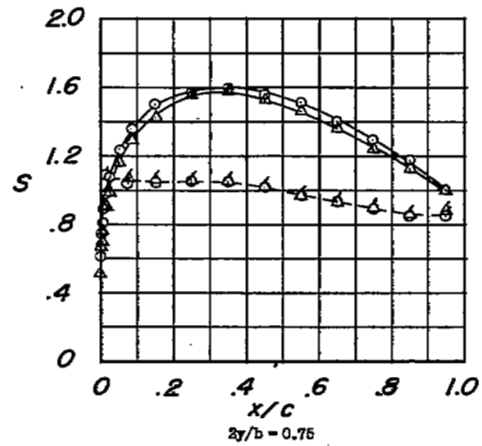
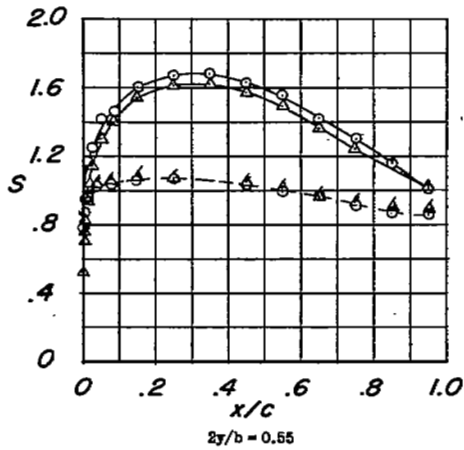


(f) $\alpha = 6.8^\circ$.

Figure 9.- Continued.

- Plain wing $R = 4.0 \times 10^6$
- Plain wing $R = 1.5 \times 10^6$
- ◇ Wing with fences at 0.45, 0.70, and 0.89 $b/2$ $R = 4.0 \times 10^6$
- △ Wing with leading-edge roughness $R = 4.0 \times 10^6$

—○— Upper surface
 -◇- Lower surface

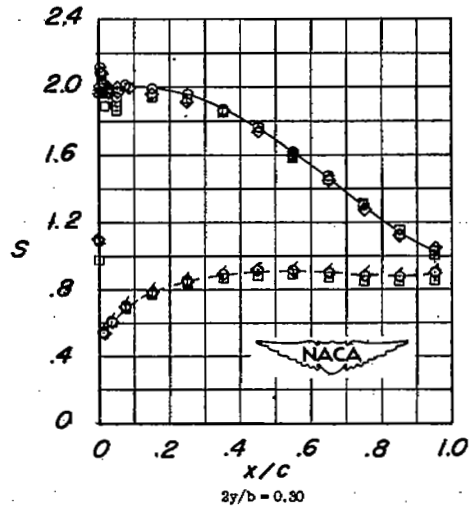
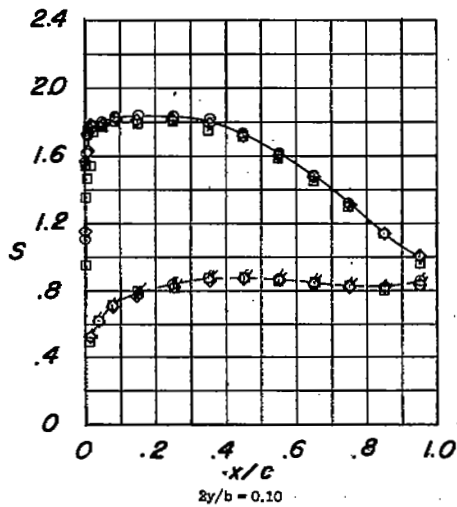
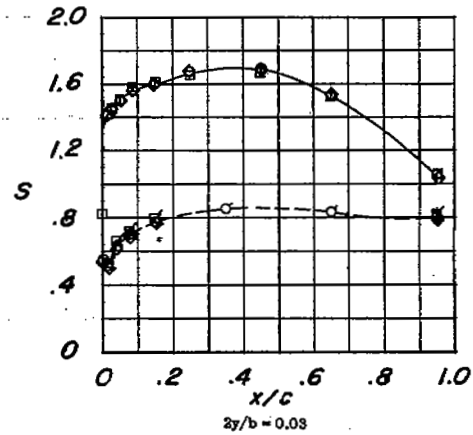
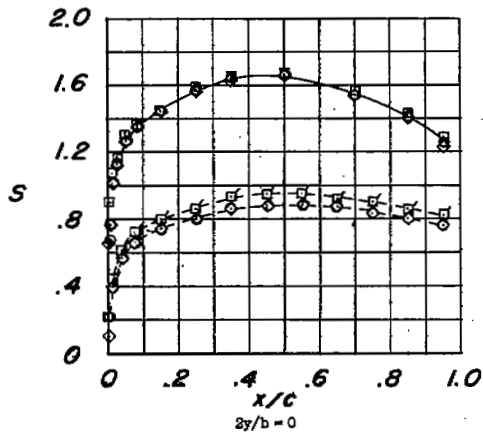


(f) Concluded. $\alpha = 6.8^\circ$.

Figure 9.- Continued.

○ Plain wing $R = 4.0 \times 10^6$
 □ Plain wing $R = 1.5 \times 10^6$
 ◇ Wing with fences at 0.45, $R = 4.0 \times 10^6$
 0.70, and 0.89 $b/2$
 Wing with leading-edge roughness $R = 4.0 \times 10^6$

—○— Upper surface
 - - -○- - Lower surface

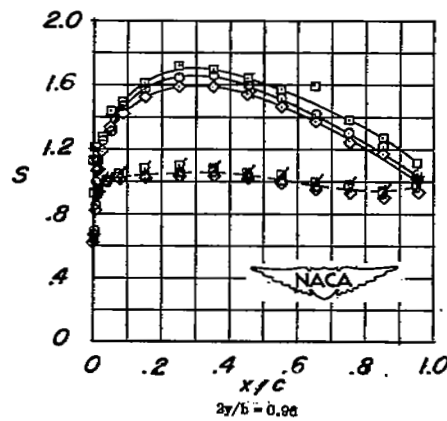
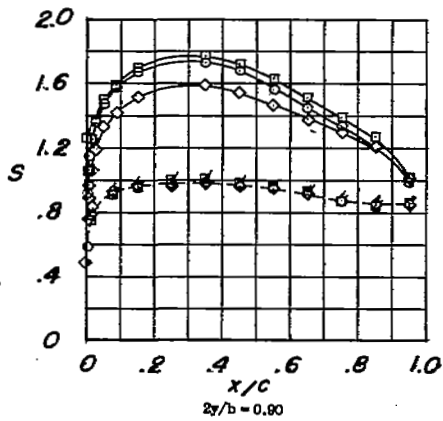
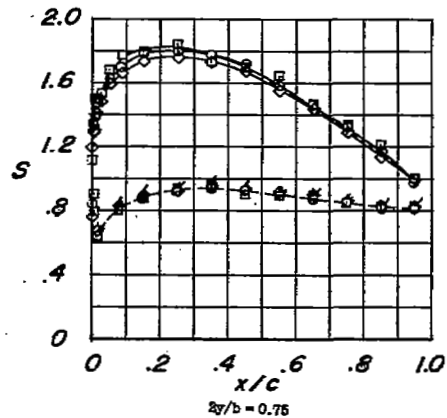
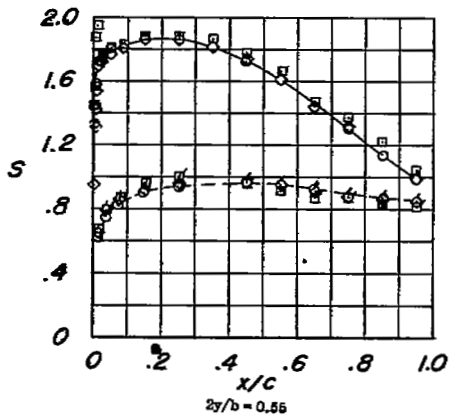


(g) $\alpha = 9.9^\circ$.

Figure 9.- Continued.

- Plain wing $R = 4.0 \times 10^6$
- Plain wing $R = 1.5 \times 10^6$
- ◇ Wing with fences at 0.45, 0.70, and 0.89 $b/2$ $R = 4.0 \times 10^6$
- △ Wing with leading-edge roughness $R = 4.0 \times 10^6$

—○— Upper surface
 - - -○- - Lower surface

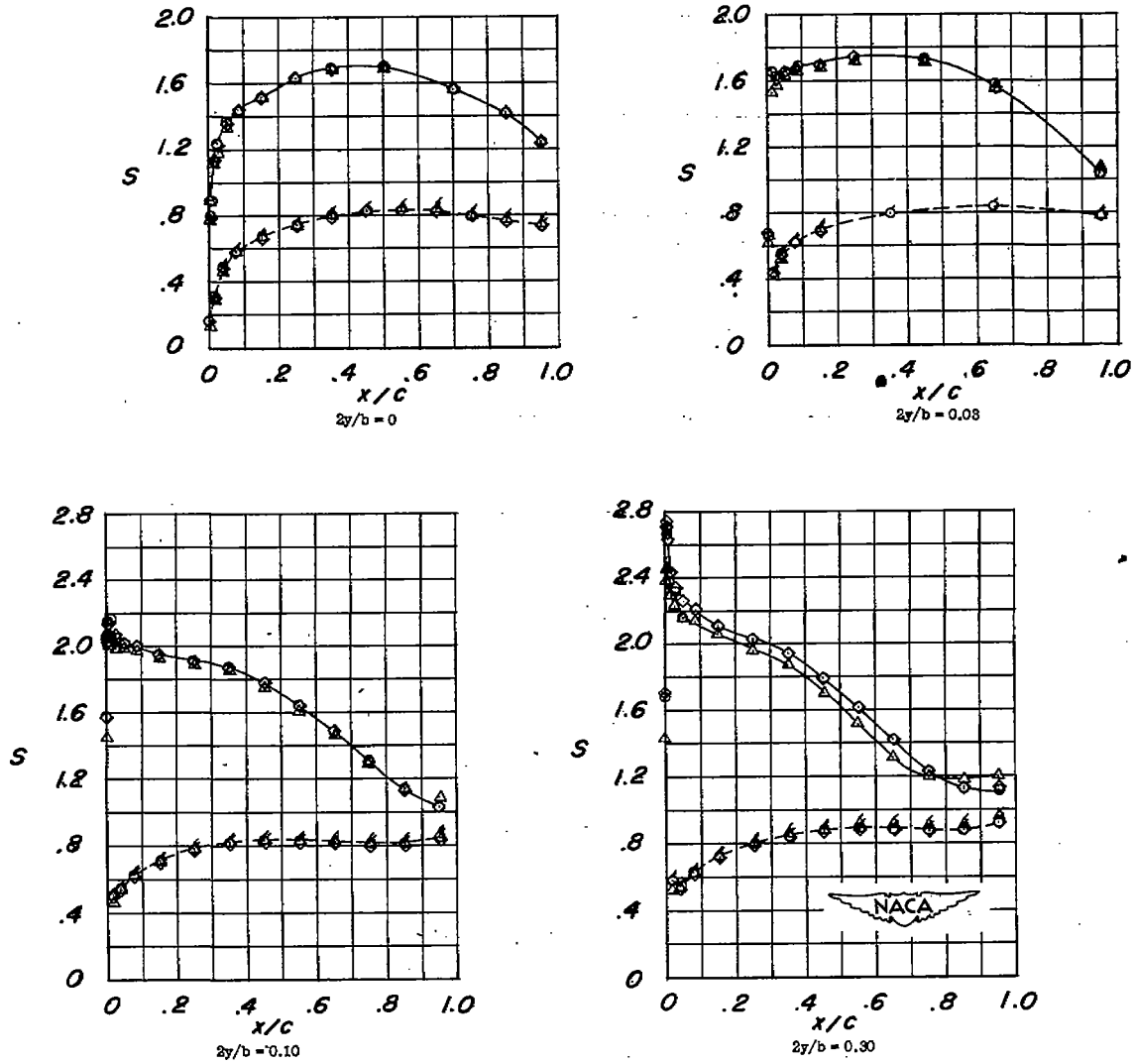


(g) Concluded. $\alpha = 9.9^\circ$.

Figure 9.- Continued.

- Plain wing $R = 4.0 \times 10^6$
 Plain wing $R = 1.5 \times 10^6$
 ◇ Wing with fences at 0.45, $R = 4.0 \times 10^6$
 0.70, and 0.89 $b/2$
 △ Wing with leading-edge roughness $R = 4.0 \times 10^6$

—○— Upper surface
 - - -○- - Lower surface

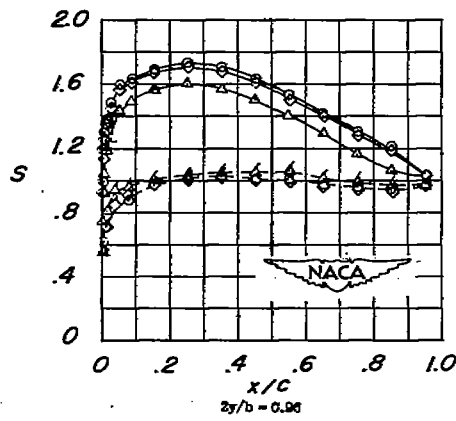
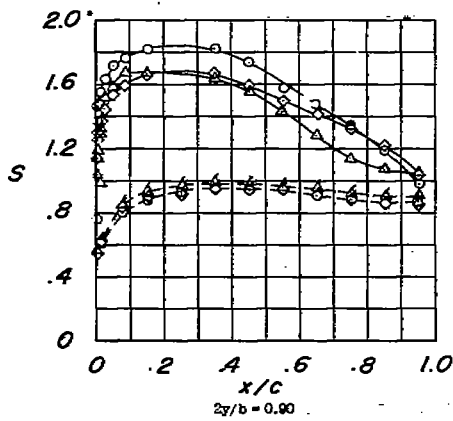
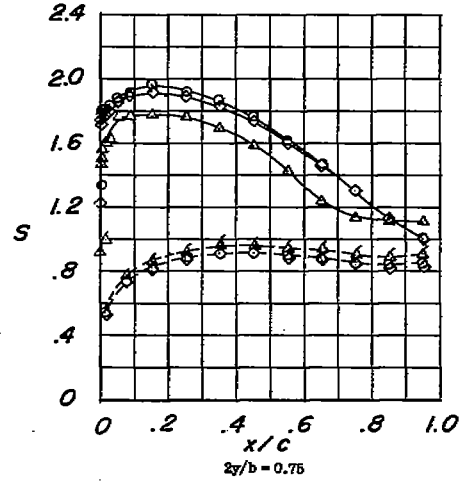
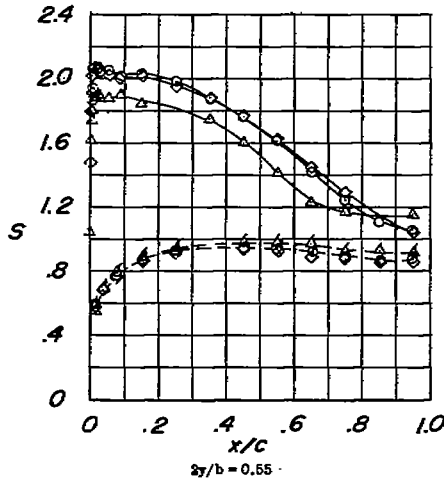


(h) $\alpha = 11.9^\circ$.

Figure 9.- Continued.

- Plain wing $R = 4.0 \times 10^6$
- Plain wing $R = 1.5 \times 10^6$
- ◇ Wing with fences at 0.46, 0.70, and 0.89 $l/3$ $R = 4.0 \times 10^6$
- △ Wing with leading-edge roughness $R = 4.0 \times 10^6$

—○— Upper surface
 - - -○- - Lower surface



(h) Concluded. $\alpha = 11.9^\circ$.

Figure 9.- Continued.

- | | |
|--|-----------------------|
| ○ Plain wing | $R = 4.0 \times 10^6$ |
| ○ Plain wing | $R = 1.5 \times 10^6$ |
| ◇ Wing with fences at 0.45, 0.70, and 0.89 $b/2$ | $R = 4.0 \times 10^6$ |
| Wing with leading-edge roughness | $R = 4.0 \times 10^6$ |

—○— Upper surface
 - - -○- - Lower surface

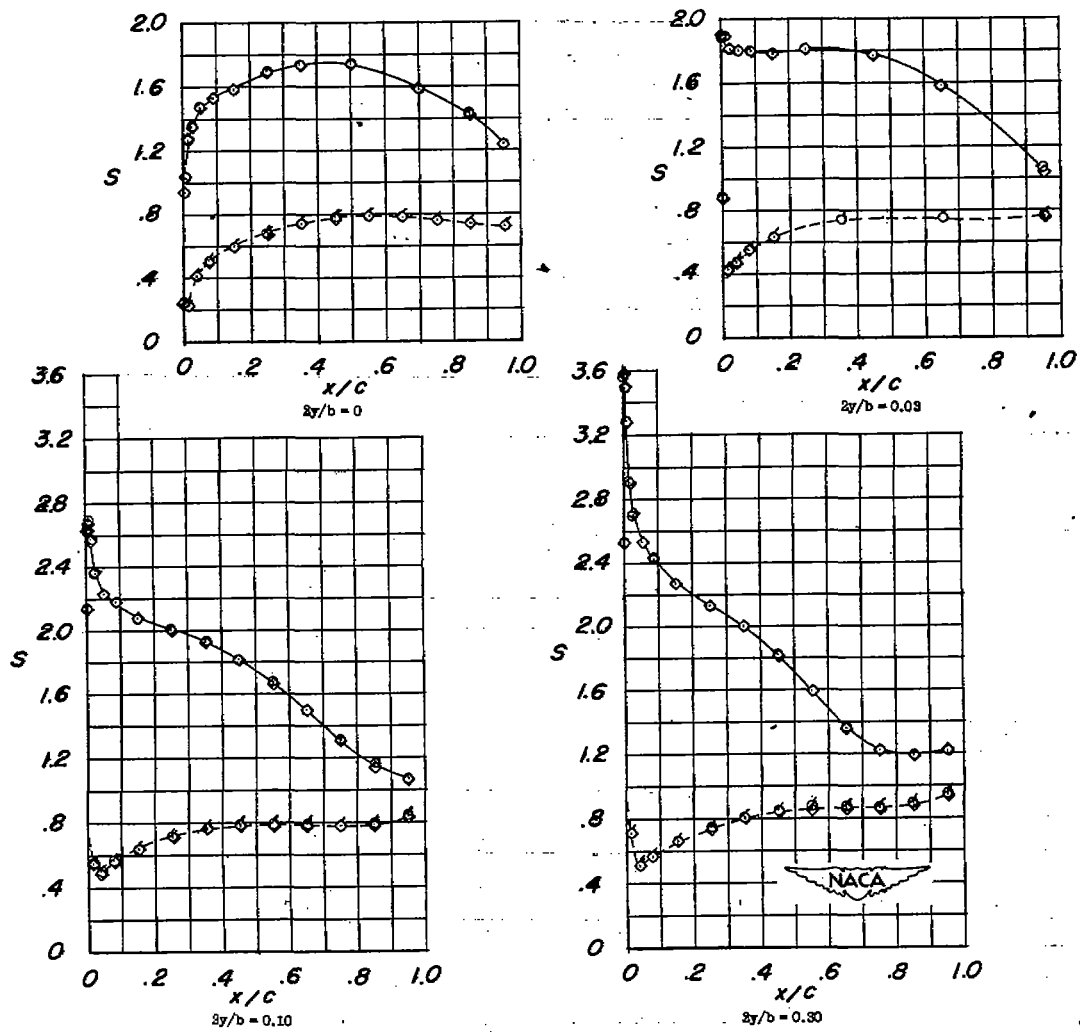
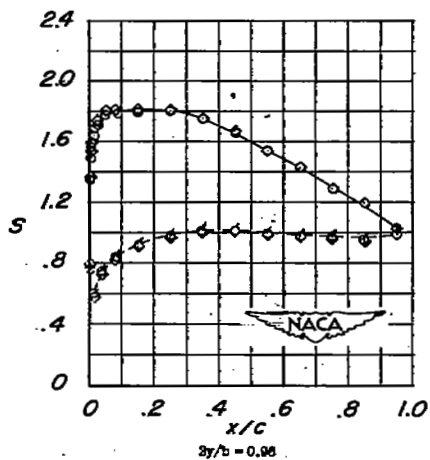
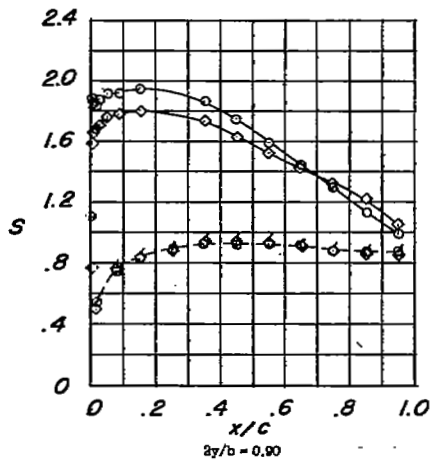
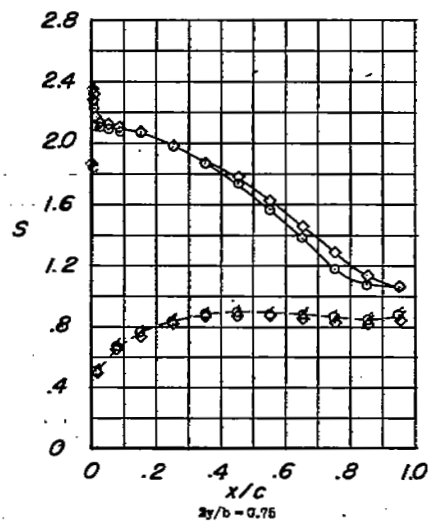
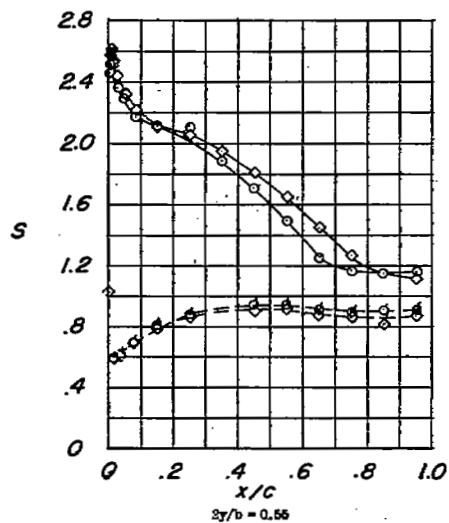


Figure 9.- Continued.

- | | |
|--|-----------------------|
| ○ Plain wing | $R = 4.0 \times 10^6$ |
| ○ Plain wing | $R = 1.5 \times 10^6$ |
| ◇ Wing with fences at 0.45, 0.70, and 0.88 $b/2$ | $R = 4.0 \times 10^6$ |
| Wing with leading-edge roughness | $R = 4.0 \times 10^6$ |

—○— Upper surface
 -◇- Lower surface

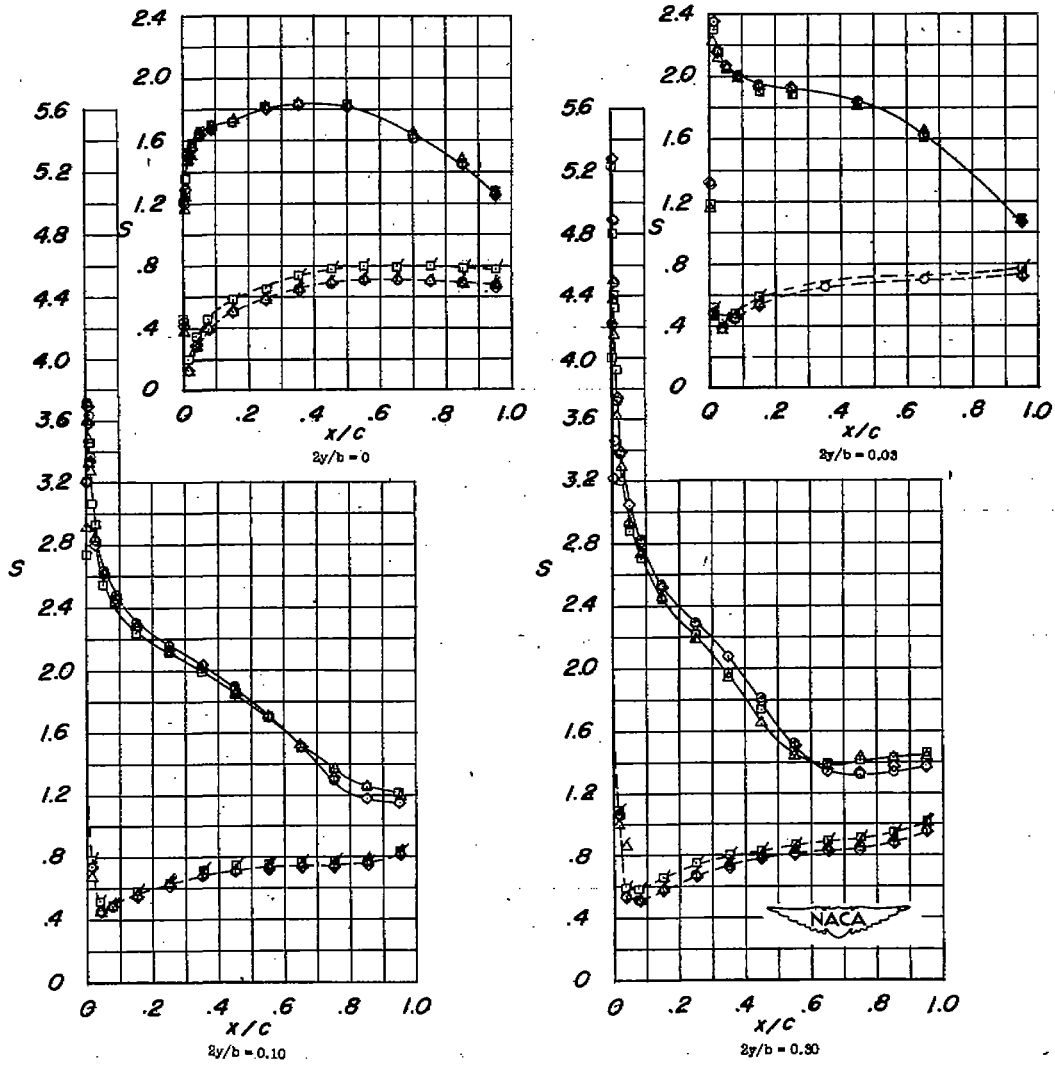


(i) Concluded. $\alpha = 13.9^\circ$.

Figure 9.- Continued.

- | | | |
|---|---------------------------|-----------------------|
| ○ | Plain wing | $R = 4.0 \times 10^6$ |
| □ | Plain wing | $R = 1.6 \times 10^6$ |
| ◇ | Wing with fences at 0.45, | $R = 4.0 \times 10^6$ |
| | 0.70, and 0.89 $b/2$ | |
| △ | Wing with leading-edge | $R = 4.0 \times 10^6$ |
| | roughness | |

- | | |
|-------------|---------------|
| —○— | Upper surface |
| - - -○- - - | Lower surface |

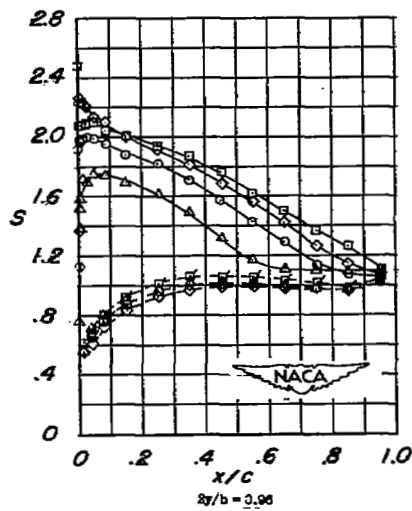
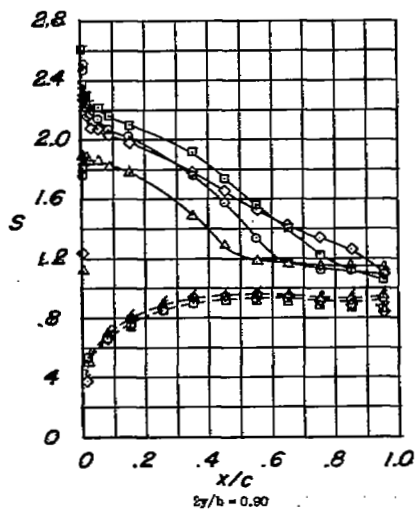
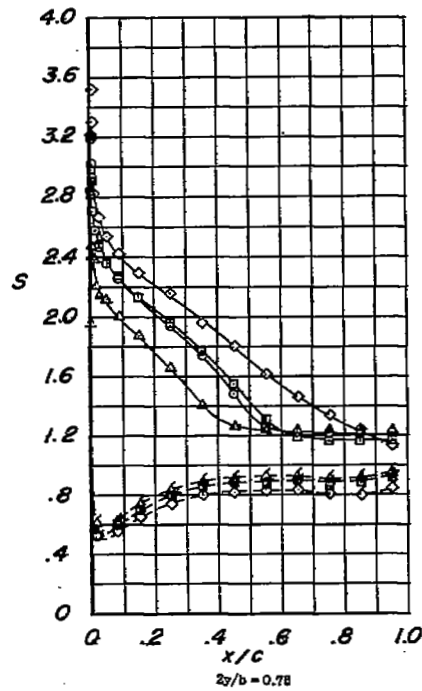
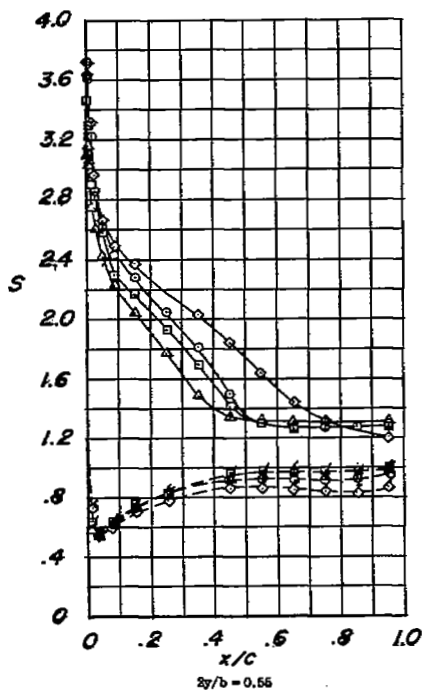


(j) $\alpha = 17.0^\circ$.

Figure 9.- Continued.

- | | |
|--|-----------------------|
| ○ Plain wing | $R = 4.0 \times 10^6$ |
| □ Plain wing | $R = 1.5 \times 10^6$ |
| ◇ Wing with fences at 0.45, 0.70, and 0.89 $b/2$ | $R = 4.0 \times 10^6$ |
| △ Wing with leading-edge roughness | $R = 4.0 \times 10^6$ |

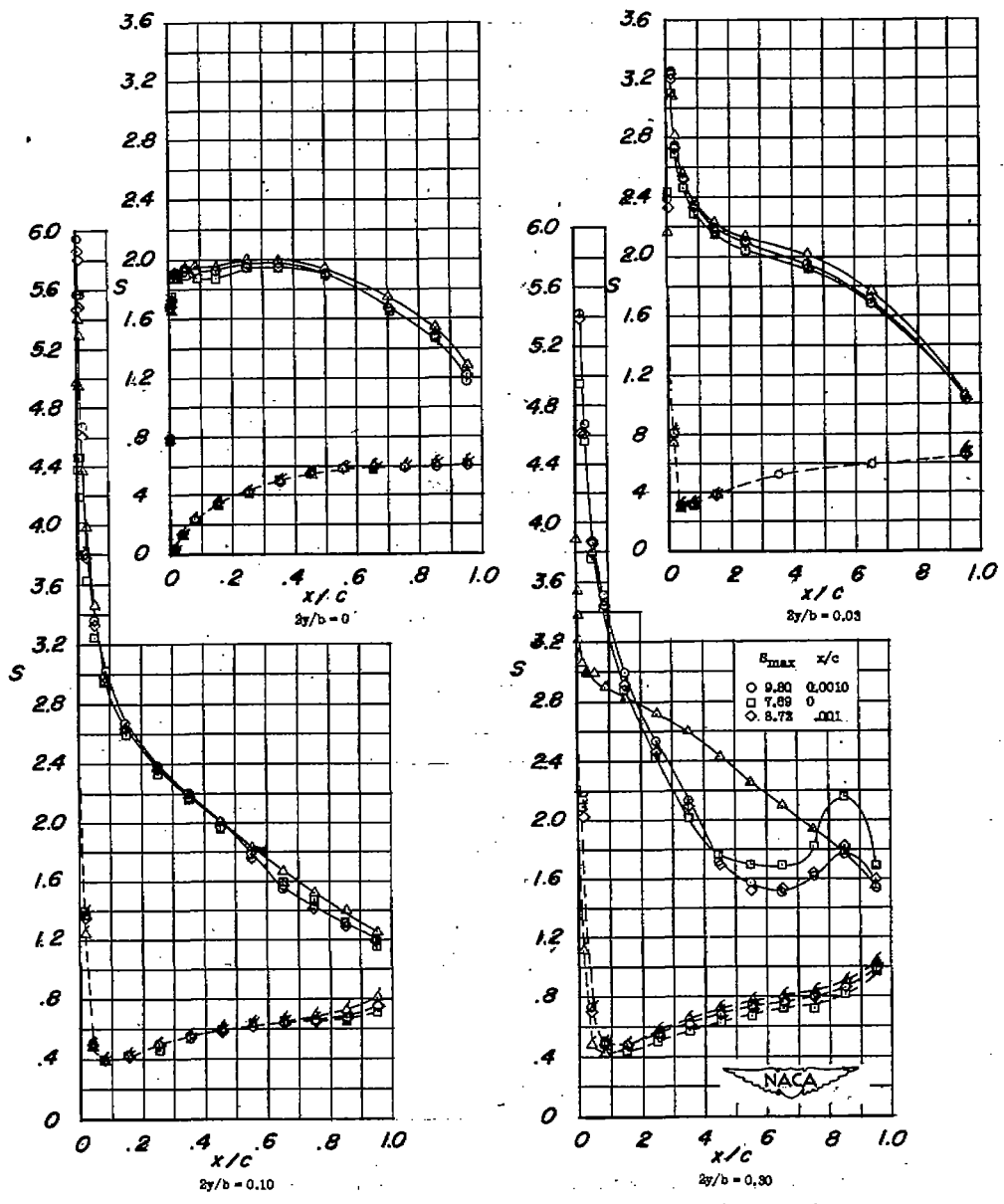
—○— Upper surface
 - -○- - Lower surface



(j) Concluded. $\alpha = 17.0^\circ$.

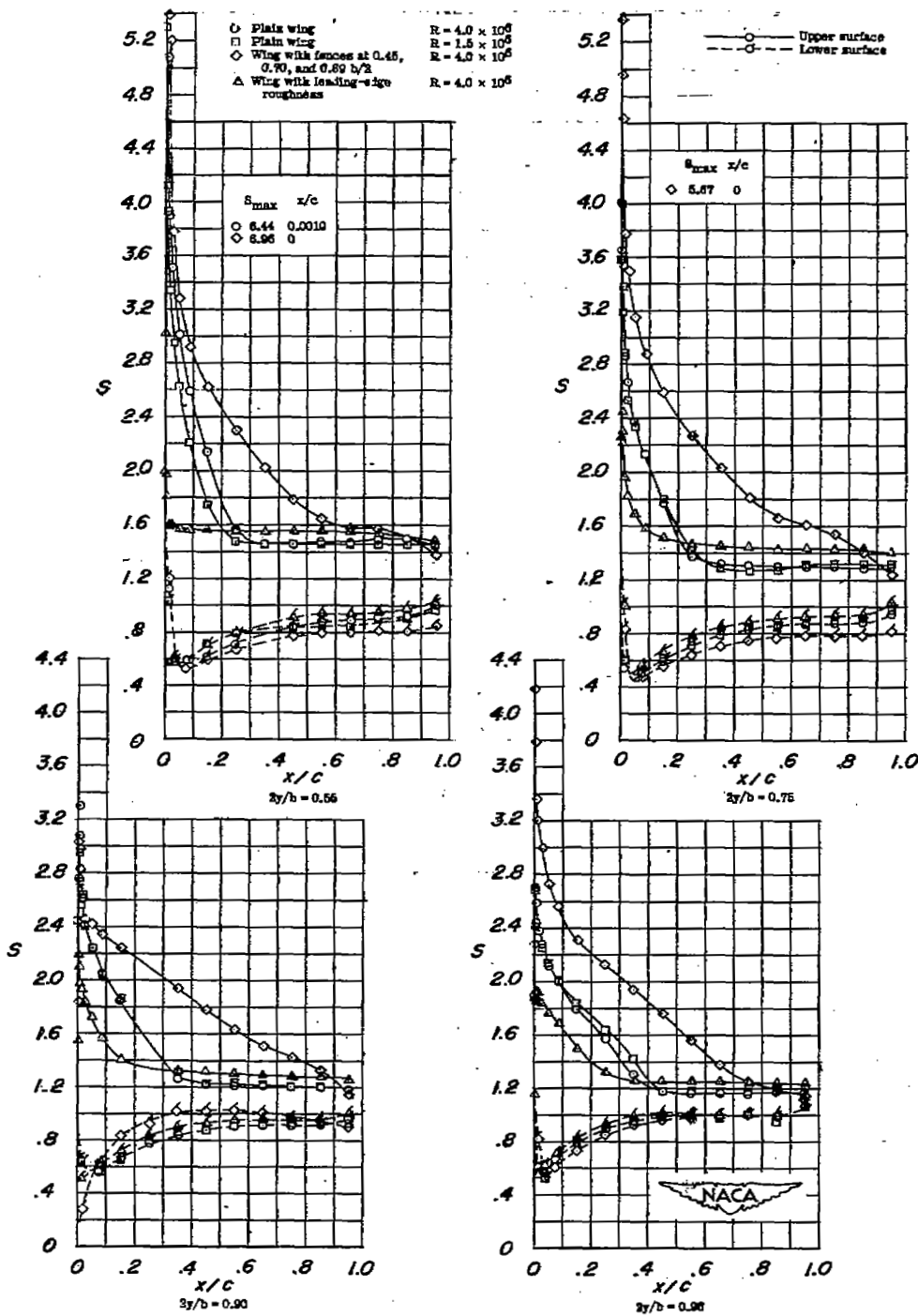
Figure 9.- Continued.

- Plain wing $R = 4.0 \times 10^6$
 - Plain wing $R = 1.5 \times 10^6$
 - ◇ Wing with fences at 0.45, 0.70, and 0.89 b/s $R = 4.0 \times 10^6$
 - △ Wing with leading-edge roughness $R = 4.0 \times 10^6$
- Upper surface
 - - Lower surface



(k) $\alpha = 22.0^\circ$.

Figure 9.- Continued.

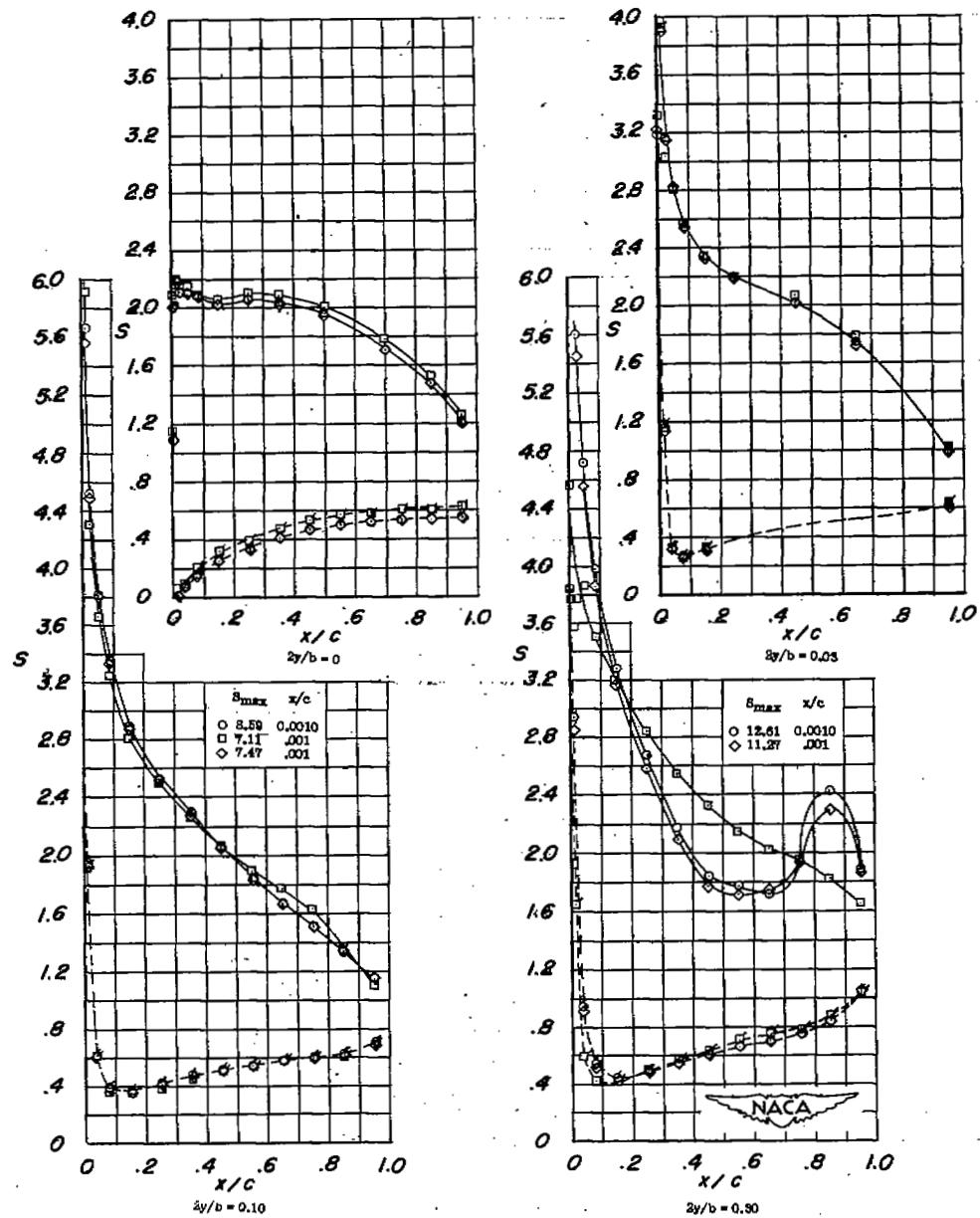


(k) Concluded. $\alpha = 22.0^\circ$.

Figure 9.- Continued.

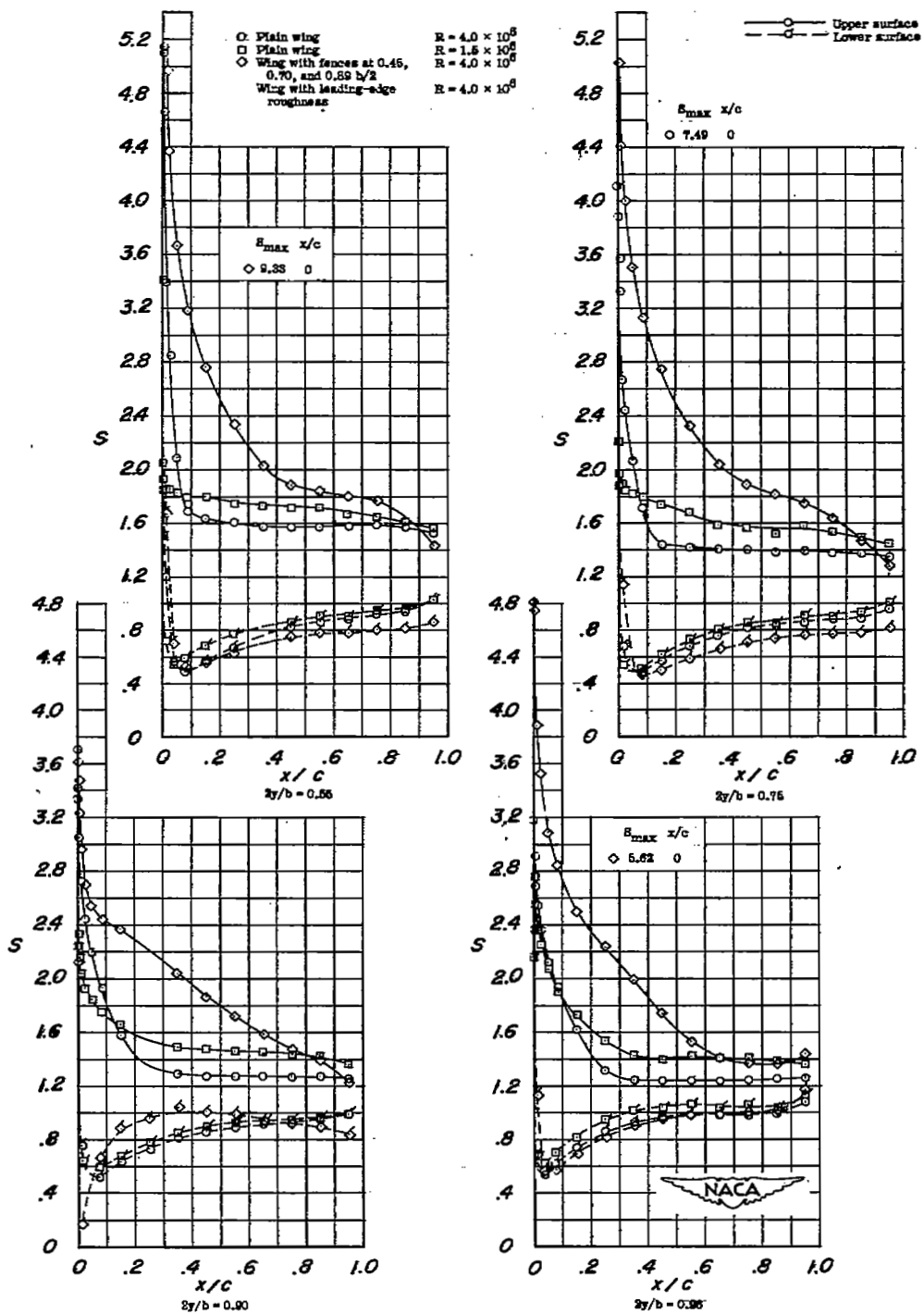
- Plain wing $R = 4.0 \times 10^6$
 □ Plain wing $R = 1.5 \times 10^6$
 ◇ Wing with fences at 0.45, 0.70, and 0.89 $b/3$ $R = 4.0 \times 10^6$
 Wing with leading-edge roughness $R = 4.0 \times 10^6$

—○— Upper surface
 - - -○ - - Lower surface



(2) $\alpha = 25.1^\circ$.

Figure 9.- Continued.

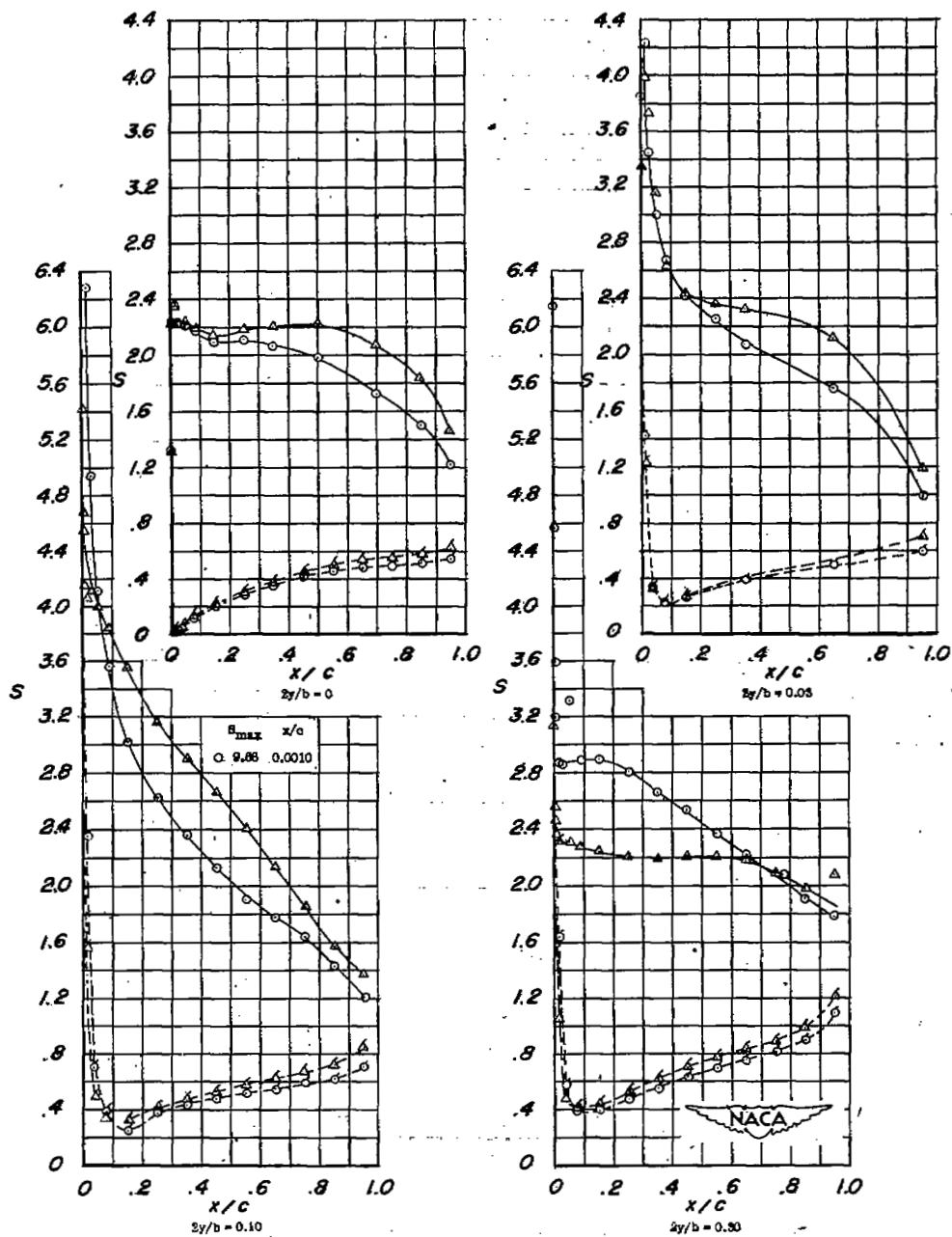


(1) Concluded. $\alpha = 25.1^\circ$.

Figure 9.- Continued.

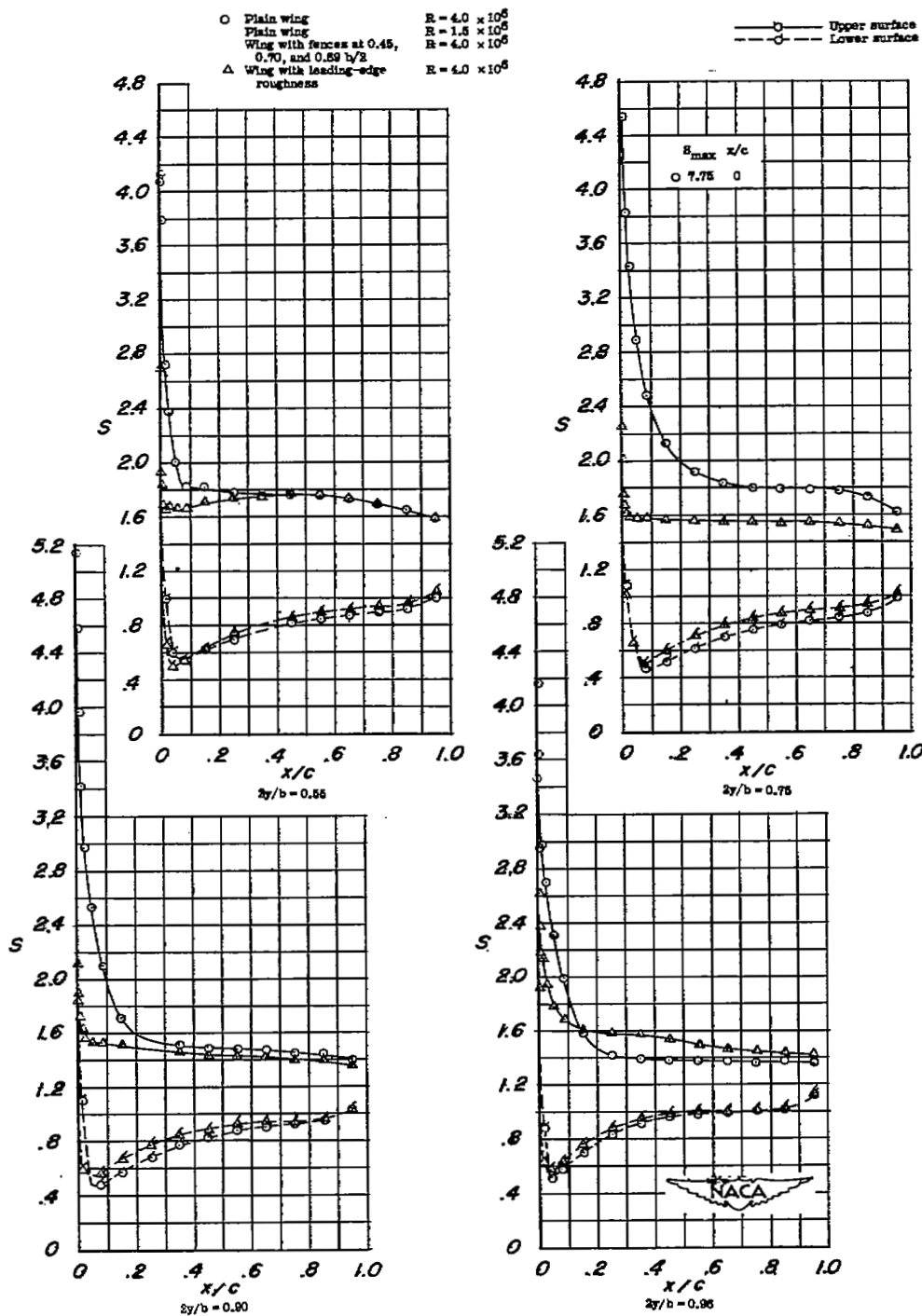
- Plain wing $R = 4.0 \times 10^6$
 Plain wing $R = 1.6 \times 10^6$
 Wing with fences at 0.46, 0.70, and 0.89 $b/2$ $R = 4.0 \times 10^6$
 △ Wing with leading-edge roughness $R = 4.0 \times 10^6$

—○— Upper surface
 - - -○ - - Lower surface



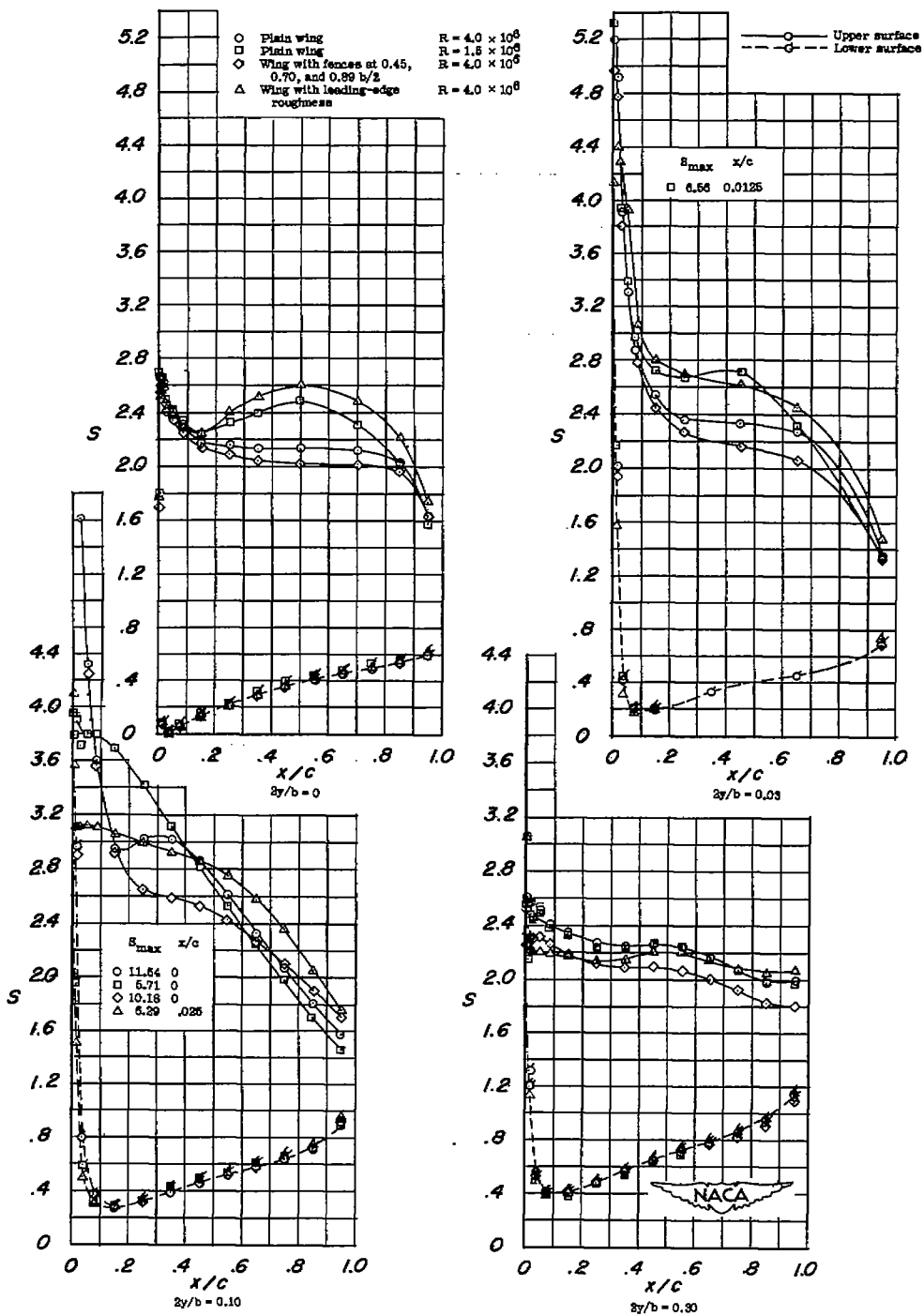
(m) $\alpha = 27.1^\circ$.

Figure 9.- Continued.



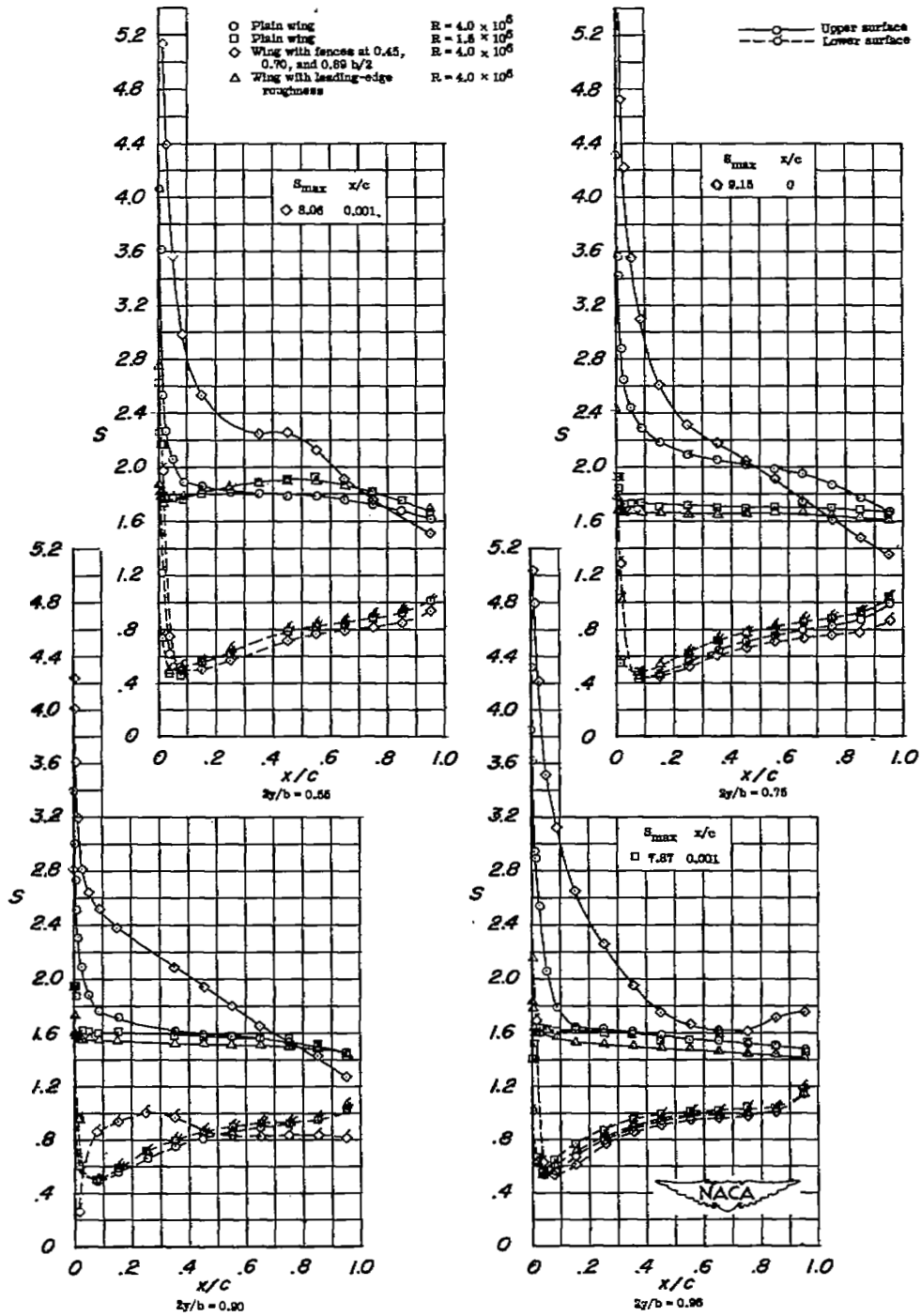
(m) Concluded. $\alpha = 27.1^\circ$.

Figure 9.- Continued.



(n) $\alpha = 31.1^\circ$.

Figure 9.- Continued.



(n) Concluded. $\alpha = 31.1^\circ$.

Figure 9.- Concluded.

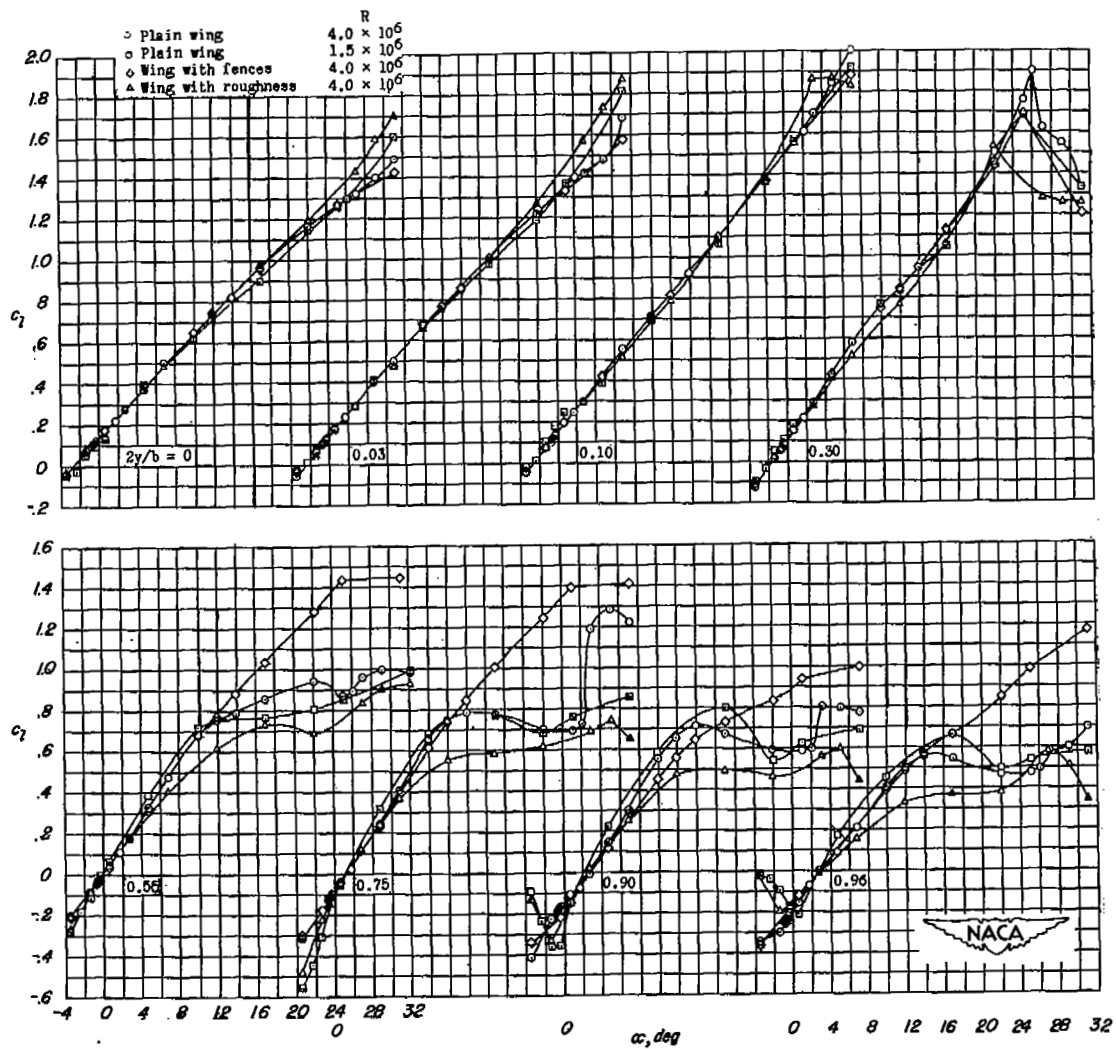
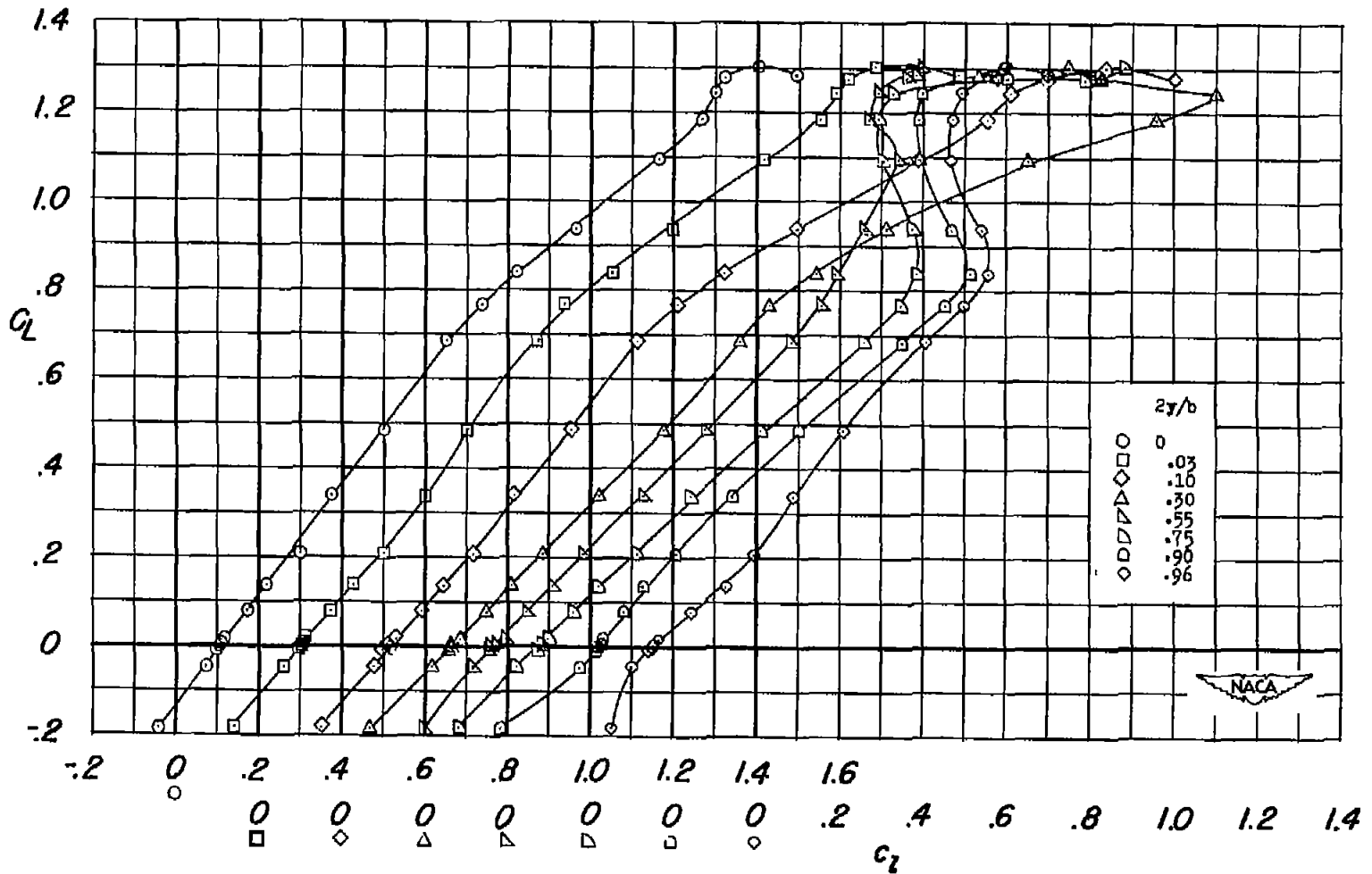
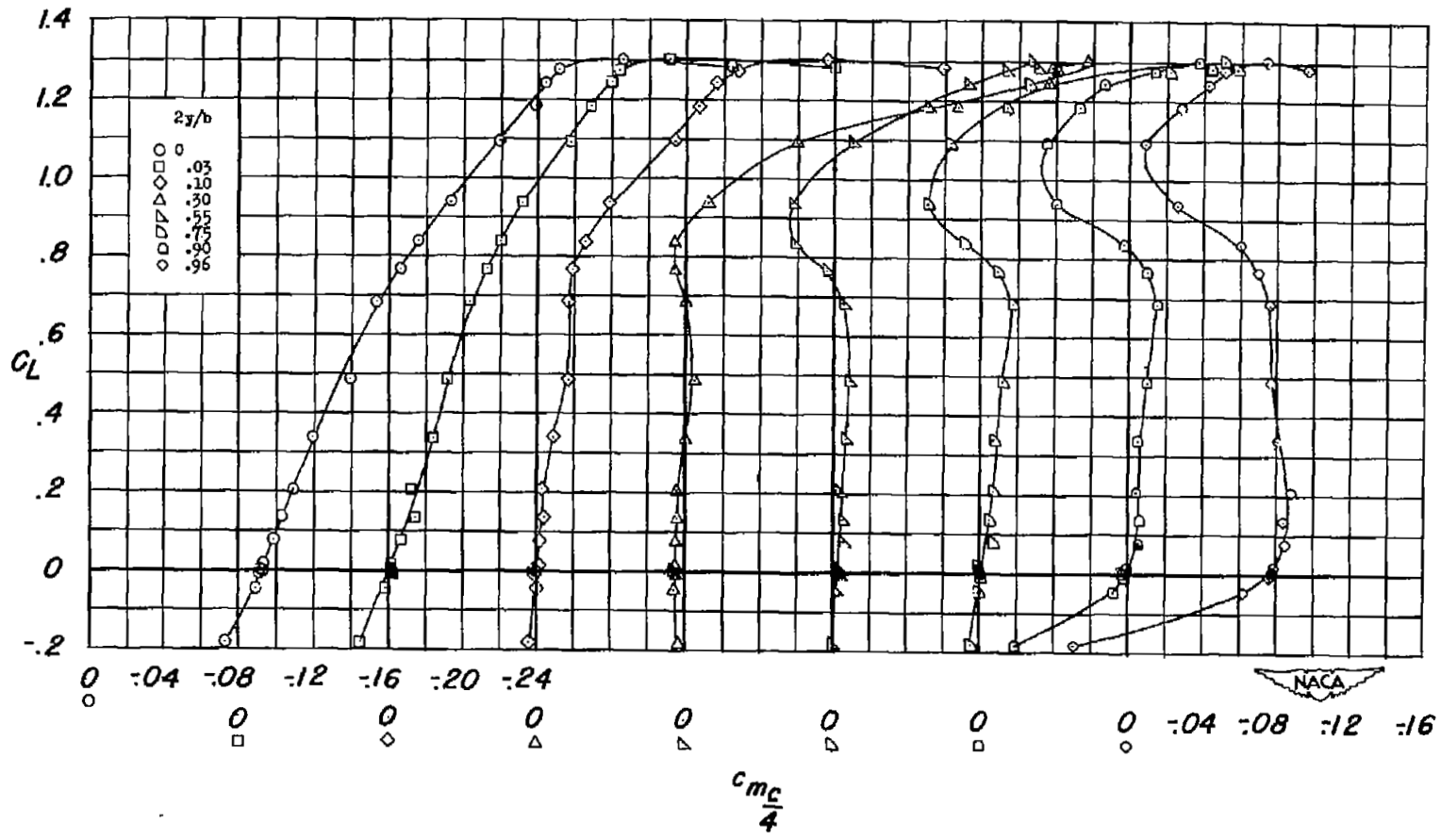


Figure 10.- Effects of Reynolds number, fences, and leading-edge roughness on the section lift characteristics of the twisted and cambered wing.



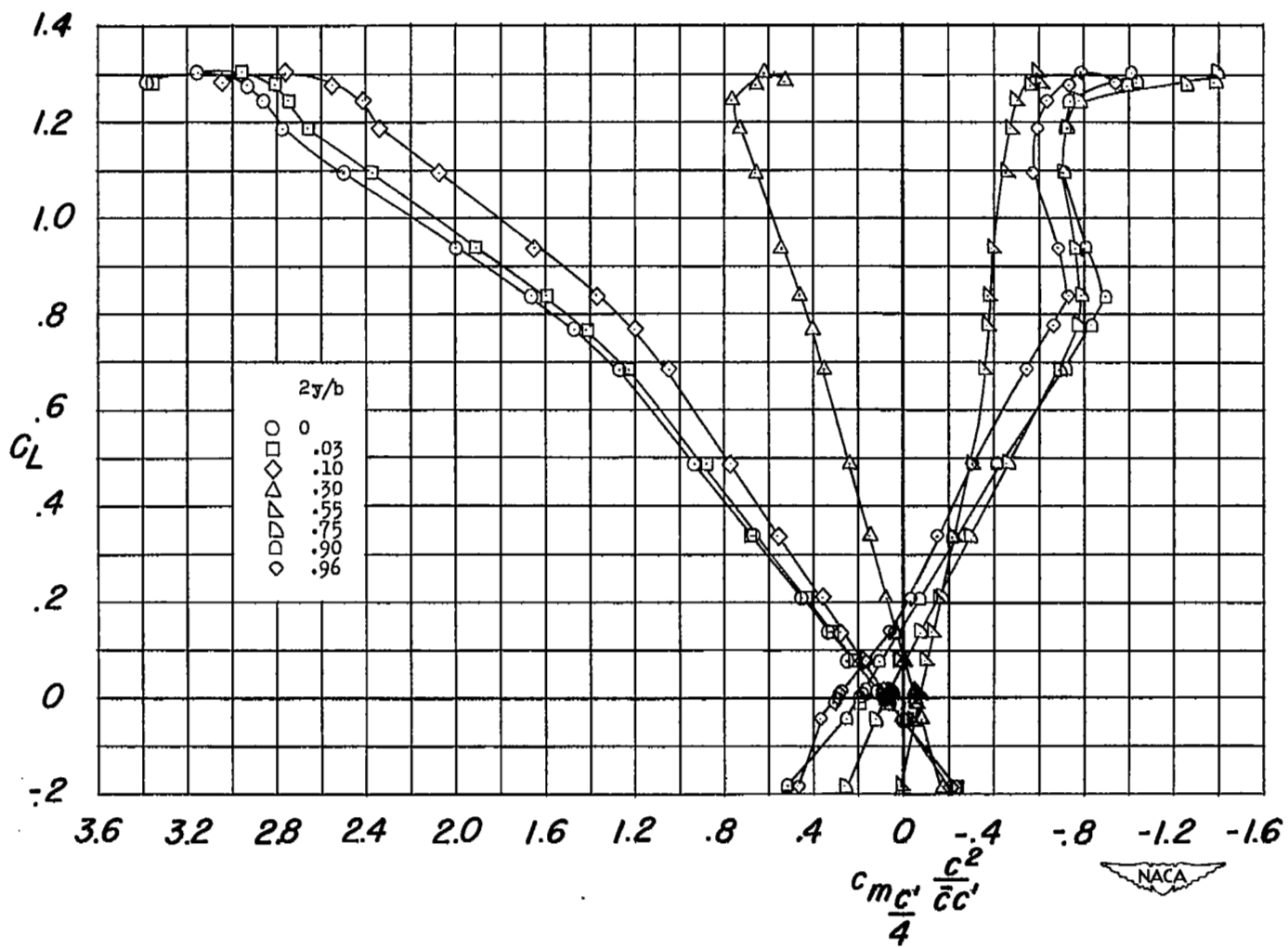
(a) Section lift.

Figure 11.- Section lift, pitching-moment, and drag characteristics on the twisted and cambered wing.



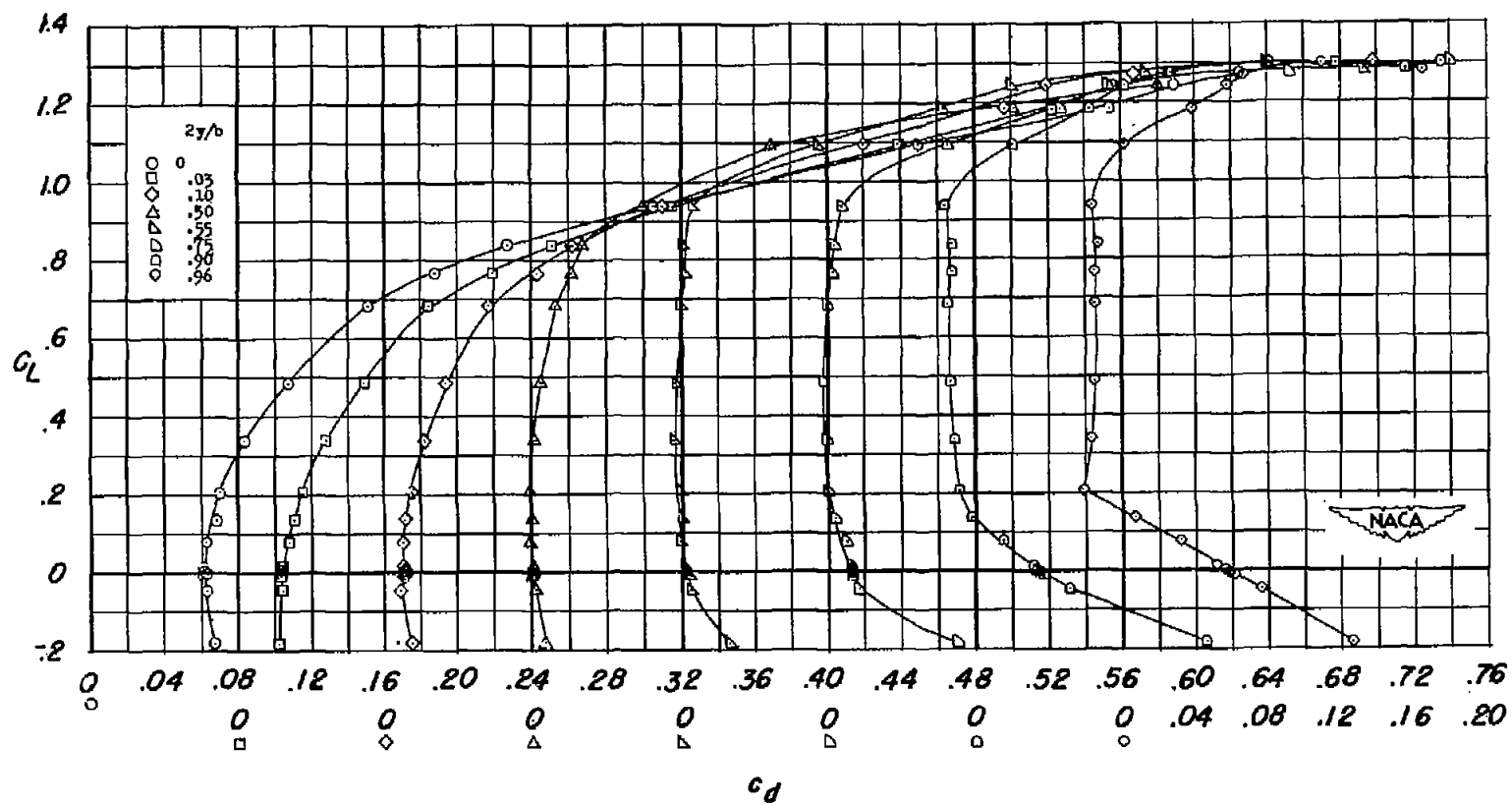
(b) Section pitching moment.

Figure 11.- Continued.



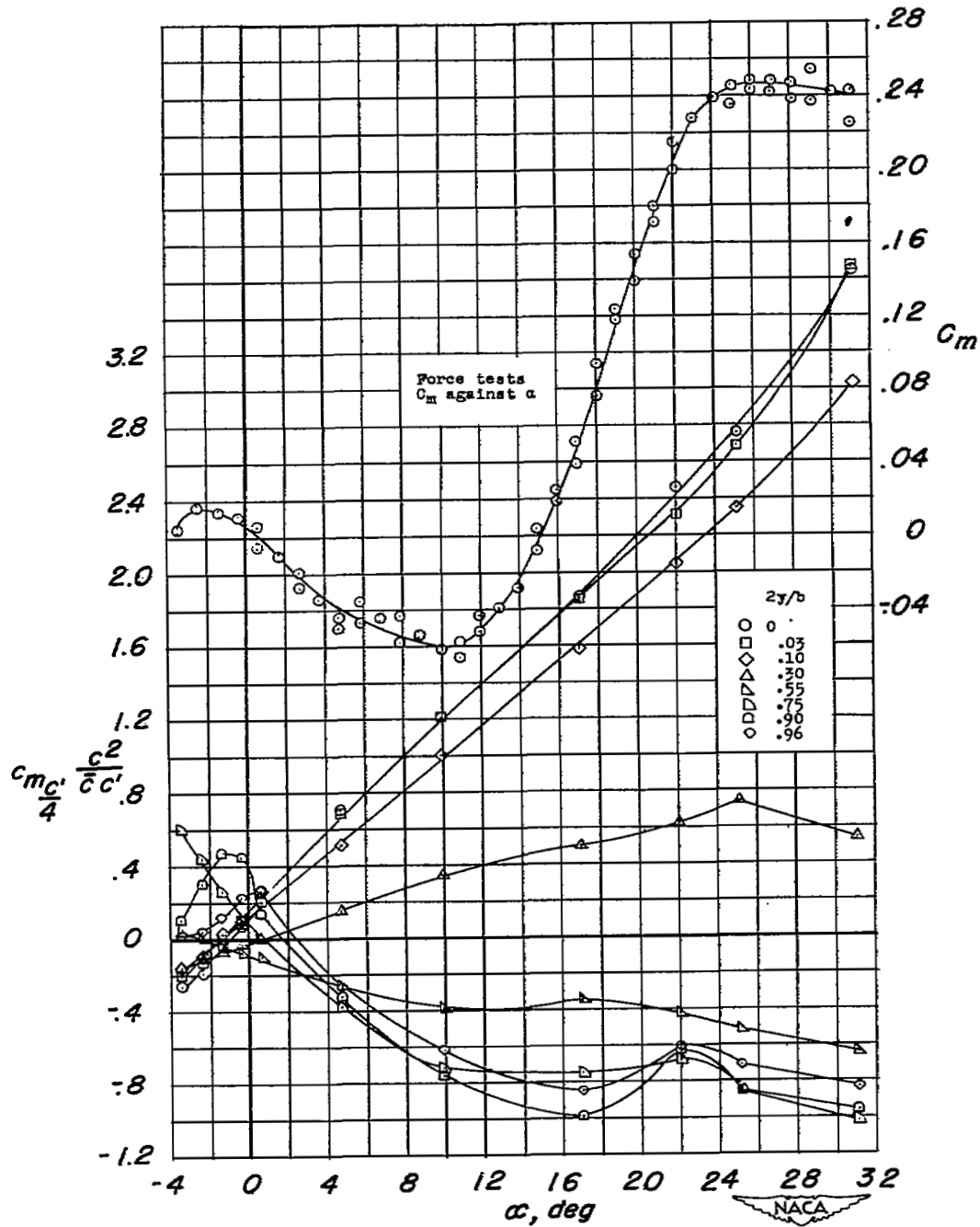
(c) Section pitching-moment parameter.

Figure 11.- Continued.



(d) Section pressure drag.

Figure 11.- Concluded.



(a) Plain wing; $R = 1.5 \times 10^6$.

Figure 12.- Comparison of section pitching-moment parameters and force-test pitching-moment coefficients on twisted and cambered wing.

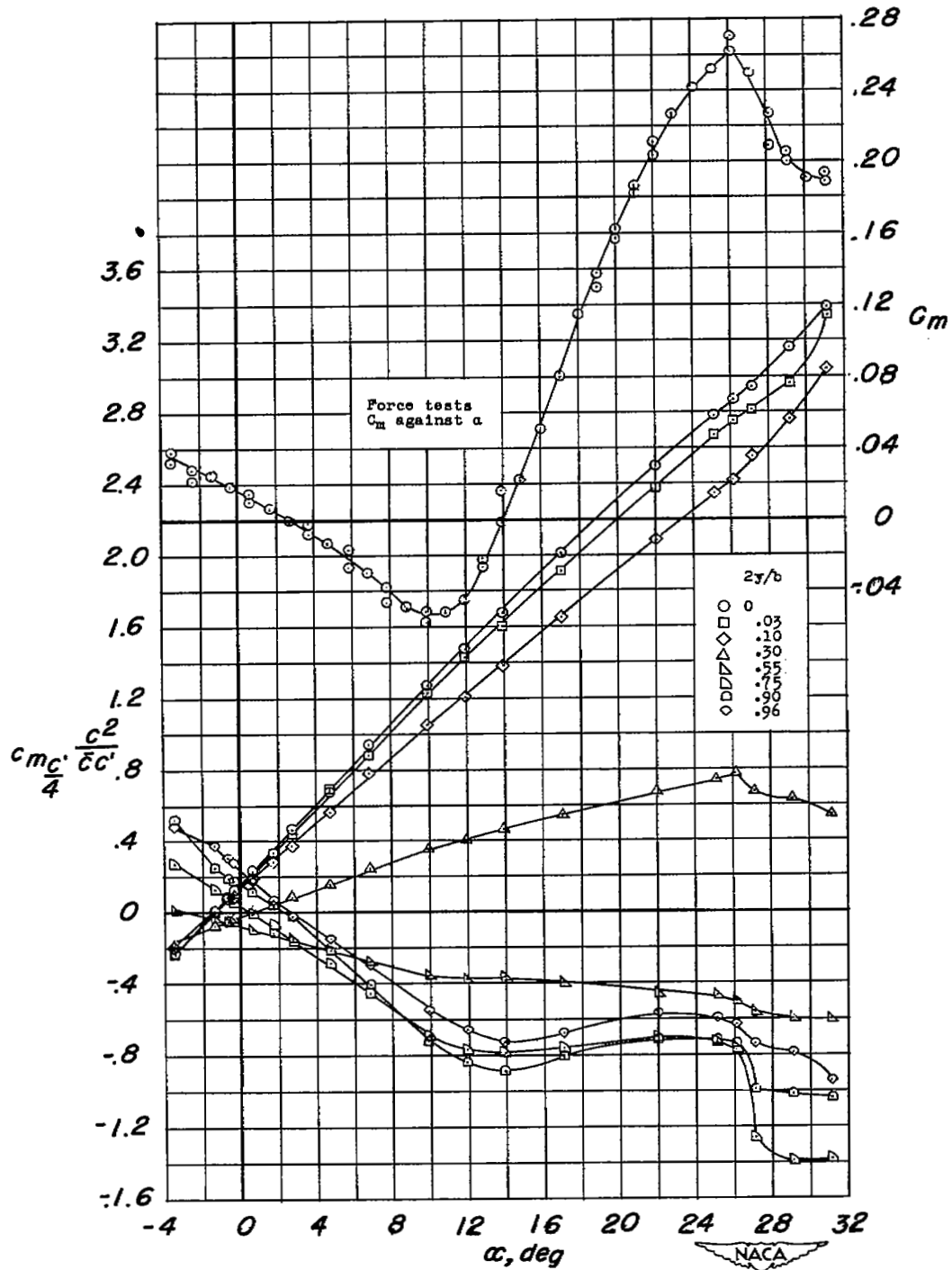
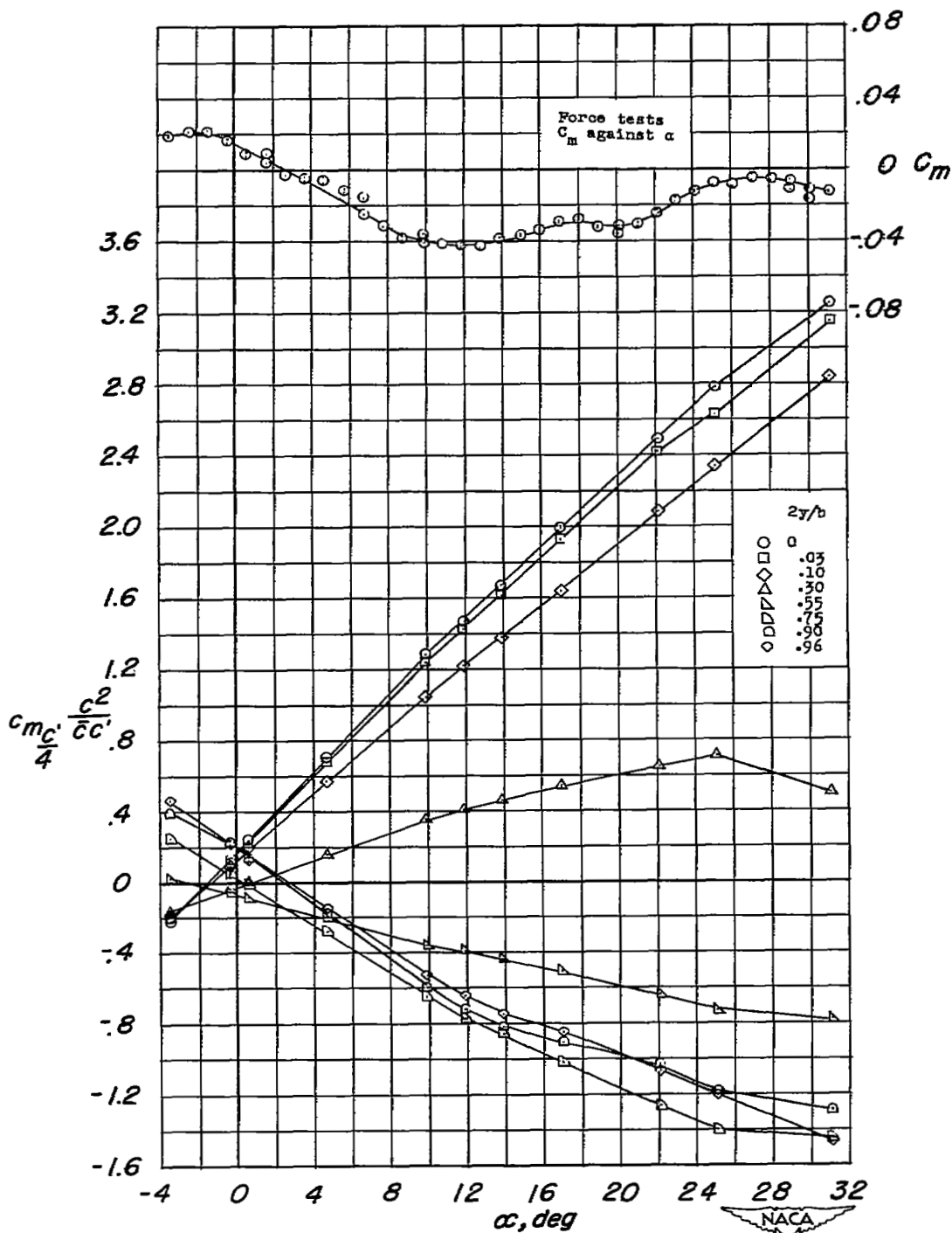
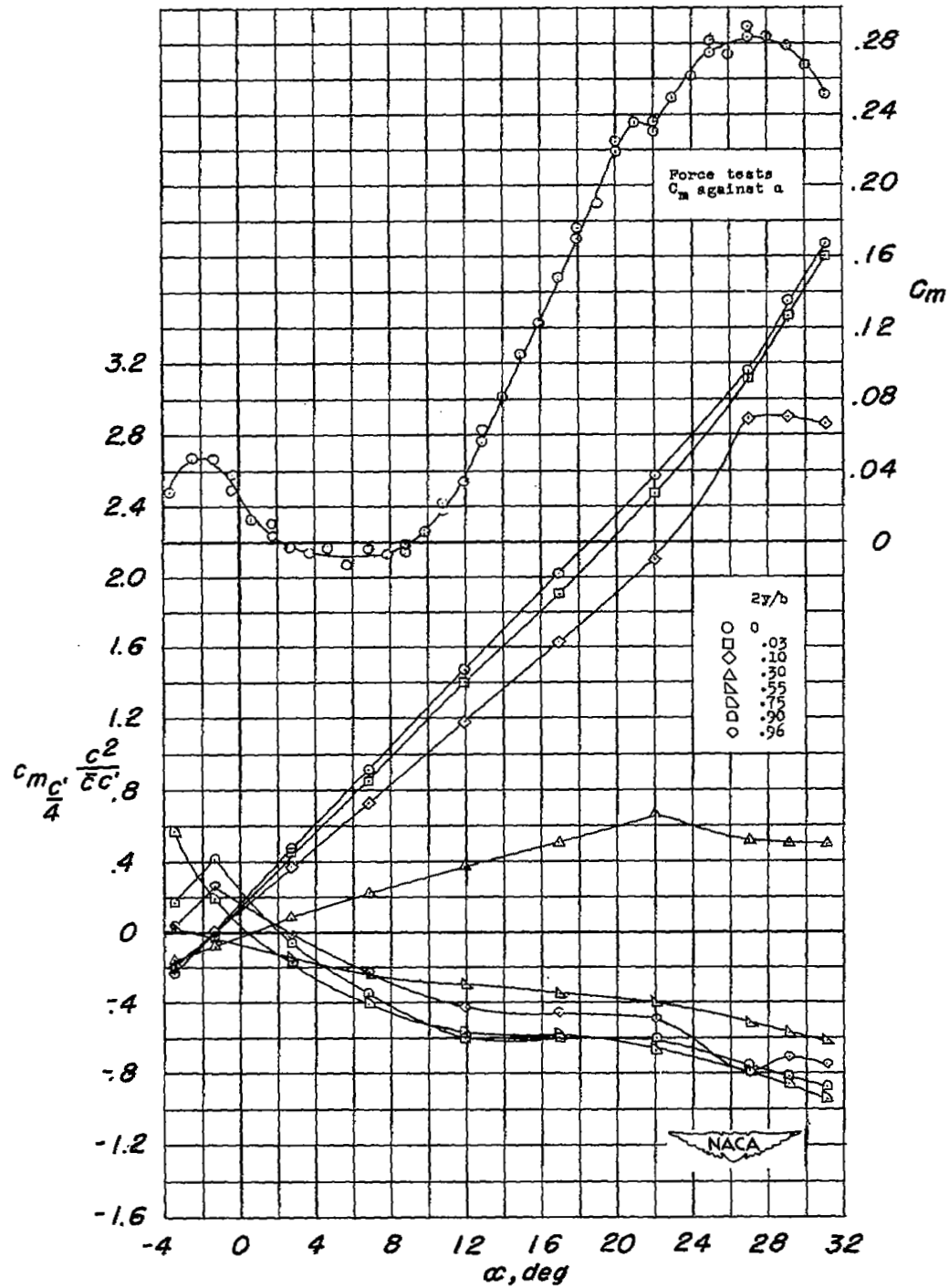
(b) Plain wing; $R = 4.0 \times 10^6$.

Figure 12.- Continued.



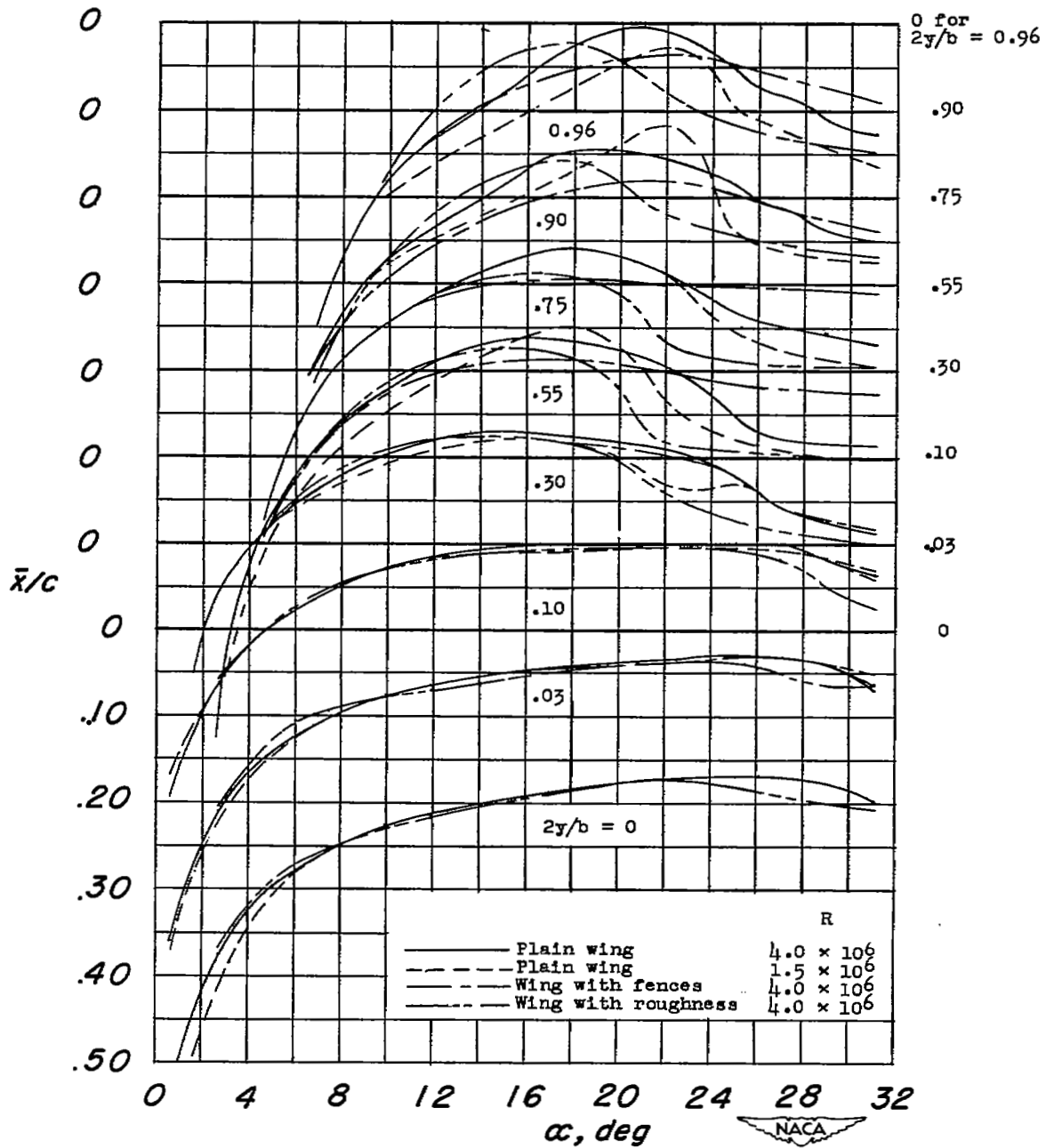
(c) Wing with fences; $R = 4.0 \times 10^6$.

Figure 12.- Continued.



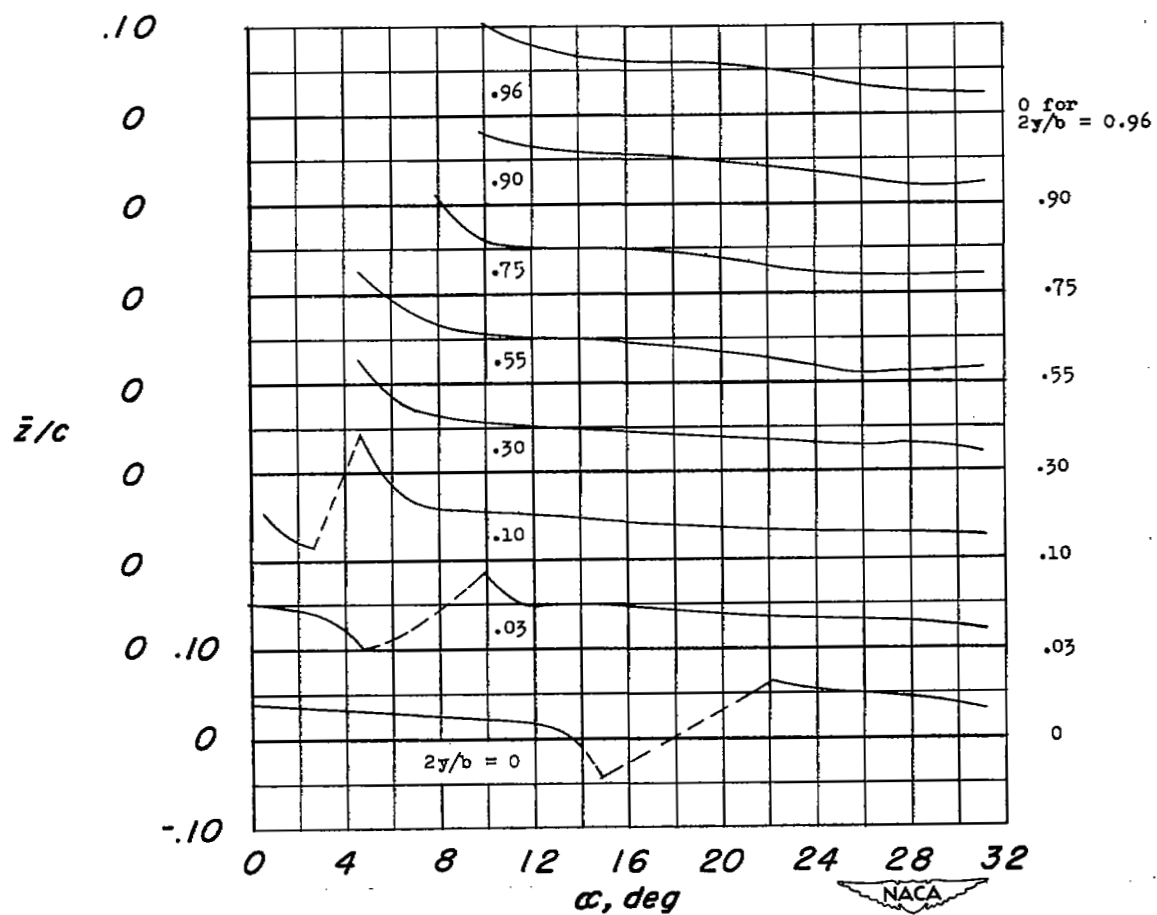
(d) Wing with leading-edge roughness; $R = 4.0 \times 10^6$.

Figure 12.- Concluded.



(a) Section chordwise center of pressure.

Figure 13.- Section chordwise and vertical centers of pressure for twisted and cambered wing.



(b) Section vertical center of pressure. Plain wing; $R = 4.0 \times 10^6$.

Figure 13.- Concluded.

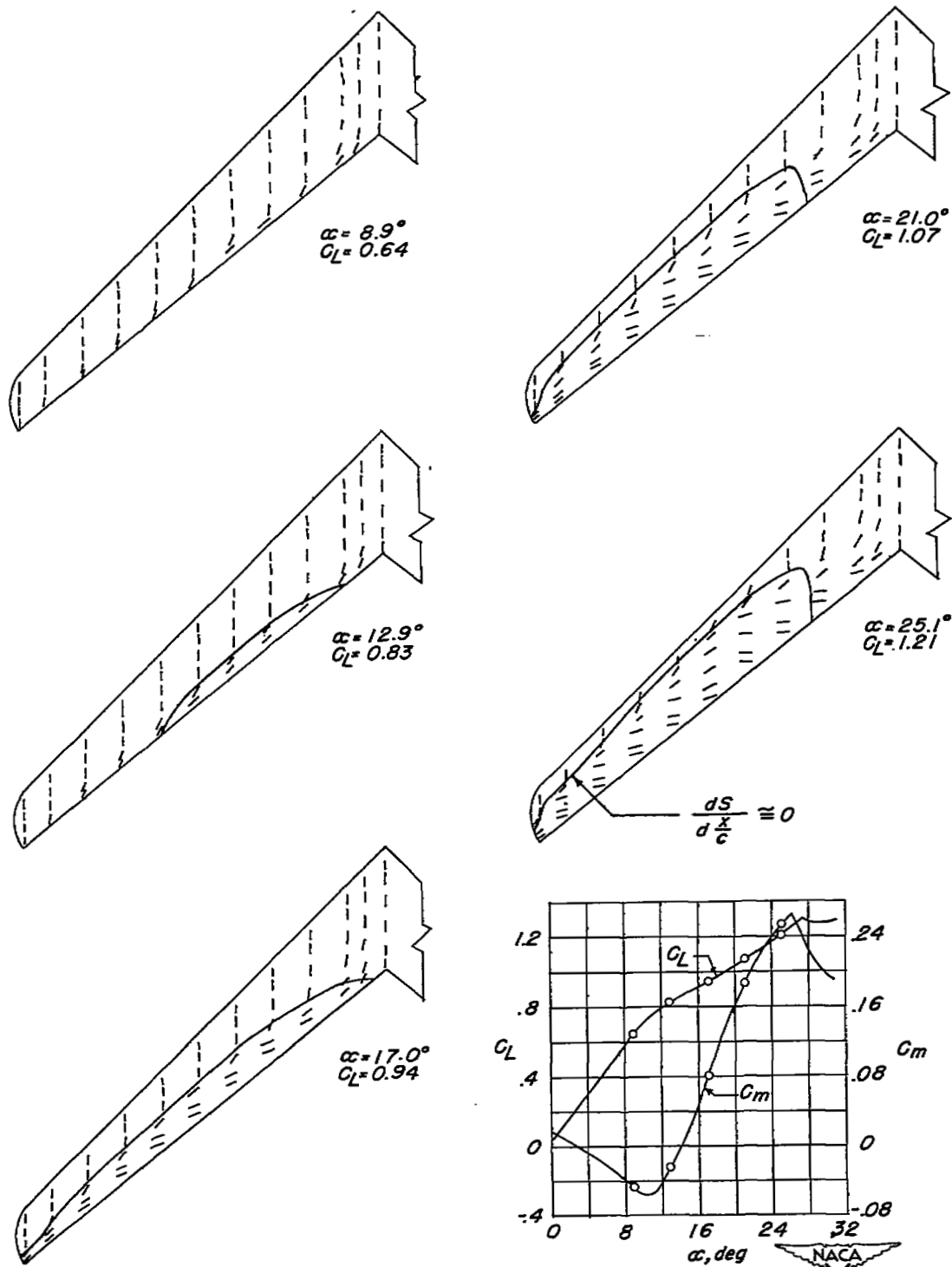
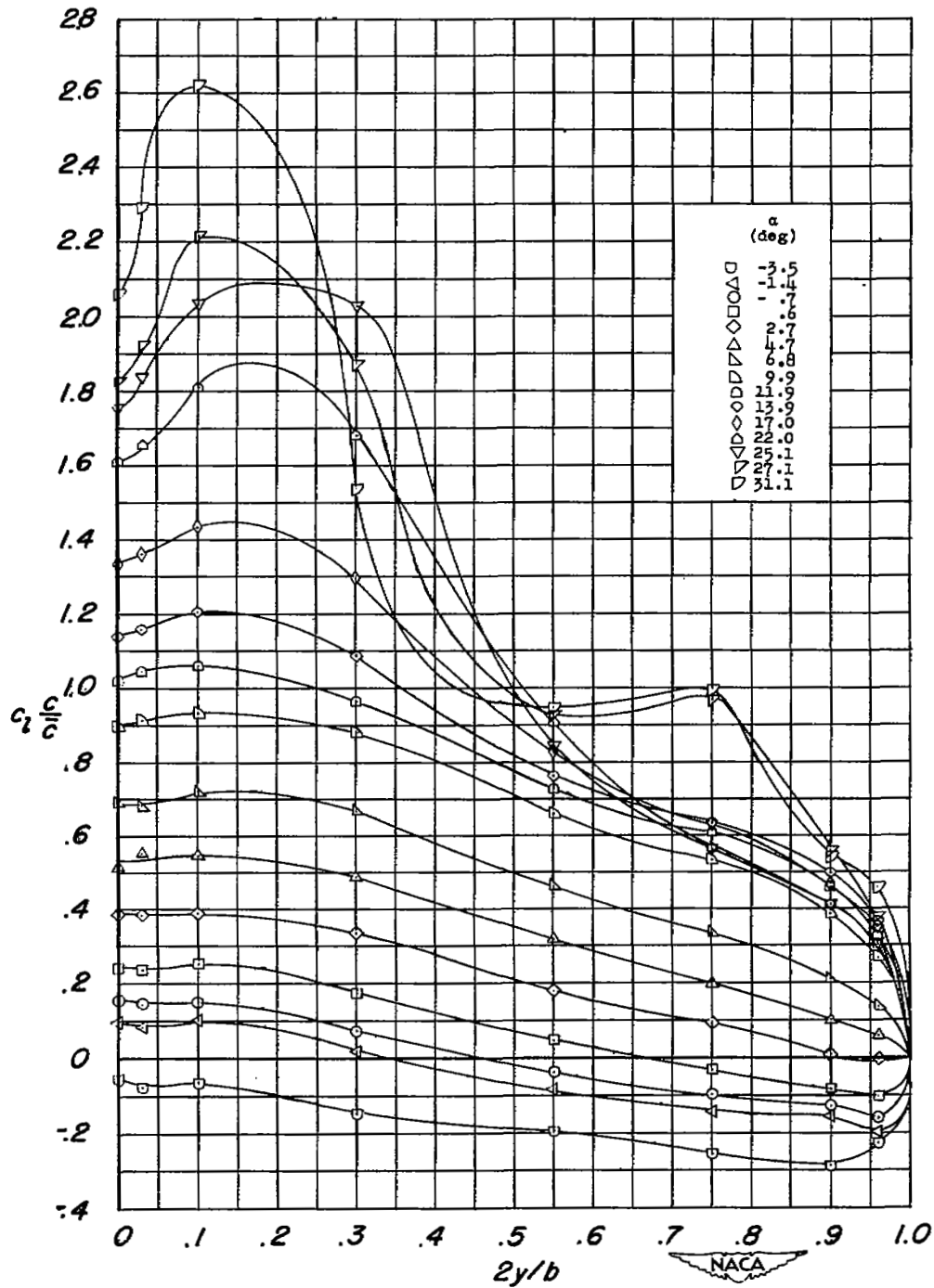
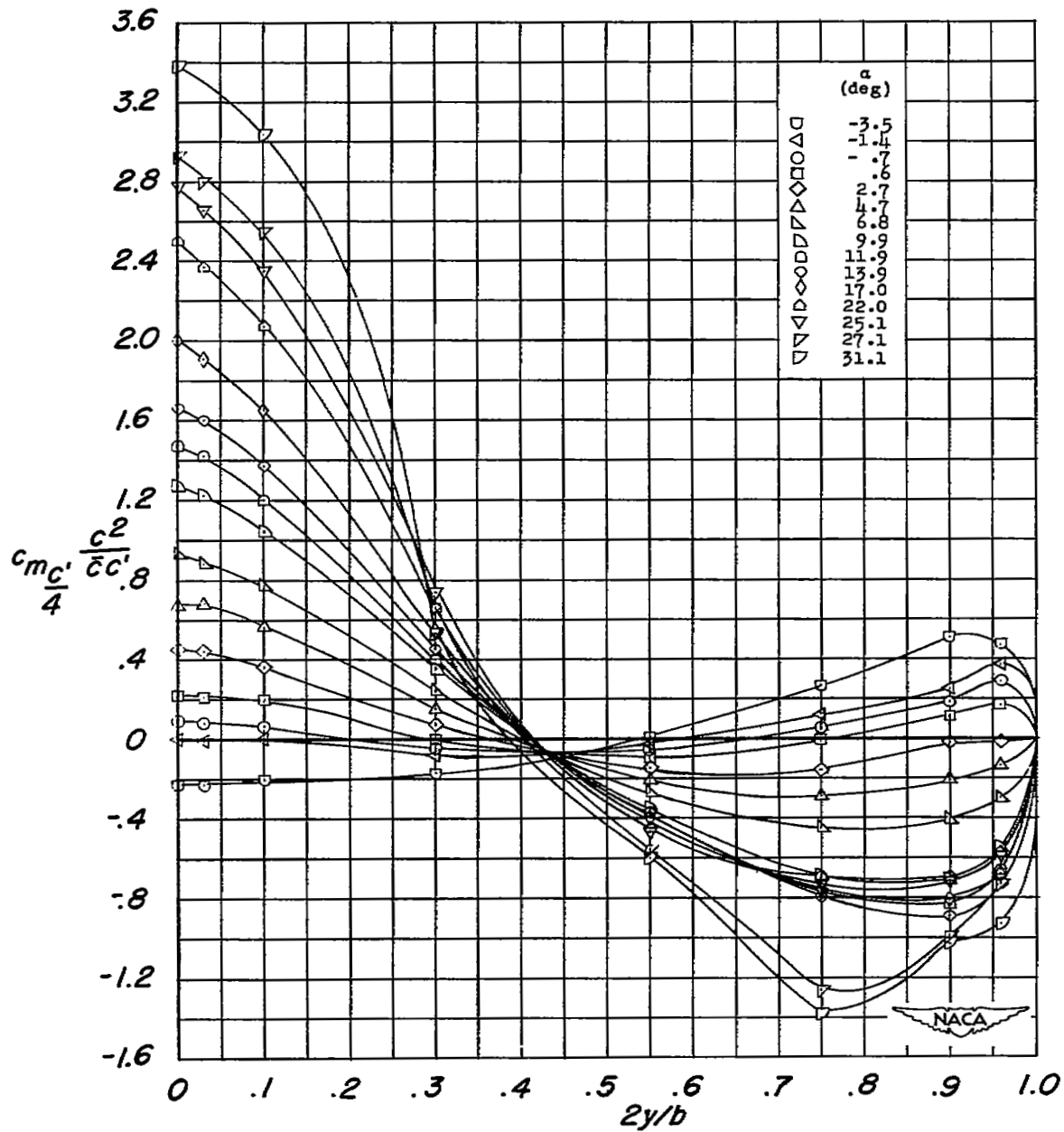


Figure 14.- Tuft studies on twisted and cambered wing. $R = 4.0 \times 10^6$.



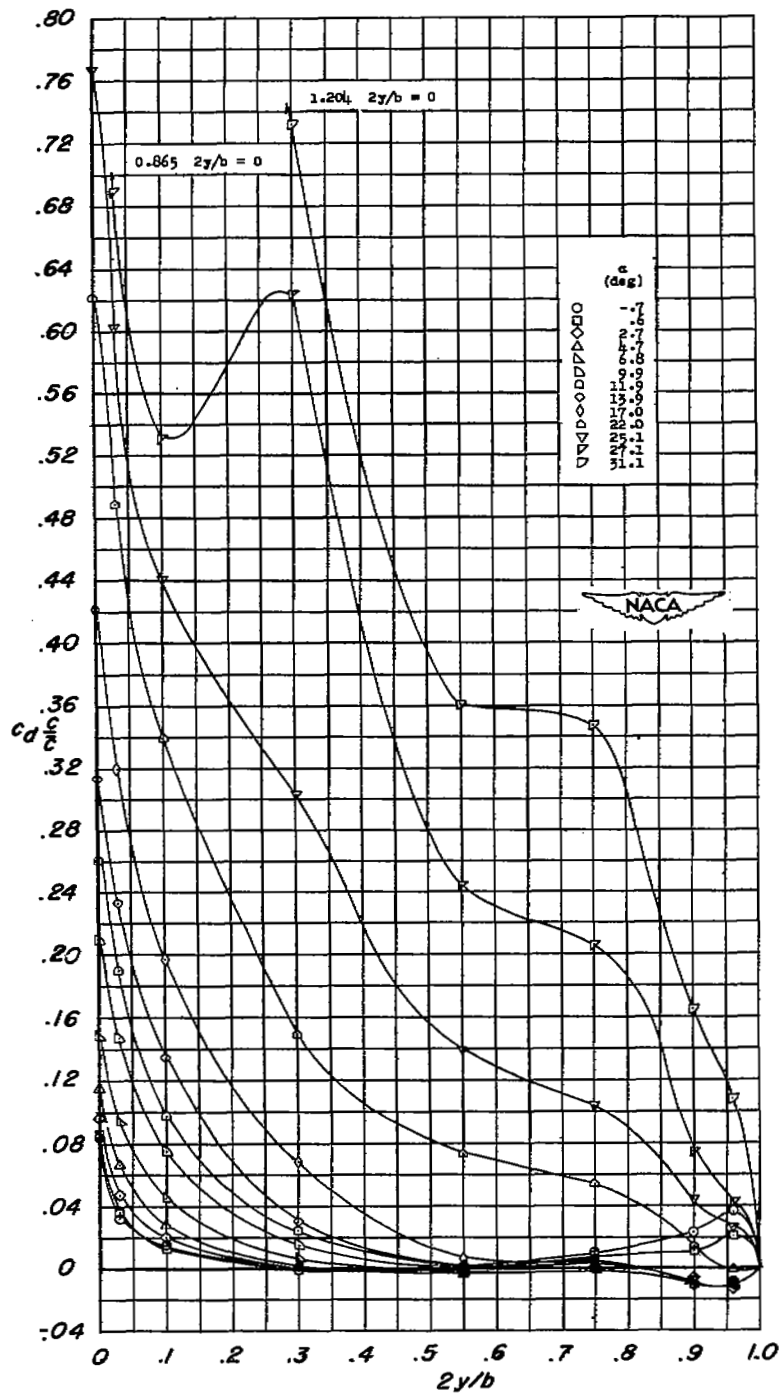
(a) Lift.

Figure 15.- Spanwise lift, pitching-moment, and drag-loading characteristics of the twisted and cambered wing. $R = 4.0 \times 10^6$.



(b) Pitching moment.

Figure 15.- Continued.



(c) Drag.

Figure 15.- Concluded.

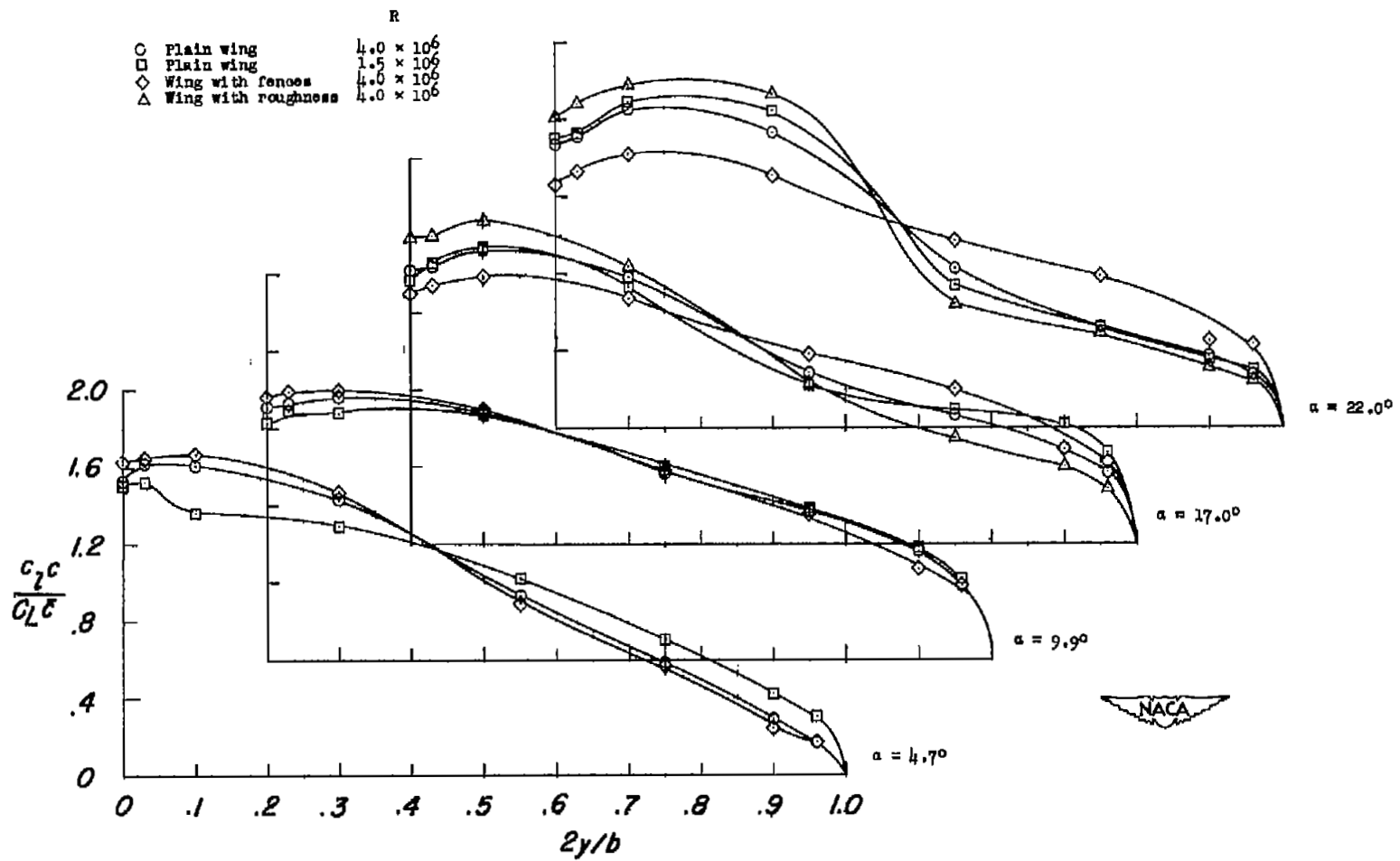


Figure 16.- Effect of Reynolds number, fences, and leading-edge roughness on the spanwise lift loading characteristics.

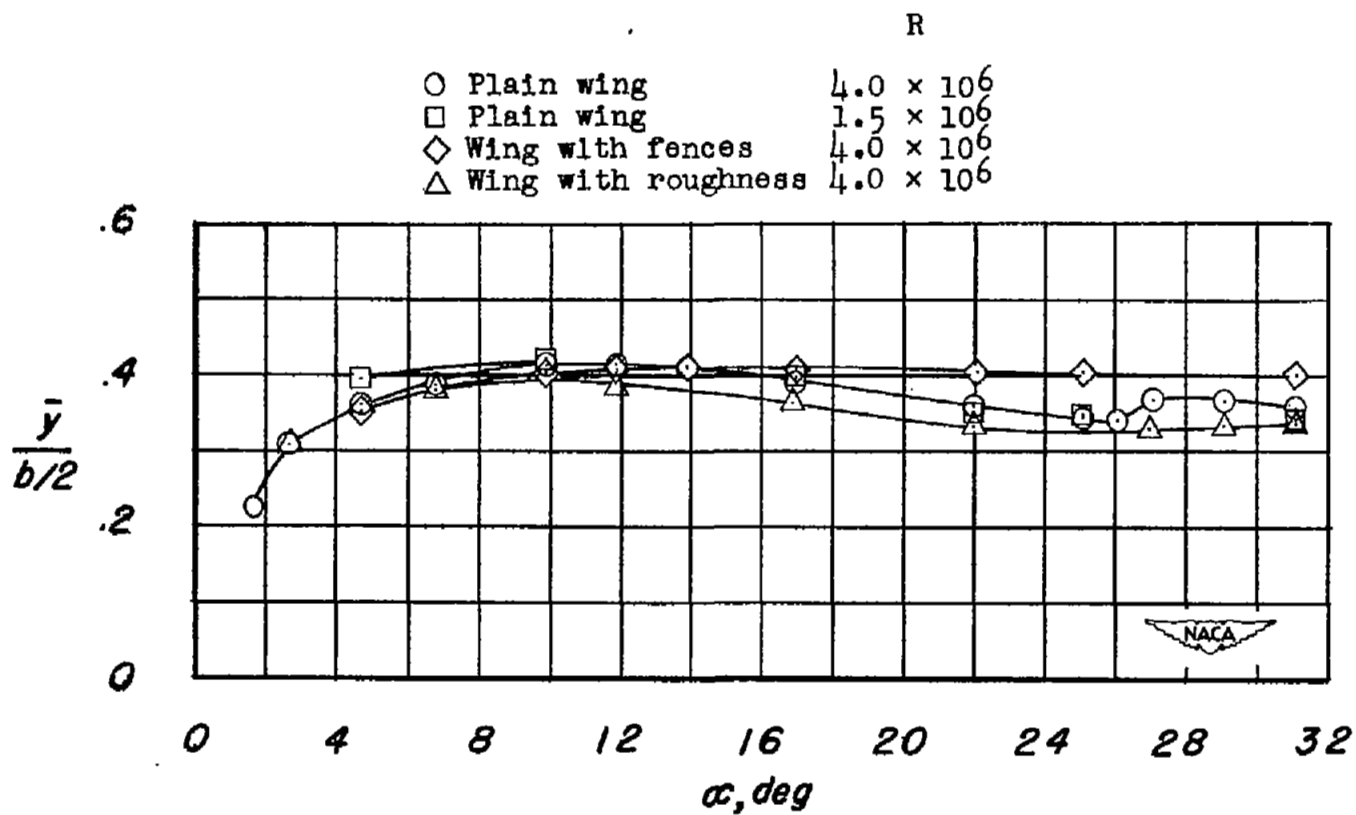
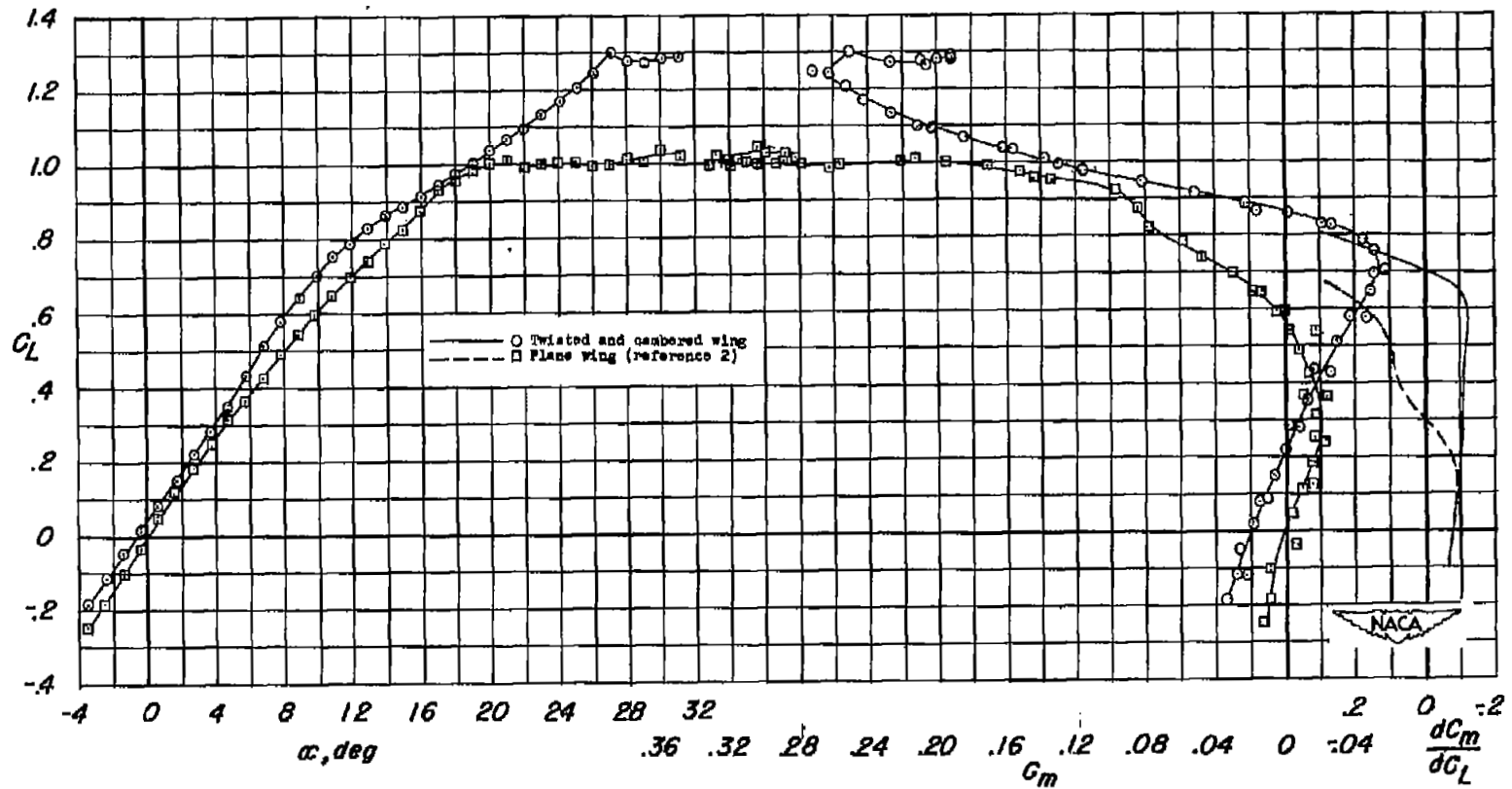


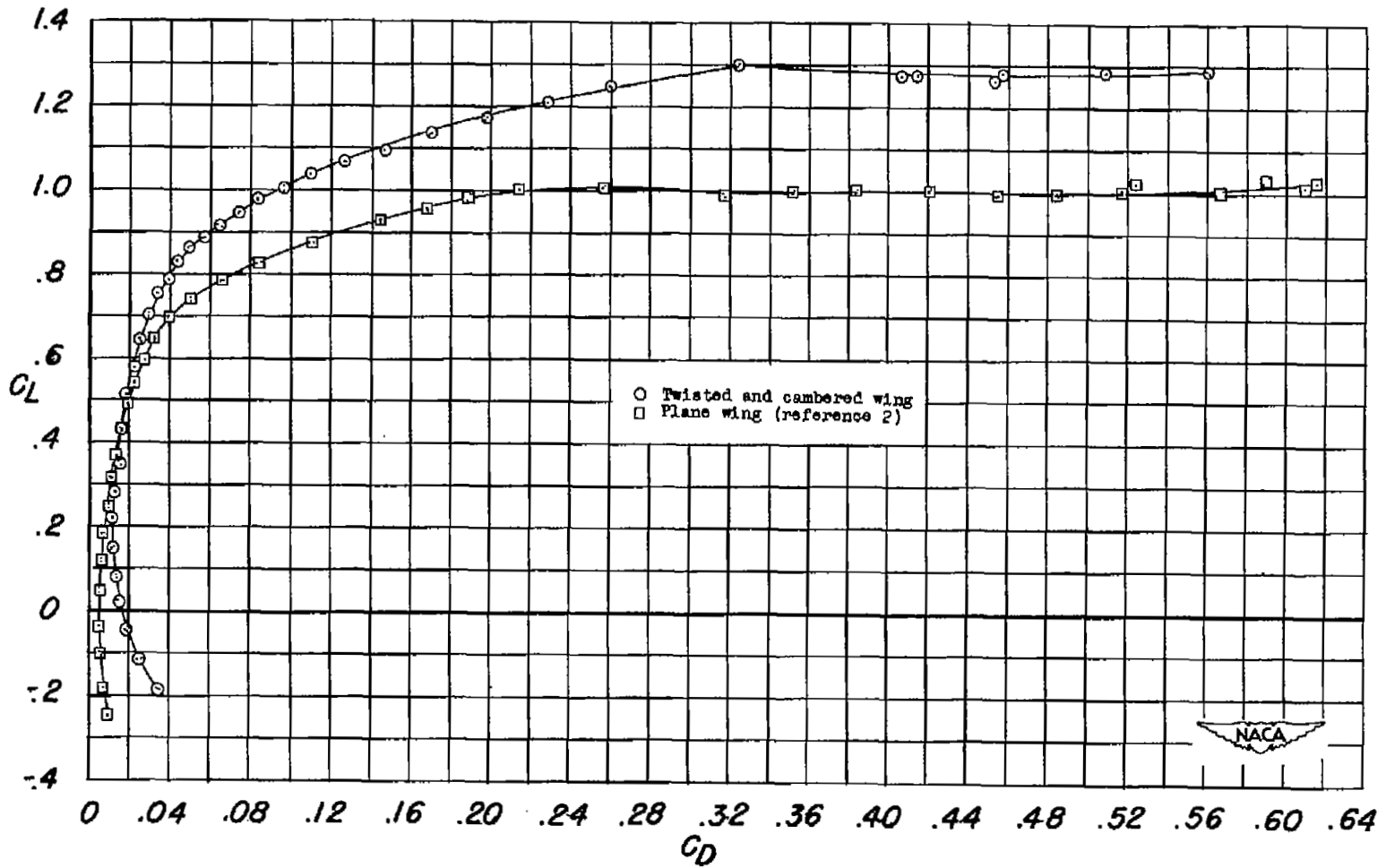
Figure 17.- Spanwise location of wing center of pressure.



(a) Lift and pitching moment.

Figure 18.- Effect of twist and camber on the lift, drag, and pitching-moment characteristics of a 45° sweptback wing of aspect ratio 8.

$$R = 4.0 \times 10^6.$$



(b) Drag.

Figure 18.- Concluded.

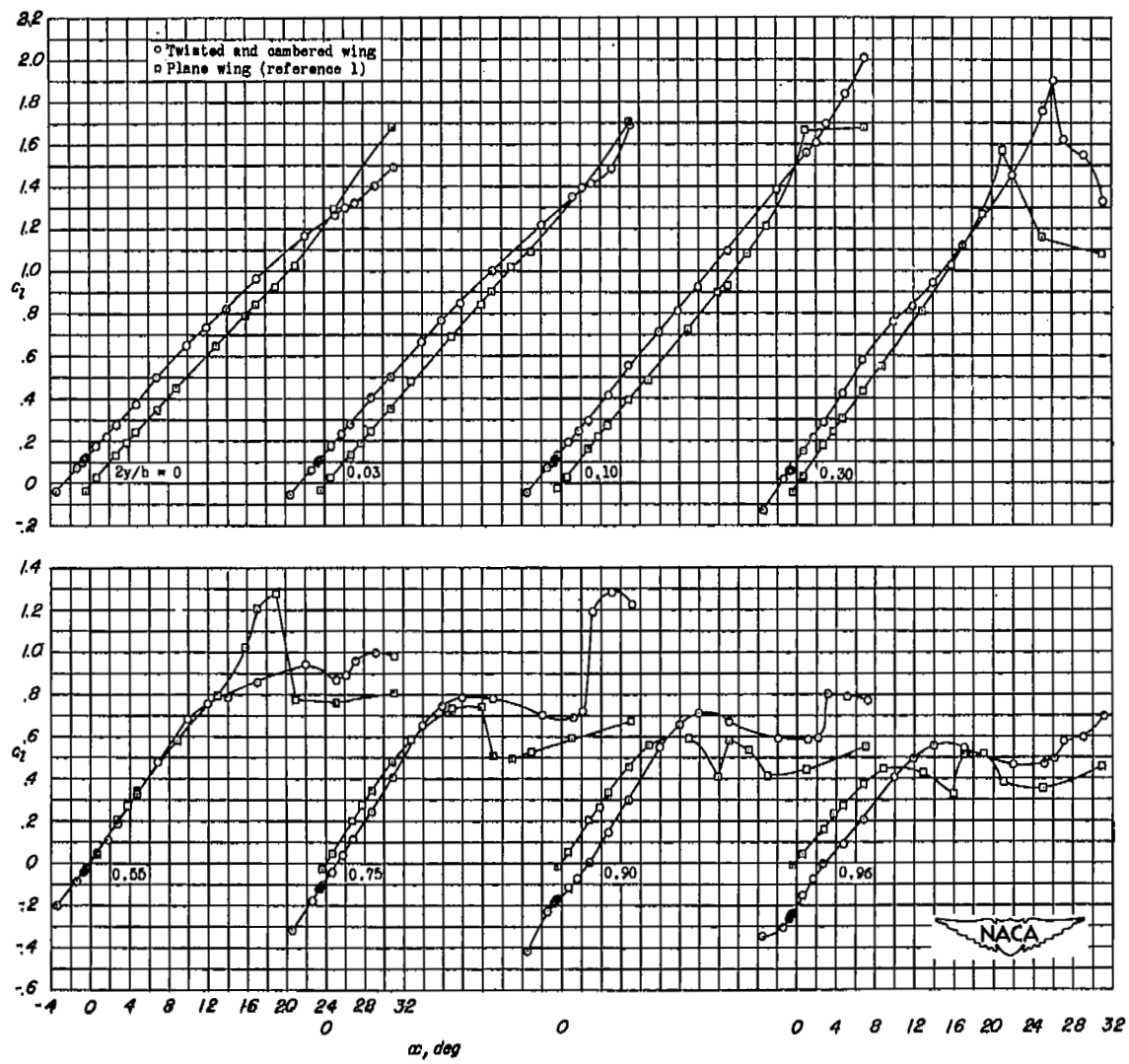
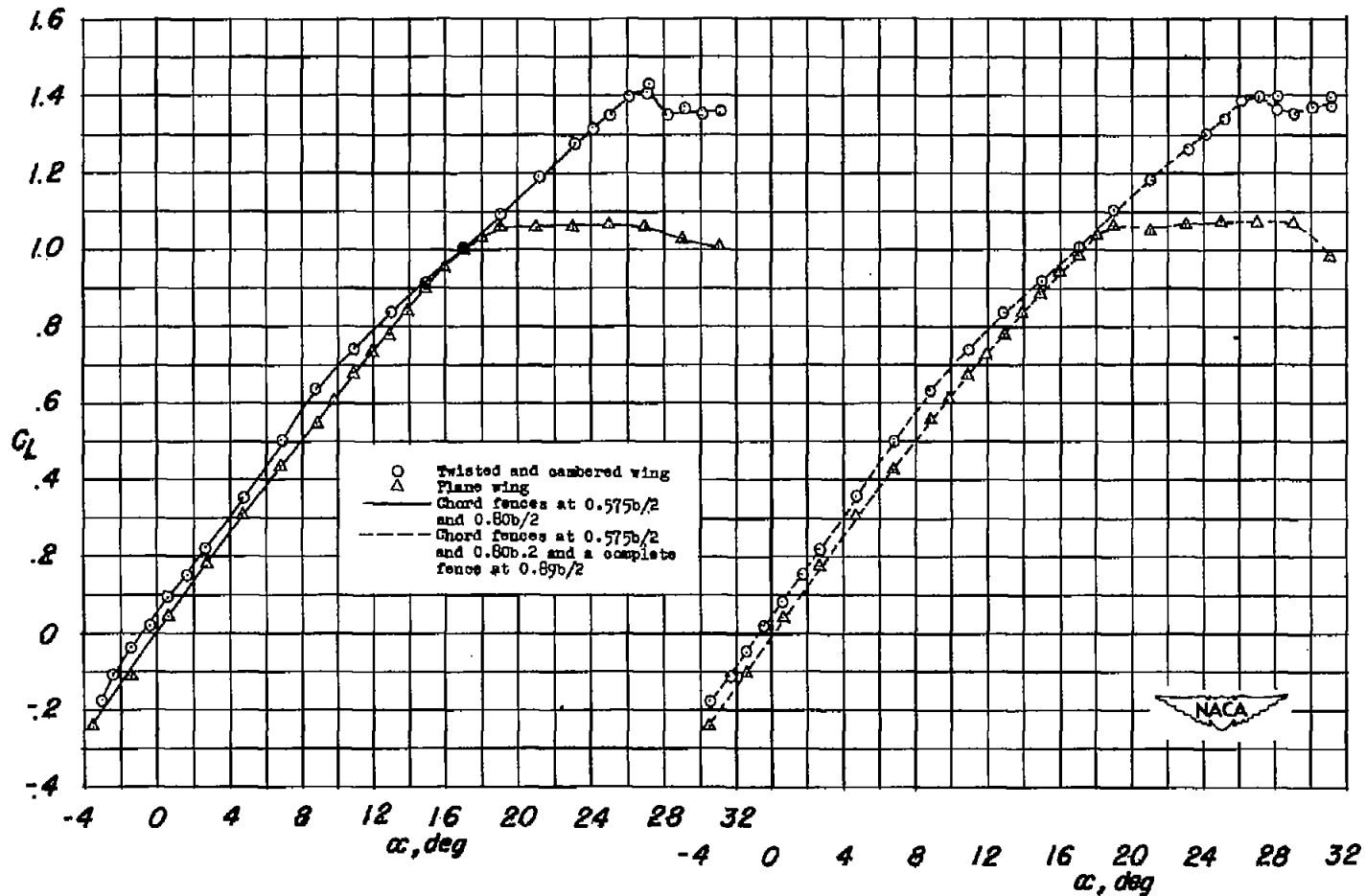
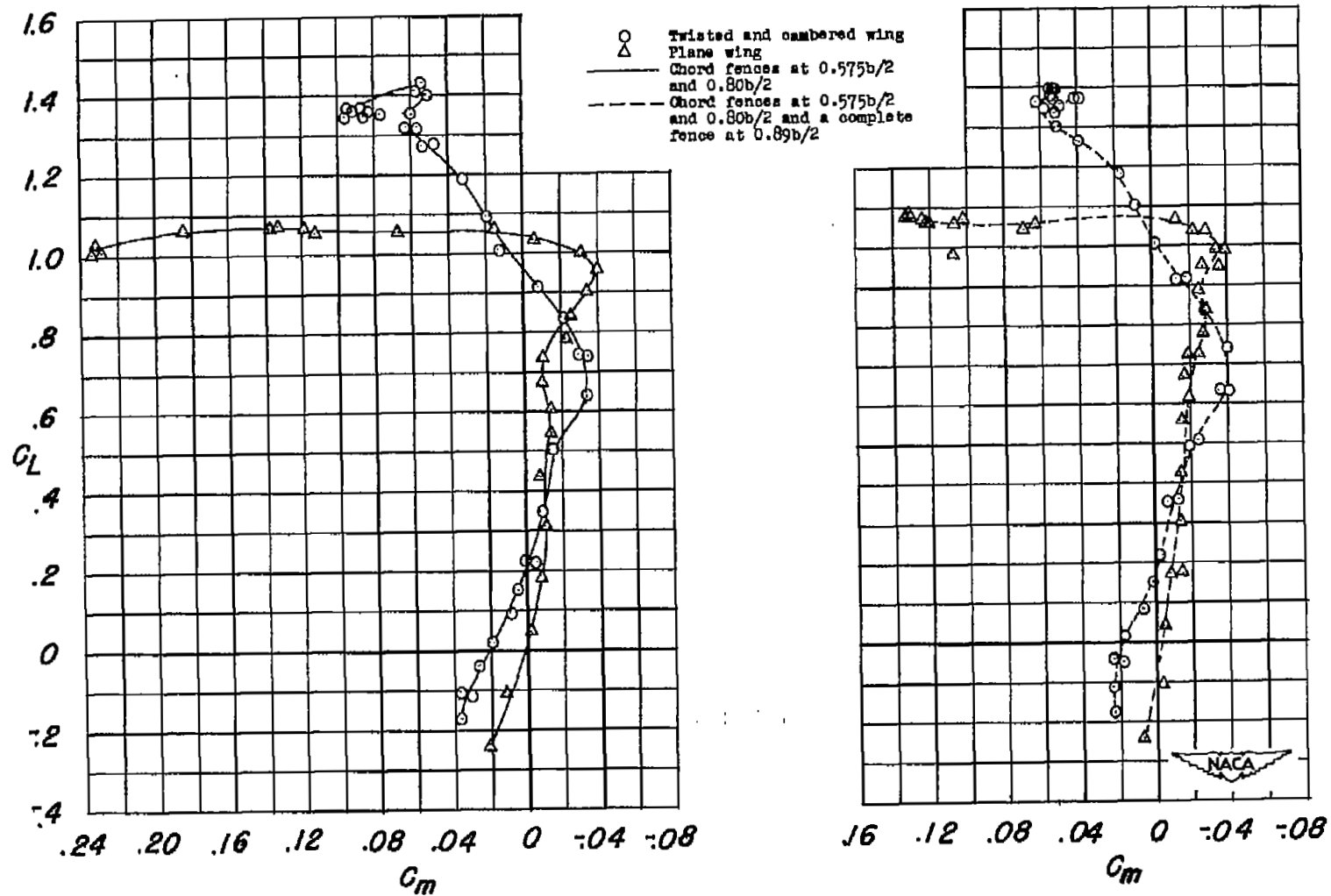


Figure 19.- Effect of twist and camber on the section lift characteristics of a 45° sweptback wing of aspect ratio 8. $R = 4.0 \times 10^6$.



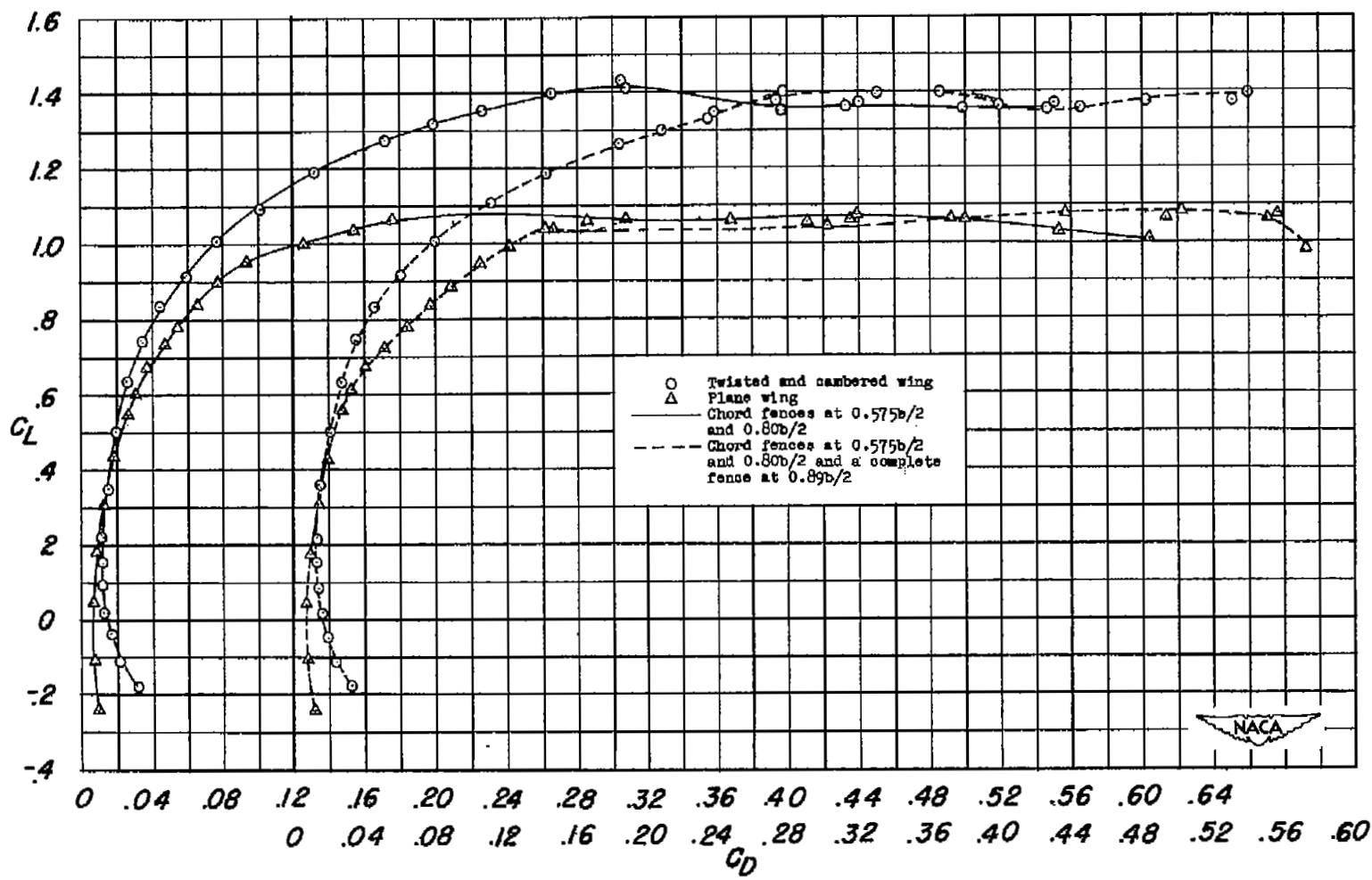
(a) Lift.

Figure 20.- Effect of various upper-surface fence configurations on aerodynamic characteristics of the plane and the twisted and cambered wings. $R = 4.0 \times 10^6$.



(b) Pitching moment.

Figure 20.- Continued.



(c) Drag.

Figure 20.- Concluded.



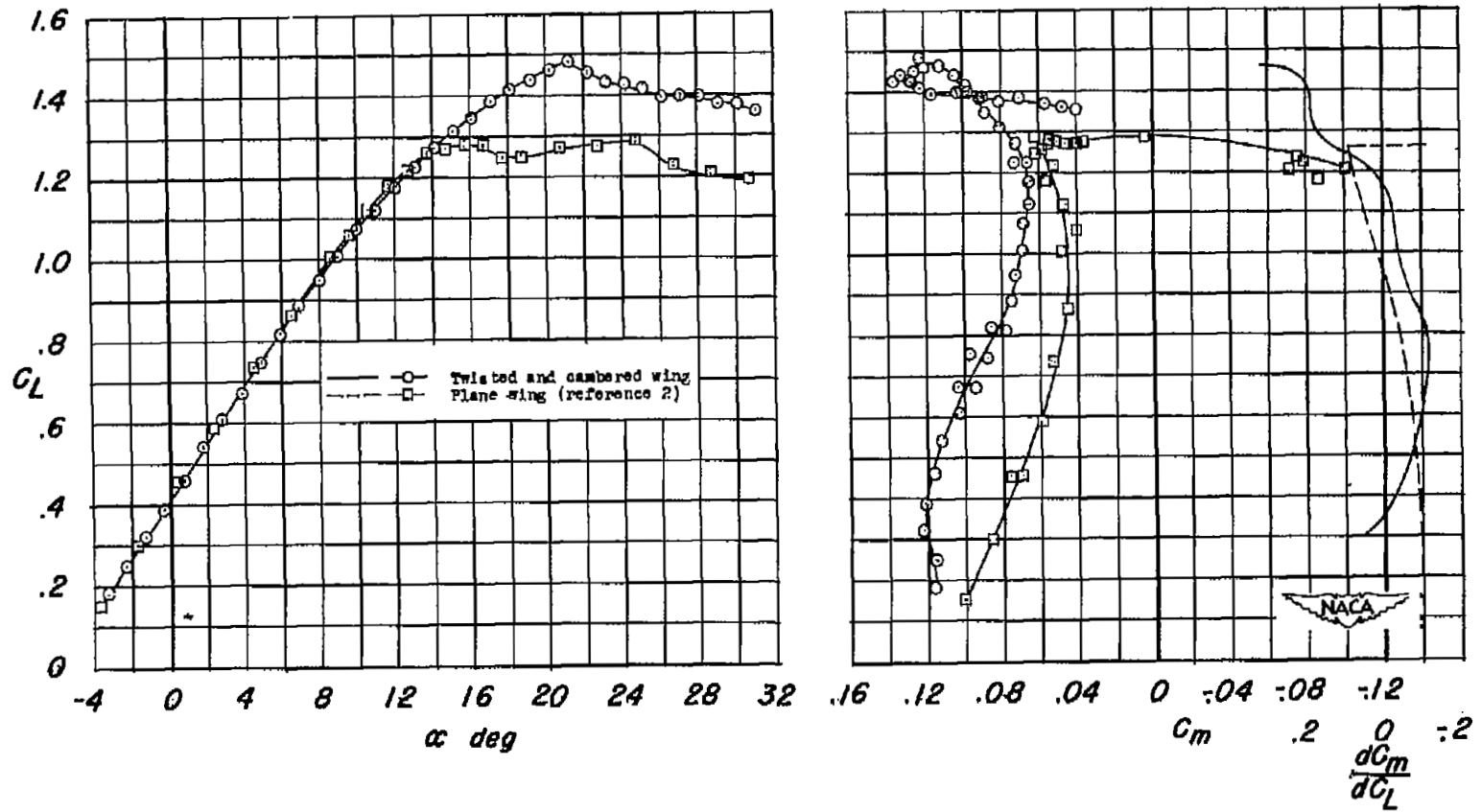


Figure 21.- Effect of twist and camber on the lift and pitching-moment characteristics of a 45° sweptback wing of aspect ratio 8 with leading-edge and trailing-edge flaps and upper-surface fences. $R = 4.0 \times 10^6$.

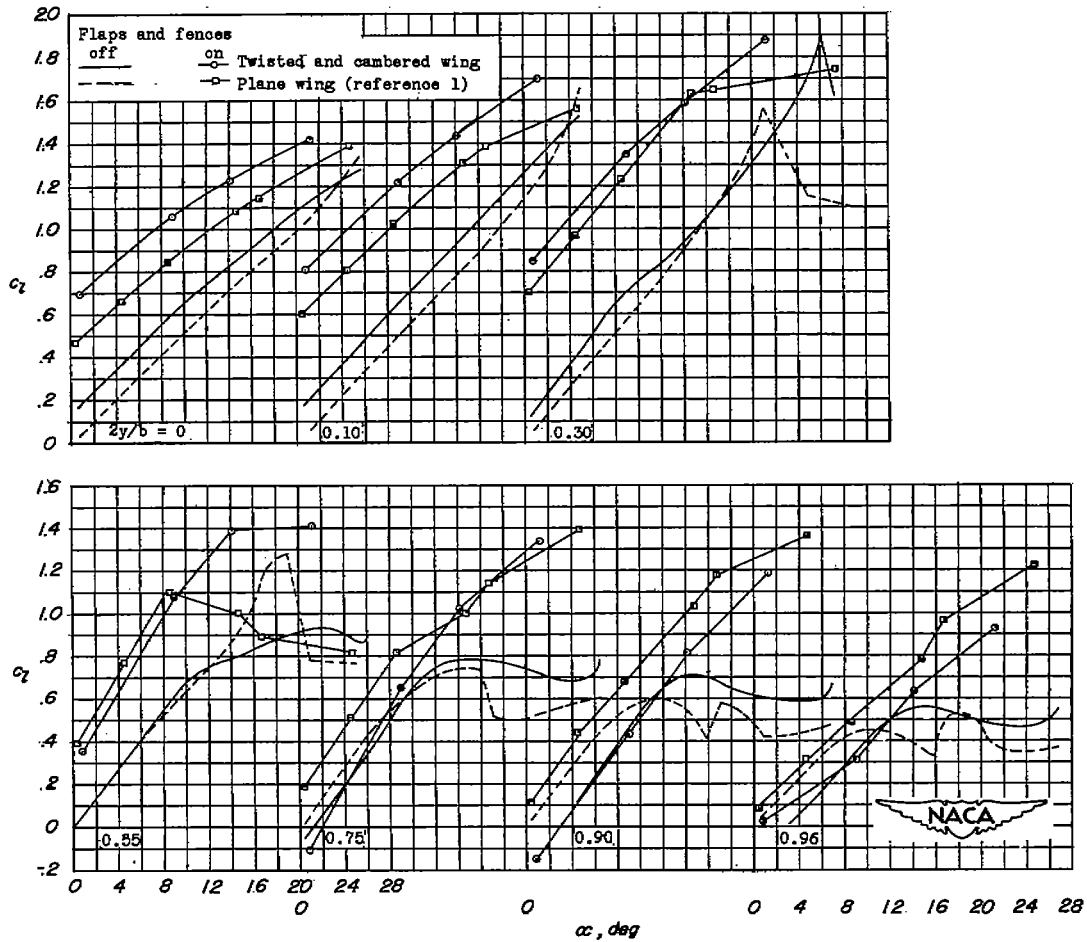


Figure 22.- Effect of twist and camber on the section lift characteristics of a 45° sweptback wing of aspect ratio 8 with leading-edge and trailing-edge flaps and upper-surface fences. $R = 4.0 \times 10^6$.

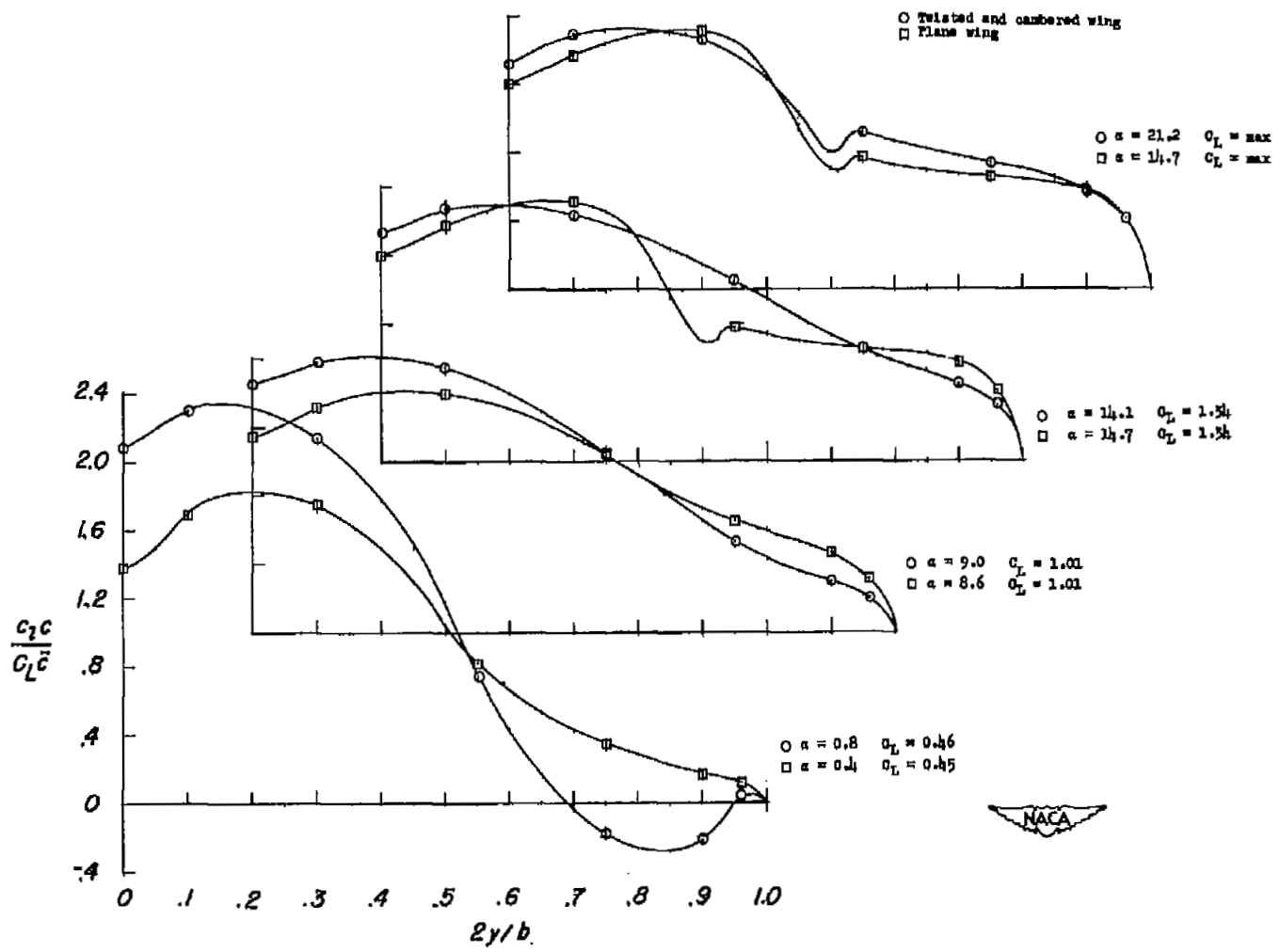


Figure 23.- Effect of twist and camber on span loading characteristics of a 45° sweptback wing of aspect ratio 8 with leading-edge and trailing-edge flaps and upper-surface fences. $R = 4.0 \times 10^6$.

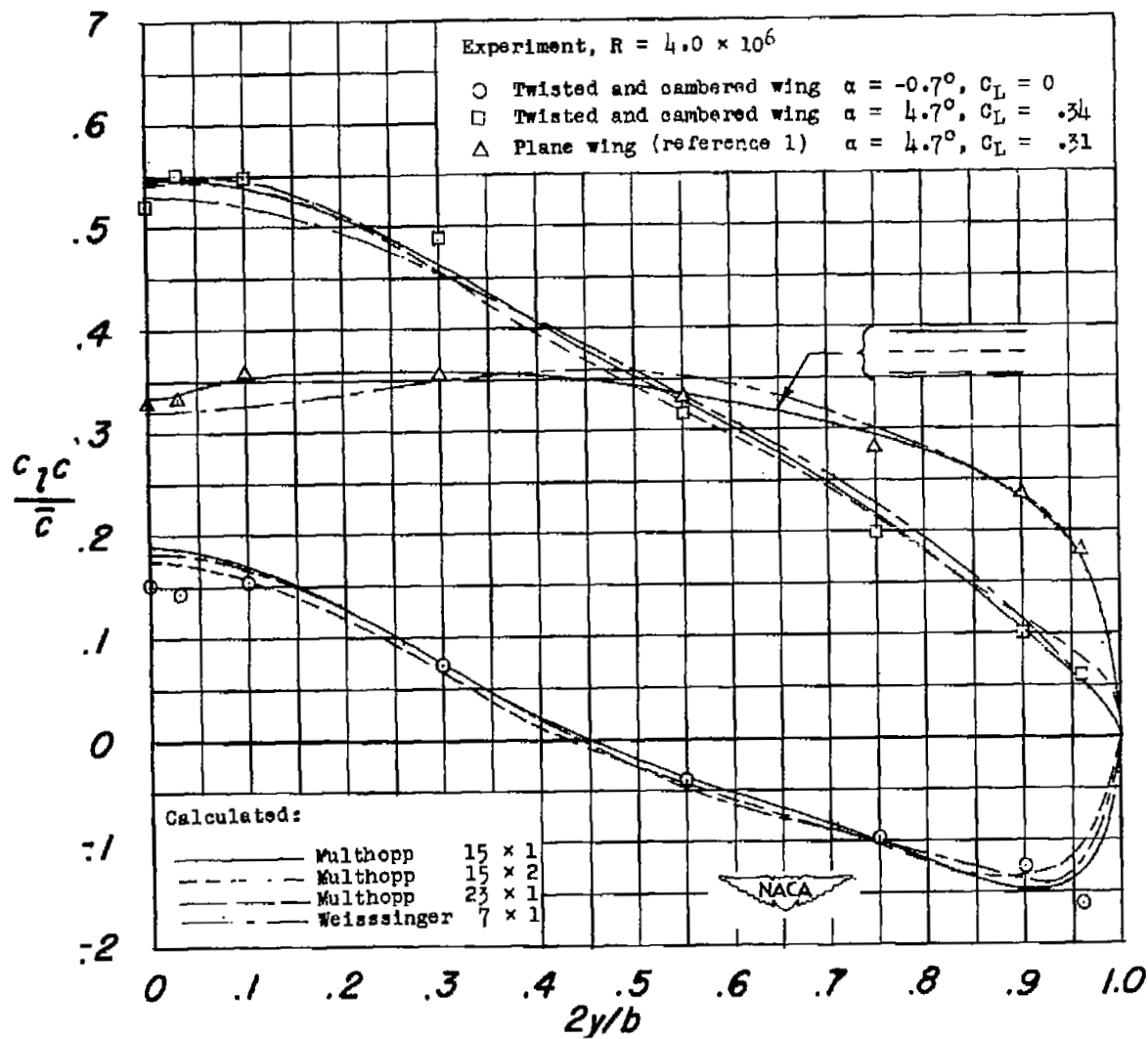


Figure 24.- Comparison of the calculated and experimental span loadings on the plane wing and on the twisted and cambered wing.

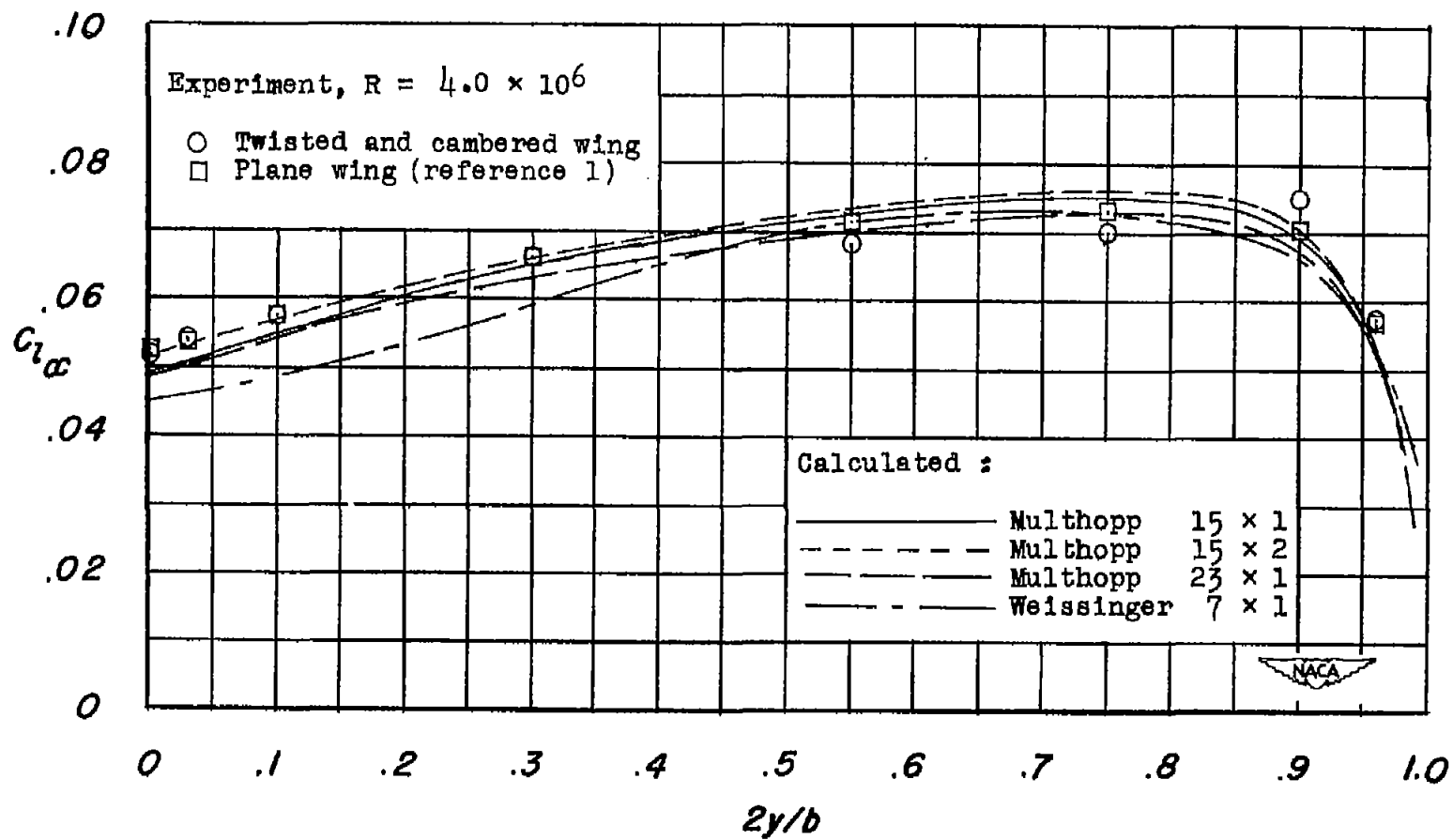


Figure 25.- Comparison of experimental and calculated section lift-curve slopes.

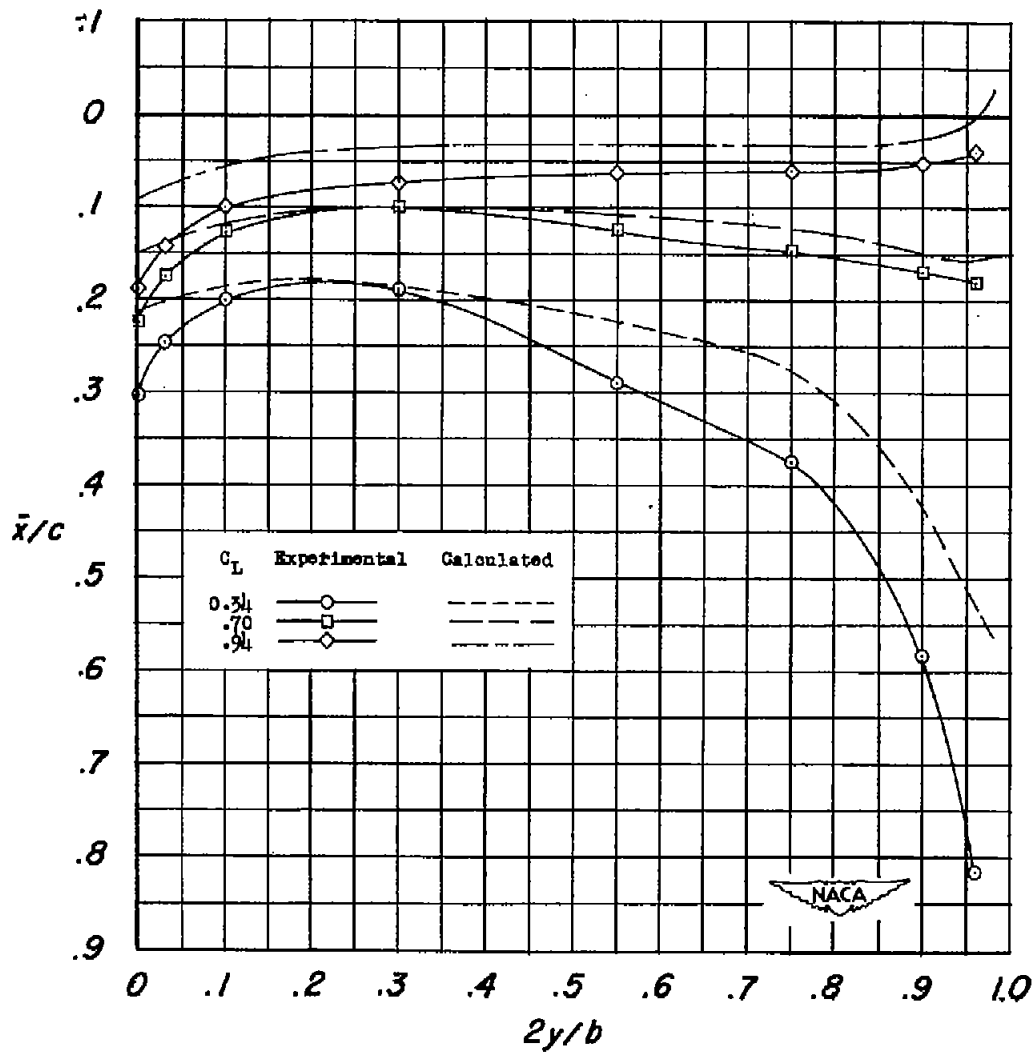


Figure 26.- Comparison of experimental section centers of pressure with centers of pressure calculated by the Multhopp 15 x 2 solution.

SECURITY INFORMATION



LANGLEY RESEARCH CENTER

3 1176 00518 2499

